annual report

2021 / 2022

INSTITUT FÜR
TECHNISCHE OPTIK
UNIVERSITÄT STUTTGART

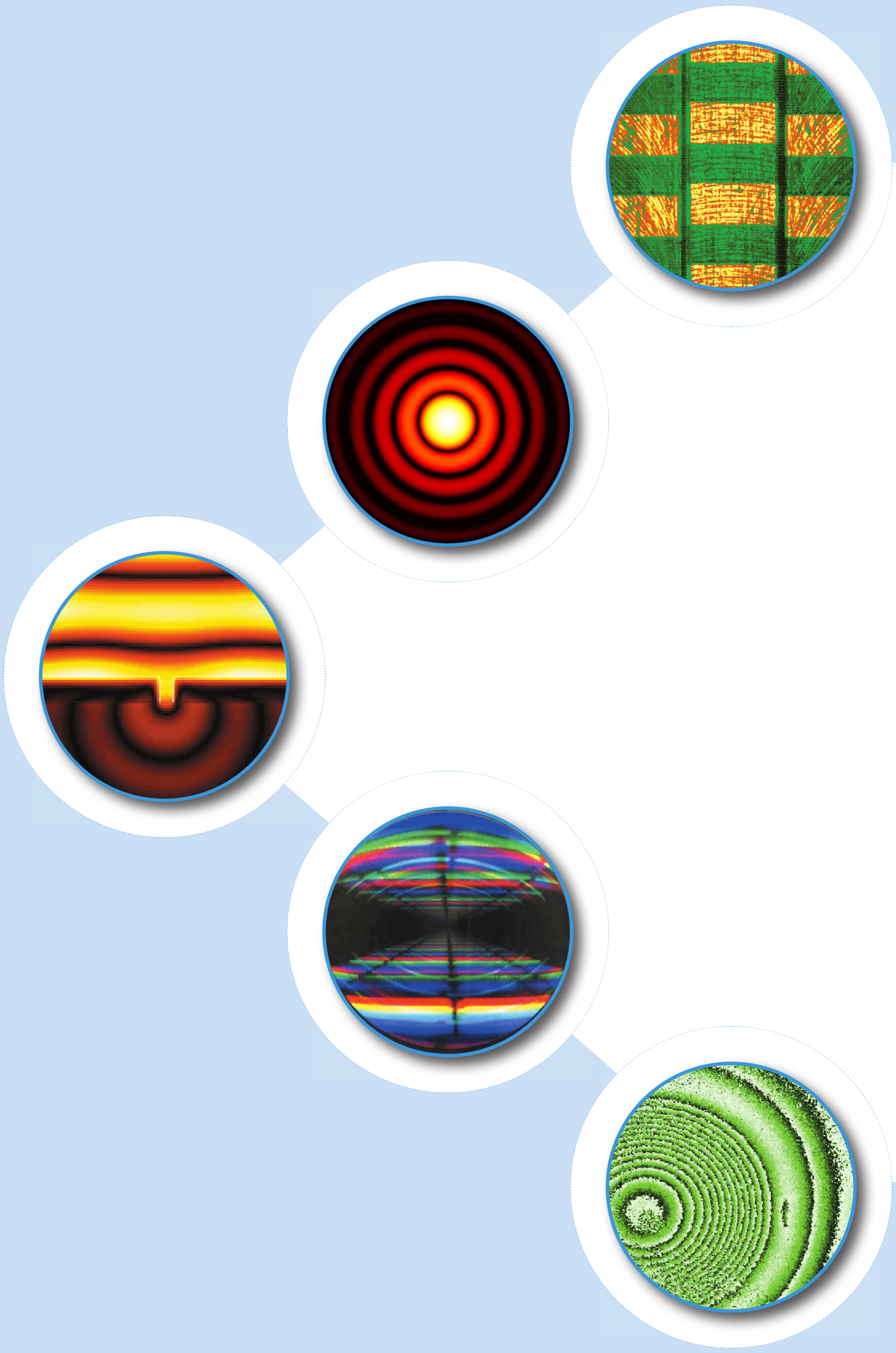

Universität Stuttgart

INSTITUT FÜR TECHNISCHE OPTIK
UNIVERSITÄT STUTTGART

Prof. Dr. S. Reichelt
Prof. Dr. A. Herkommer

Pfaffenwaldring 9
D-70569 Stuttgart
Tel.: +49(0)711 685-66075
https://www.ito.uni-stuttgart.de

ANNUAL REPORT 2021/2022

Optics is our future – But how do we get young people to get excited about it as well?

Dear readers, dear friends and partners of the ITO,

The 21st century is often referred to as the “Century of the Photon”, with optics and photonics playing a crucial role as a key technology in many areas. Over the last decades, optics and optical technologies have evolved from a specialized field to a cross-cutting, enabling technology. Whether in manufacturing technology, image processing, data transmission, medical technology, biotechnology, energy and environmental technology, or transportation, the contributions of optical technologies are indispensable. We encounter the achievements of optical technologies every day, and we equally appreciate their use. The microprocessors in our mobile devices are manufactured using EUV lithography, miniaturized optical systems ensure the impressive image quality of our photos, which, in turn, are displayed in high resolution on the display. But how do we manage to turn (some of the) users into designers, engineers and researchers of these fascinating optical technologies? It is our daily commitment to achieve this through engaging teaching and exciting research projects.

When we reflect on the progress made over the past two years, we realize that a lot has been achieved and put in place, but there are just as many new challenges ahead of us. Our teaching program is well established and we have still a good number of interested students. However, the overall number of first-year students in technical programs has declined in recent years. To somehow counteract this trend, the ITO has been actively engaging in the ‘Science Day’ of the University of Stuttgart for years. This involvement includes organizing optical experiments and workshops for school children, students and families (e.g. exposure of analog holograms).

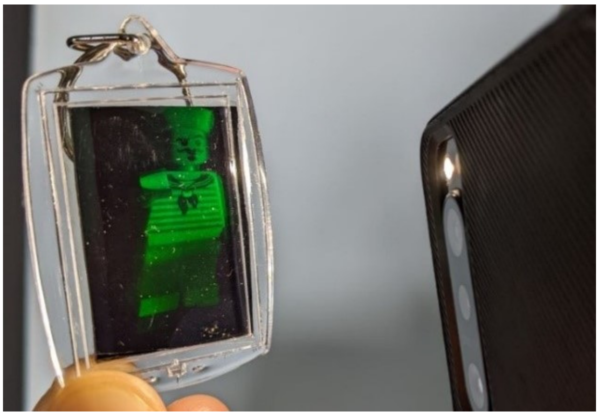

Fig. 1: Impressions of the ´Science Day´ at the ITO, here: exposure of analog holograms

On the research side, we have successfully completed several projects and acquired new research projects. Examples of some of the new projects include the development of an adaptive digital microscope, holographic light field generation, time-gated single pixel camera, correlation-based imaging through scattering media and the development of endoscopic bio-3D printing. It is with great pleasure that I present to you our latest achievements in the field of fundamental and applied research in optics in the new Annual Report of the Institute of Applied Optics (ITO). The report reflects our exciting activities in the research areas of 3D surface metrology, high resolution metrology, interferometry, diffractive optics design and fabrication, coherent metrology as well as optical design, simulation and 3D micro-optics manufacturing. All in all, this report attempts to summarize the journey we have taken in the field of applied optics, demonstrating our dedication to excellence in research, education, and innovation.

Equally important and beneficial is the close collaboration with our industrial partners. These collaborations give us some insight into relevant R&D challenges, enable joint projects and allow us to tailor our research accordingly.

I extend my heartfelt gratitude to everyone who has been a part of this journey. This applies in particular to all team members and third-party funders who made this research possible: BMBF, BMWi, DFG, AiF, ZIM, Baden-Württemberg Stiftung, all our industrial partners and the good cooperation with all the research institutes and institutions involved.

As we look to the future, let us continue to push the boundaries of what is possible and inspire generations to come. Above all, enjoy reading this report! And share it with young people who have an interest in optics so that the promises of the photonic century can continue to be realized!

Stuttgart, 2023

Stephan Reichelt

Index

Institute structure

3D-Surface Metrology

High Resolution Metrology and Simulation

Interferometry and Diffractive Optics

Coherent Metrology

Optical design and Simulation

Publications & Colloquium

A large part of the ITO Team hiking in the Wental nearby Oberkochen (Oct. 2023)

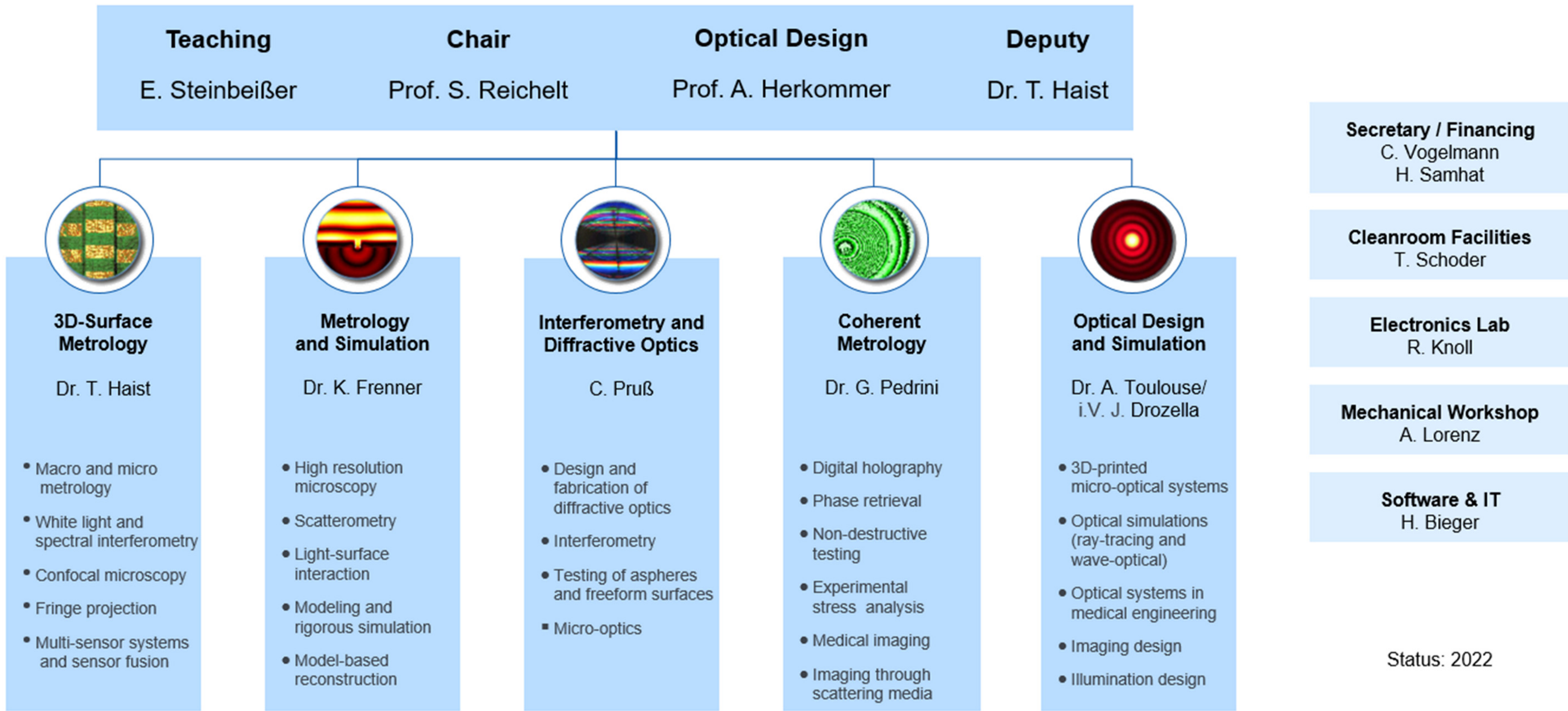
Teaching
E. Steinbeißer
Chair
Prof. S. Reichelt
Optical Design
Prof. A. Herkommer
Deputy
Dr. T. Haist
3D-Surface Metrology
Dr. T. Haist
Macro and micro metrology
White light and spectral interferometry
Confocal microscopy
Fringe projection
Multi-sensor systems and sensor fusion
Metrology and Simulation
Dr. K. Frenner
High resolution microscopy
Scatterometry
Light-surface interaction
Modeling and rigorous simulation
Model-based reconstruction
Interferometry and Diffractive Optics
C. Pruß
Design and fabrication of diffractive optics
Interferometry
Testing of aspheres and freeform surfaces
Micro-optics
Coherent Metrology
Dr. G. Pedrini
Digital holography
Phase retrieval
Non-destructive testing
Experimental stress analysis
Medical imaging
Imaging through scattering media
Optical Design and Simulation
Dr. A. Toulouse/
i.V. J. Drozella
3D-printed micro-optical systems
Optical simulations (ray-tracing and wave-optical)
Optical systems in medical engineering
Imaging design
Illumination design
Secretary / Financing
C. Vogelmann
H. Samhat
Cleanroom Facilities
T. Schoder
Electronics Lab
R. Knoll
Mechanical Workshop
A. Lorenz
Software & IT
H. Bieger
Status: 2022

Studying Optics

Traditionally our curriculum is primarily directed towards the students in upper-level diplom courses of **Mechanical Engineering, Cybernetic Engineering, Mechatronics, and Technology Management**. Since the academic year 2011/12 this courses are offered as master courses and an increasing number of master students is going to join our lectures.
This applies especially for the new master programme **“Micro-, Precision- and Photonics Engineering”** which enjoys great popularity also by students from other universities even from other countries.
Since the academic year 2009/10 we also offer our optics courses within the new bachelor and master program **“Medical Engineering”**, and since 2012 also within the new master program **“Photonic Engineering”**.
We also welcome students from other courses, such as “Physics” and “Electrical Engineering” and “Information Technology”.

The following list should give you an overview about the lectures given at the ITO. Be aware that not all lectures are suitable for all courses and that most lectures are held in German language.

Core subjects in Bachelor and Master Courses (6 ECTS - Credit Points):

- **Fundamentals of Engineering Optics**

  Lecture: Prof. Dr. S. Reichelt
  Exercise: K. Doth, A. Gronle, E. Steinbeißer

- **Optical Measurement Techniques and Procedures**

  Lecture: Prof. Dr. S. Reichelt
  Exercise: S. Hartlieb, E. Steinbeißer, M. Zimmermann

- **Optical Information Processing**

  Lecture: Prof. Dr. S. Reichelt
  Exercise: Dr. K. Frenner

- **Fundamentals of Optics** (only for B.Sc.)

  Lecture: Prof. Dr. A. Herkommer
  Exercise: F. Rothermel, M. Wende

- **Optical Systems in Medical Engineering**

  Lecture: Prof. Dr. A. Herkommer
  Exercise: F. Rothermel, M. Wende

- **Development of Optical Systems**

  Lecture: Prof. Dr. A. Herkommer
  Exercise: C. Reichert, A. Herkommer

- **Optical Sensors for Autonomous Systems**

  Lecture: Dr. T. Haist
  Exercise: Dr. T. Haist

Elective subjects in Bachelor and Master Courses (3 ECTS - Credit Points):

- **Optical Phenomena in Nature and Everyday Life**
  Lecture: Dr. T. Haist
- **Image Processing Systems for Industrial Applications**
  Lecture: Dr. T. Haist
- **Optical Measurement** (only for B.Sc.)
  Lecture: C. Pruß, Dr. T. Haist
- **Polarization Optics and Nanostructured Films**
  Lecture: Dr. K. Frenner
- **Introduction to Optical Design**
  Lecture: Prof. Dr. A. Herkommer, F. Rothermel
- **Advanced Optical Design**
  Lecture: Dr. Ch. Menke, Prof. Dr. A. Herkommer
- **Illumination Systems**
  Lecture: Prof. Dr. A. Herkommer
- **Current Topics and Devices in Biomedical Optics** (only for B.Sc.)
  Seminar: Prof. Dr. A. Herkommer

Additional studies:

- project work and thesis within our fields of research
  (you will find a list of all student project works at the end of this annual report)

- practical course “Optic-Laboratory”
  ⇒ speckle measurement
  ⇒ holographic projection
  ⇒ digital microscopy
  ⇒ computer aided design of optical systems
  ⇒ measurement of the spectral power distribution
  ⇒ Köhler illumination
  ⇒ 3D measurement with stereo vision

- practical course “Optical Measurement Techniques”
  ⇒ high contrast microscopy
  ⇒ digital holography
  ⇒ 2D-interferometry and measurement
  ⇒ quality inspection of photo-objectives with the MTF measuring system
  ⇒ ellipsometry

- common lab for mechanical engineering (APMB)

Activities of the Univ. Stuttgart SPIE Student Chapter

A. Birk, J. Drozella, F. Fischer, S. Hartlieb, F. Rothermel, C. Schober, A. Toulouse, C. Pruß

Since its founding in 2018, the Univ. Stuttgart SPIE Student Chapter plays an important role for optics-inclined students at the University of Stuttgart. The Student Chapter is an officially recognized student group at the University and we have students of all levels among our members, many of whom are with ITO, including past and present officers. Our goal is to deepen connections between students, the optics and photonics industry, and other researchers in the field. Despite the COVID 19 pandemic, we were able to do so with exciting activities during the past two years.

In 2021, we hosted a new event that we call Chapter Seminar. The aim is to increase professional exchange among our students in terms of their individual research and personal and career development. Chapter members could vote and sign up for their favourite series of talks, such as “Learning from Each Other” or “Increasing Motivation”, to discuss their goals and problems as well as share their insights with fellow students. Great emphasis was placed on the “By students, for students” mode of presentation, giving everyone ample time to leave their own mark and maximize their personal takeaways. To strengthen the team, we ended the event with a get-together of Chapter members and interested students.

The event was a resounding success, which is why we repeated it in 2022 with a greater, two-day scope. On top of the talks and discussions, it included the voted-upon lecture “Fourier Optics for Dummies” and a professional discussion with Nils Fahrbach, co-founder of SPIE Prism award 2023 finalist Printoptix, about start-up founding in the field of optics and photonics.

In Sept. 2021, we invited career coach Janina Hartlieb to host the seminar “Kompetent Kommunizieren” for our Chapter members. We gained many insights on engaging and efficient communication strategies with our scientific peers and future colleagues outside of academia.

To deepen our connection with other Student Chapters around the world, we joined TU Dresden Chapter (Germany), Stellenbosch Univ. Chapter and Wits Optics Chapter (both South Africa) for an international online workshop in Nov. 2021. With five talks by members of each chapter, this gave us the opportunity to share our results with peers outside of the usual scope of the University or local conferences and to learn about the exciting research directions that are being pursued elsewhere.

We had the exciting opportunity to invite guest speakers to give prolific talks for our chapter members and interested audience from the rest of the University. Thus, it was our pleasure to welcome Dr. David Andrews, Professor at the University of East Anglia, Norwich, UK and President of SPIE at that time, in 2021 and Dr. Michael Totzeck, Fellow at Carl Zeiss AG, Oberkochen, Germany, in 2022. Both used the opportunity not only to share some of their research with us, but also to spend a day learning about optics and photonics research at the University and especially ITO.

In addition to these professional events, we continued having regular outreach activities to make the chapter known to interested (prospective) students. Among those are our participations at Girls’ Day, Science Day and our annual barbecue, where we invite active Chapter members and interested new students for them to get in touch with each other.

Supported by: SPIE – The International Society for Optics and Photonics

SPIE. STUDENT CHAPTER UNIVERSITY OF STUTTGART

Fig. 1: Get-Together after the Chapter Seminar 2021.

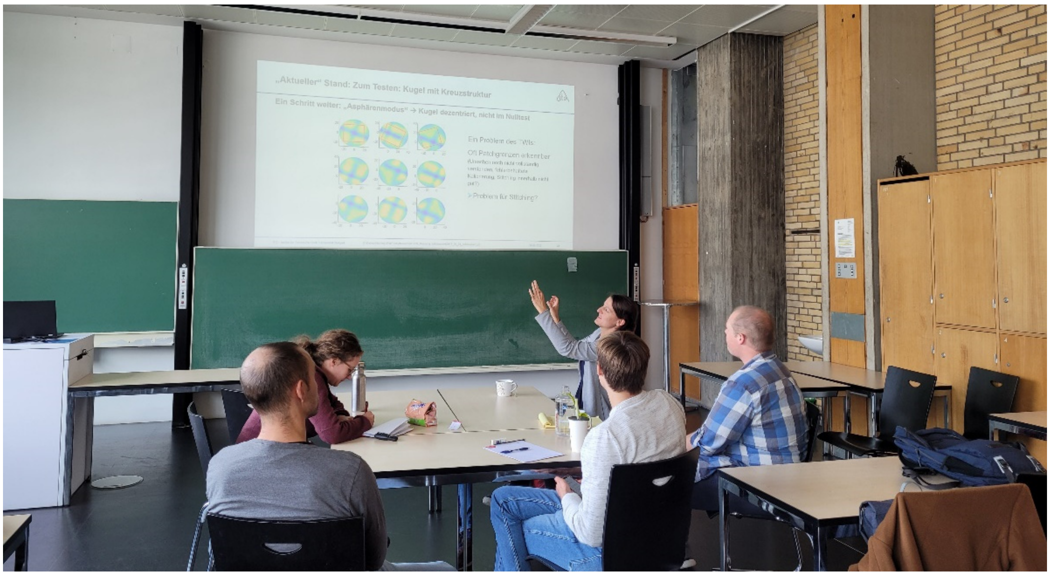

Fig. 2: Discussion during Chapter Seminar 2022.

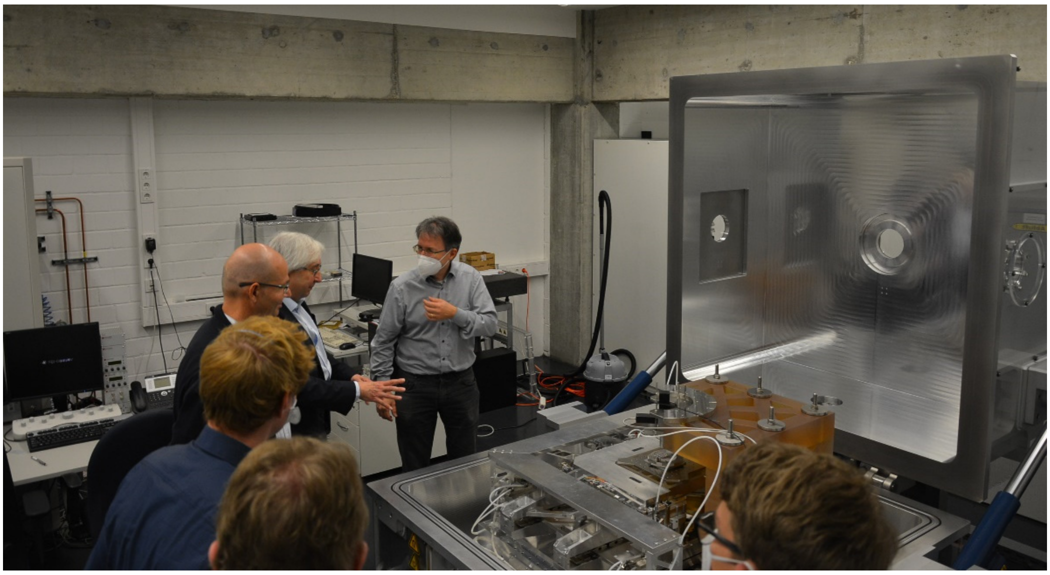

Fig. 3: Christof Pruß explaining the NPMM-200 to Prof. Andrews.

The research groups

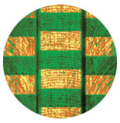

3D-Surface Metrology

The objective of the group is the analysis and the implementation of new principles for the acquisition of optical 3D-surface data of engineering and biological objects over a wide scale. Our main focus is on the enhancement of the metering capacity by a combination of physical models and optimized system design.

Current research activities are:

- 3D-measurement applying fringe projection and deflectometry (macroscopic and microscopic)
- adaptive techniques using spatial light modulators
- confocal microscopy
- white light interferometry
- hyperspectral imaging
- sensor fusion and data interpretation strategies

Contact: haist@ito.uni-stuttgart.de

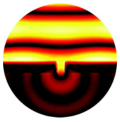

High Resolution Metrology and Simulation

The goal of this research group is the investigation of the interaction of light with 3d object structures in the micro and nano domain. Along with experimental research, one major aspect is the rigorous modelling and simulation as an integral part of the active metrology process. The analysis of all information channels of the electromagnetic field (intensity, phase, polarisation state of light) allows us to obtain sub-wavelength information about the structure.

Current research areas:

- modelling and rigorous simulation
- computational electromagnetics
- inverse problems
- high resolution microscopy
- scatterometry
- optical metamaterials

Contact: frenner@ito.uni-stuttgart.de

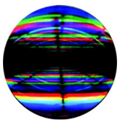

Interferometry and Diffractive Optics

The goal of our research activity is to explore new measurement concepts using diffractive optics. One important application is the testing of optical surfaces, in particular, aspheric lenses. For this purpose we design and produce computer generated holograms (CGH). At the same time, we develop flexible measurement techniques for aspheres and freeform surfaces that aim to replace static null correctors. In addition to CGH for interferometry, our in house production facilities allow us to produce diffractive elements and micro-optics for a wide variety of applications such as imaging systems, UV-measurement systems, beam shaping applications and wavefront sensing.

Our research areas include:

- testing of aspheric and freeform surfaces
- design, fabrication and testing of hybrid refractive/diffractive systems
- interferometry and wavefront sensors
- tailored optics for metrology applications
- fabrication of diffractive elements and micro-optics

Contact: pruss@ito.uni-stuttgart.de

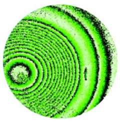

Coherent Metrology

Our research objective is the analysis and application of methods based on coherent optics for the measurement of 3D-shape and deformation and to determine the material properties of technical objects and biological tissues. Aside from the quantitative measurements of form and deformation, methods for non destructive material testing are also analysed and applied.

Research areas include:

- computational imaging
- imaging through scattering media
- holographic microscopy
- experimental stress analysis
- shape measurement

Contact: pedrini@ito.uni-stuttgart.de

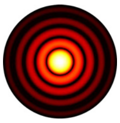

Optical Design and Simulation

In our research group we focus on the development of novel tools for simulation and optimization, and the design of innovative complex optical systems for industrial or medical purposes. A strong focus lies on the realization of novel micro-optical systems fabricated via two-photon-polymerization. The classical optical design of imaging and illumination systems, as well as ray-based and wave-optical system simulations remain core competencies and research fields of our group.

Research areas include:

- design, simulation and manufacturing of 3D-printed micro-optical systems
- optical simulations (ray-tracing and wave-optical)
- optical systems in medical engineering
- imaging design
- illumination design
- phase space methods in optical design and simulation

Contact: toulouse@ito.uni-stuttgart.de, herkommer@ito.uni-stuttgart.de

3D-Surface Metrology

Snapshot hyperspectral sensor based on diffraction at microgratings

R. Hahn, T. Haist

A new method for single-shot (snapshot) multispectral imaging has been developed. The core idea is the use of a diffractive optical element (DOE) in an intermediate image plane. The main advantages are the potentially low-cost implementation for various applications, e.g. for classification and the possibility and capability to use different spatial-spectral scans in different field positions.

By choosing the DOE appropriately, it is possible to select different spectral and spatial sampling patterns. Here, spatial and spectral resolution are coupled via an uncertainty relation, i.e. a high spatial resolution leads to a large spectral half-width.

Fig. 1 shows the basic structure of a corresponding sensor. The DOE is located in an intermediate image plane and deflects the light depending on the wavelength. To understand the principle of operation, it is advantageous to first assume image-side telecentricity of the first imaging stage and a large grating with a constant grating period as the DOE.

Due to the telecentricity, the main rays hit the DOE at the same angle and are deflected according to their wavelength. Different wavelengths then impinge on the filter plane (actually the Fourier plane of the second image) at different points, and we can, through a suitable aperture, pass a certain spectrum through the filter aperture. The rest of the second imaging system focuses the light onto the monochrome (or color, if we want to combine with absorption-based filtering) image sensor.

Now, however, one can replace the simple grating by a more complicated diffraction structure. For example, different micro-gratings can be used.

The sensor was used, for example, to record the topography in a chromatic confocal microscope in a single shot. For this purpose, stripe-shaped grids of different periods were used. Spectral shifts can thus be determined very precisely (in the example set-up to 0.5 nm) and height measurements can be carried out with it.

Fig. 2: Intensity on image sensor in stripe-shaped microgratings for detection of the spectral shift in a chromatic confocal microscope.

Supported by: BMBF and BMWI under the grant 13N15161 and 16KN075722

References:

(1) R. Hahn, T. Haist, K. Michel, and W. Osten, "Diffraction-based hyperspectral snapshot imager," Optical Engineering, vol. 61, no. 1, p. 015106, (2022).

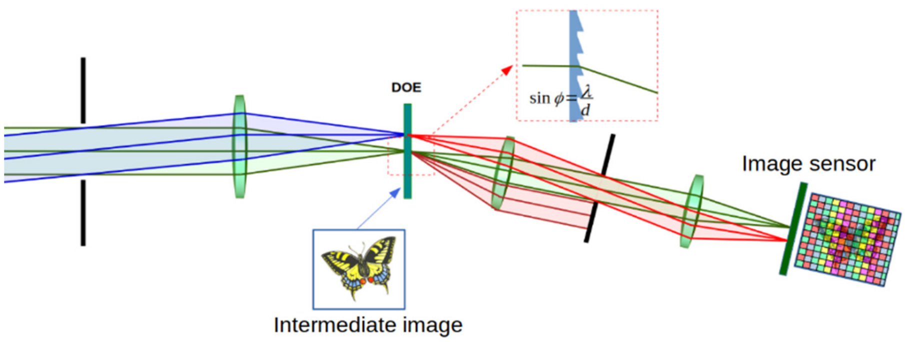

Fig. 1: Principle of the diffraction-based snapshot sensor.

Optical tweezers for pathogen detection

K. Doth, T. Haist

The significance of hand hygiene as an infection prevention measure has clearly been demonstrated during the corona virus pandemic. But even apart from pandemics, with the increase in multi-resistant pathogens and the high mobility, the probability of pathogenic infections is increasing. An early-warning system for pathogenic infections would be a useful tool in not only detecting but also preventing infections by dynamically adapting the hygiene measures in closed systems (e.g. hospitals). In the BMBF-funded project GeDeSens2Virus, the aim is to integrate a multi-sensor detection of bacteria and viruses into a dispenser system, which analyses the so-called overspray after a hand hygiene event. The ITO is investigating different methods for the optical detection of pathogens in order to miniaturize the most promising one for integration into the dispenser system. One of the investigated methods is the optical tweezer for pathogen detection.

Optical tweezers make use of the radiation forces present in a focused laser beam to trap particles in the focus of the beam. The trapping efficiency depends on various parameters, e.g. the particle size, refractive index of the particle and the surrounding medium, laser power, as well as the numerical aperture (NA) of the focused beam. This dependence on different particle and laser parameters can be used to differentiate between particles. For example, optical tweezers enable the differentiation between healthy and cancerous cells (1).

Usually, stable particle trapping requires a high NA of the focus generating microscope objective. With a holographic twin trap, the required NA for stable trapping can be significantly reduced. Holographic twin traps use a diffractive optical element in front of the objective to generate two axially separated traps. A mirror redirects the focus of second trap to the focus of the first trap (2).

We implemented a lab setup for analyzing the trapping efficiency for different microscopic objects like polystyrene particles from 500 nm to 30 µm or E. Coli bacteria. A Fresnel zone plate was produced to realize a holographic twin trap. We investigated different trapping techniques and compared the required NA for stable trapping of the single trap and the holographic twin trap approach. The results showed a NA-reduction of 40% when working with the holographic twin-trap setup. Therefore, the holographic-twin trap approach was chosen to be advantageous over the single trap approach.

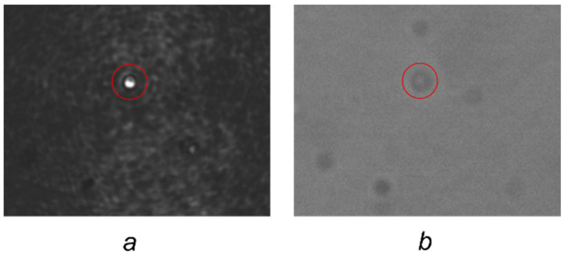

Fig. 1: Trapped 1 µm polystyrene-particle.
a: Reflection of trapping laser.
b: Blocked trapping laser. Object in transmission illumination.

Part of the project is the miniaturization of the optical detection and its integration into a microfluidic system. For this purpose, we work with a 3D-printer for microoptics using two photon polymerization. This additive manufacturing allows for rapid prototyping and the combination of diffractive and reflective surfaces in a single optical design to manufacture an objective that generates two axially separated focal points. A first prototype for the miniaturized holographic optical tweezer was designed and printed. The next step is the analysis of the trapping performance and the integration into a microfluidic channel.

Supported by: BMBF
Project: Miniaturisiertes Elektroniksystem zur schnellen Detektion von Viren und Bakterien im Desinfektionsmittelspender
In cooperation with: OPHARDT HYGIENE-TECHNIK, ALU Freiburg, ibidi, ADDI-DATA, Sciospec Scientific Instruments

References:

(1) F. Schaal, et al., “Marker-free cell discrimination by holographic optical tweezers.”, Journal of the European Optical Society - Rapid publications, Vol 4, (2009).

(2) S. Zwick, et al., “Holographic twin traps.”, Journal of Optics A: Pure and Applied Optics 11 03401, (2009).

Multipoint method for industrial applications

S. Hartlieb, T. Haist

The multipoint technique allows one to extend the precision, resolution and potentially the accuracy of camera-based position sensing. To this end a computer-generated hologram in the imaging system (ideally located in the Fourier plane) replicates images of active emitters (typically LEDs). On the image sensor, we therefore have N copies of the imaged LEDs and straightforward center-of-gravity based evaluation of the LED's image positions. Subsequent averaging over the N copies leads to very precise measurements (precision in the range of thousands of a pixel). Discretization errors as well as photon and camera noise will be reduced in theory by a factor of the square root of N. In practice, statistical measurement uncertainties in the range of thousands of a pixel can be reached.

We successfully used this technique in the project for improving the accuracy of a commercial coordinate measurement machine, building an improved Shack-Hartmann wavefront sensor and realizing low-cost multipoint vibrometry.

In addition, the technique can be used in combination with a PSF-based distance measurement technique (see [2]) to achieve lateral as well as axial positioning (approximate precision 1:2000 of the axial measurement range) with just one image sensor and one objective lens (plus hologram).

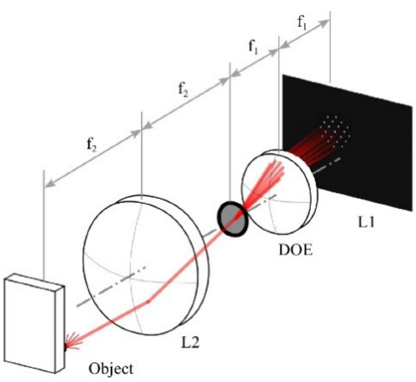

Fig. 1: The multipoint technique.

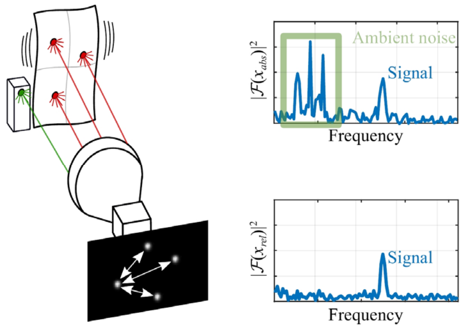

Fig. 2: Image-based multipoint vibrometry using multipoint image replication.

Supported by: DFG within project Dynref2
In cooperation with: ISYS University of Stuttgart

References:

(1) Hartlieb, S., Tscherpel, M., Guerra, F., Haist, T., Osten, W., Ringkowski, M., & Sawodny, O. (2021). Highly accurate imaging-based position measurement using holographic point replication. *Measurement*, *172*, 108852.

(2) Hartlieb, S., Schober, C., Haist, T., & Reichelt, S. (2022). Accurate single image depth detection using multiple rotating point spread functions. *Optics Express*, *30*(13), 23035-23049.

(3) Hartlieb, S., Boguslawski, M., Haist, T., & Reichelt, S. (2022, May). Holographical image-based vibrometry with monochromatic and event-based cameras. In *Optics and Photonics for Advanced Dimensional Metrology II. SPIE* Vol. 12137, p. 1213702.

(4) Hartlieb, S., Ringkowski, M., Haist, T., Sawodny, O., & Osten, W. (2021). Multi-positional image-based vibration measurement by holographic image replication. Light: Advanced Manufacturing, 2(4), 425-433.

3D measurement system for autonomous robots

A. Faulhaber, T. Haist

Within the project SEE3D, new methods for 3D acquisition in the context of robotics have been investigated. The focus of the work was on energy-efficient acquisition, which is desirable for battery-assisted systems. The main technology is triangulation, but a new perspective-based approach was also investigated. Furthermore, non-contact methods for breath and pulse detection were implemented to provide additional important information in the field of care robotics.

For triangulation-based 3D panorama acquisition, many (2×10) energy-efficient CMOS image sensors are used in combination with FPGA-based preprocessing. The inevitably large amounts of data are compressed onboard (FPGA) and transferred via WLAN to a central server (host) for further processing. This reduces the power required for the actual robot. Accordingly, triangulation is based on a mixture of passive multi-stereo and a “sparse” point projection to improve robustness and accuracy. An optimized, laser-based projection of point patterns thus leads to energy-efficient illumination of the periphery.

From our point of view, the approach pursued in the project is the most sensible one for battery-operated systems in the medium term. The main sensors can use the available ambient light and only comparatively little additional light energy (sparse projection) is necessary. The focus for the evaluation is on high-resolution 2D image information (combined to 3D, among other things) and low processing energy onboard. It could be shown that very good results with regard to sensor technology can be achieved with low energy requirements.

The differential perspective methodology developed in the project is currently being further developed in the field of driver assistance systems. The advantage of this is that it is possible to determine distances with sufficient accuracy even at great distances of up to approx. 300 m very cost-effectively with only one camera (low cost) (current status: measurement uncertainty of the distance for stationary objects approx. 1% at a distance of 200 m).

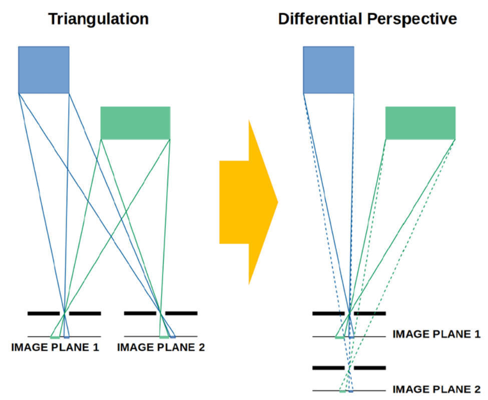

Fig. 1: Triangulation-based methods as well as a new method, differential perspective, have been investigated.

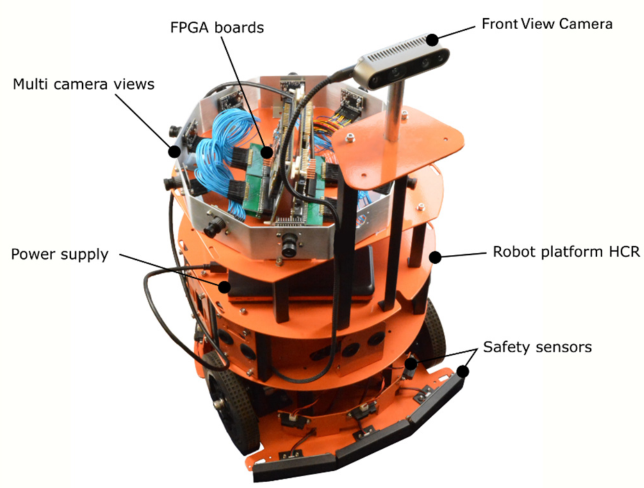

Fig. 2: Robot platform with multiple stereocameras.

Supported by: Baden-Württemberg Stiftung gGmbH
In cooperation with: IPVS Universität Stuttgart

References:

(1) Faulhaber, A., Kraechan, C., Haist, T., „Depth from axial differential perspective“, Optica Continuum, Optical Society of America (Optica), (2021).

Holographic light field generation to investigate large 3D displays

M. Zimmermann, S. Reichelt

Immersive display technologies are becoming more and more common in people's everyday lives. Today's devices are highly complex in all their different forms, from 3D cinema and stereoscopic displays to AR/VR glasses.

The main drawback of current stereoscopic displays for 3D vision is the vergence-accommodation conflict. While the object appears to be behind or in front of the screen due to the different positions of the two images for the left and right eye, the eyes are still accommodated onto the screen. For small depth deviations this is not a problem, but for larger deviations and over a longer period of time, the vergence-accommodation conflict can cause headaches and discomfort.

Holography is one way of overcoming the vergence-accommodation conflict, as it recreates the light field and the objects appear at the specified distance and not in the plane of the rendering media. Analog holography using high-resolution photographic film was popular around 1960 and 2000. However, the step from analog to digital holography is harder than one might think, as digital displays are nowhere near the resolution and "pixel sizes" of the analog films.

The pixel sizes in today's displays allow only a limited angle of diffraction and therefore a limited viewing angle. However, with a positive lens, all the rays from the display are focused in the Fourier plane of the lens (1). As long as the eye is close to the Fourier plane, the view is expanded to the full display size, as shown in the schematic setup in Figure 1.

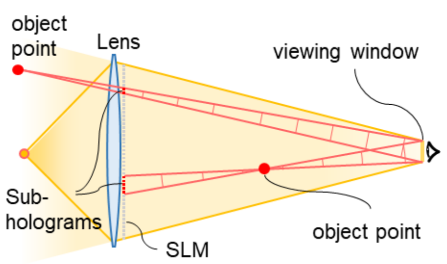

Fig. 1: Schematic principle of a large holographic display setup. The light source is imaged in the plane of the viewing window. In this example the sub-holograms are simple Fresnel lenses.

The position of the pupil is also limited to the area between the diffraction maxima resulting from the pixel matrix in the Fourier plane, called the viewing window. If the eye moves outside of the viewing window, the viewing window must be moved, which is done by beam steering and pupil tracking. Figure 2 shows two captured images taken from our current setup with the camera placed in the correct position.

In order to obtain a good visibility of the scene across the entire viewing window, the object phases are typically superimposed by a random phase distribution, which provides the desired slight scattering but also creates unwanted speckles. Our goal is to minimize the speckles and increase the image quality.

The novelty of our approach is to include the position of the pupil in the hologram optimization. This allows for more degrees of freedom during optimization.

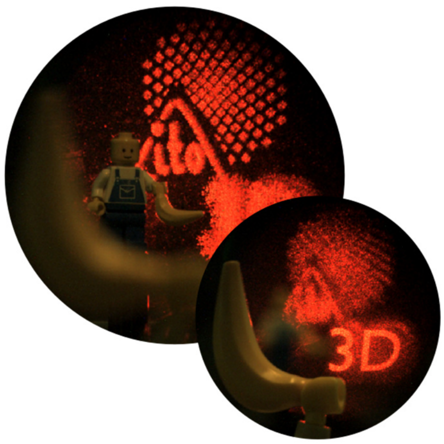

Fig. 2: In the left image, the camera is focused on the distance of the Lego figure and the ITO logo appears sharp. In the right image the camera is focused on the banana.

Supported by: Vector Stiftung

References:

(1) S. Reichelt, R. Häussler, N. Leister, G. Fütterer, H. Stolle, and A. Schwerdtner, 'Holographic 3-D Displays - Electro-holography within the Grasp of Commercialization', Advances in Lasers and Electro Optics. InTech, 2010. doi: 10.5772/8650.

Tissue differentiation using optical sensor systems

V. Aslani, T. Haist, S. Thiele, A. Herkommer

Pathologically altered tissue exhibits differences in its structural, mechanical and elastic properties compared to healthy tissue (1). Even though minimally invasive surgery has many advantages for the patient, direct contact of the surgeon to the tissue and thus direct haptic feedback is lost during these procedures (2). However, the assessment of stiffness plays an important role in tissue differentiation, which is why an optical sensor system based on the principles of elastography and triangulation was developed that allows intraoperative and minimally invasive determination of the elastic tissue properties. For this purpose, a novel 3D-printed fiber-based fringe projector is used to project a fringe pattern onto the tissue, which is detected at a triangulation angle using an endoscope. The tissue is indented in a non-contact manner by a compressed air or water jet pulse and a depth map of the deformation is reconstructed. The indentation is directly related to the stiffness of the tissue and thus allows differentiation between different tissue types. As shown in Fig. 1, the measurement system was miniaturized to the extent that it can be integrated into the working channel of a commercially available cystoscope and can be used in a minimally invasive manner, e.g. during cystoscopy or transurethral bladder tumor resection.

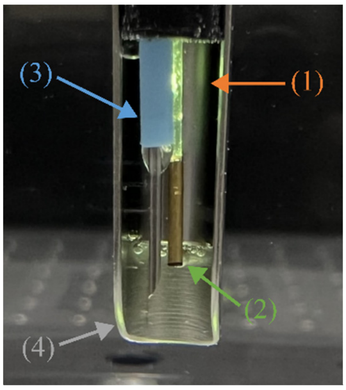

Fig. 1: (4) Distal tip of the cystoscopy system with (1) cystoscope, (2) fringe projector and (3) injection needle for force application.

The functionality of the setup was tested, for example, on the inner bladder wall of porcine bladders as demonstrated in Fig. 2. The fiber-based fringe projector was used to project the fringe pattern onto the bladder wall. The bladder was deformed via a compressed air pulse, with a constant force applied to the tissue during the pulse, and a sequence of images of the deformation was acquired. Depth maps were then reconstructed from the fringe projection images of the image sequence.

The sensor system enables the detection of viscoelastic tissue properties and is suitable for intraoperative, endoscopic and non-contact differentiation between samples with different elastic properties.

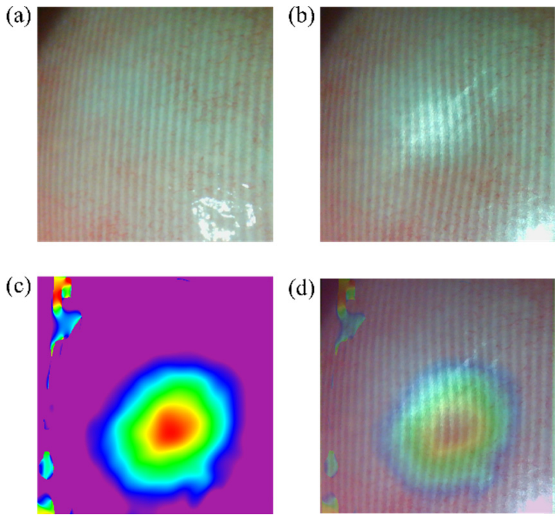

Fig. 2: Endoscope images of the fringes projected onto the inner bladder wall of the pig bladder (a) before force application and (b) deformation during force application. (d) shows an overlay from (b) with the reconstructed depth map (c).

Supported by: The work described in this report was conducted in the framework of the Graduate School 2543/1 “Intraoperative Multi-Sensory Tissue-Differentiation in Oncology” (project A1) funded by the German Research Foundation (DFG - Deutsche Forschungs-gemeinschaft).

References:

(1) Y. C. Fung, Mechanical properties of living tissues: Mechanical properties of living tissues, vol. / Y.C. Fung of Biomechanics, 2nd ed. (Springer, New York, 1993).

(2) S. Walz, V. Aslani, O. Sawodny, and A. Stenzl, “Robotic radical cystectomy - more precision needed?” Current opinion in urology 33(2), 157–162 (2023).

Averaging approaches for highly accurate image-based edge localization

V. Aslani, F. Guerra, T. Haist

We introduce an optical and a digital averaging technique that considerably improves edge localization performance. The techniques have been demonstrated for horizontal edges captured under laboratory conditions (razor blade) as well as for real world applications (building deformation measurements) using a scientific CMOS image sensor. Edge localization can be improved by up to 60% while preserving high lateral and temporal resolution.

The first approach uses an optical replication scheme based on a computer-generated hologram that optically replicates the image before photo-detection so that the same image of the edge falls onto different positions on the image sensor (as shown in Fig. 1). Thereby, different discretization errors and most time-varying errors can be reduced by spatial averaging (1). Especially for high quality images, the optical method achieves measurement uncertainties down to 5/1000-th of a pixel (36 nm in image space).

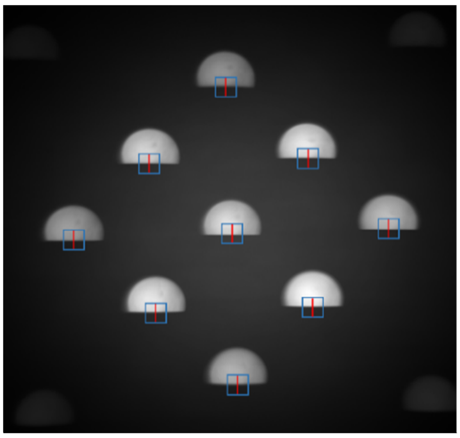

Fig. 1: Exemplary image used for evaluation. Nine replications of the original object (edge of a razor blade) are recorded by a CMOS sensor. The blue boxes indicate the regions that were used for the evaluation. The edge position is determined along the direction of the vertical red lines.

Of course, the field of view is reduced by the technique in the experimental setup. For such a limited field of view scenario, the results have to be compared to optical systems using longer focal lengths. For a 3×3 replication this would correspond to three times the focal length and, therefore, one would end up with a comparable precision of 15/1000-th of a pixel. However, for some applications, the replication can be done along one dimension. Then, the full gain of the method becomes obvious and still the full field of the original imaging can be preserved.

The second method is based on a neural network denoising architecture (U-Net (2)) and is especially suited for high levels of photon noise. In this case, a neural-net based denoising (Fig. 2) can considerably improve edge localization (improvement up to 50%).

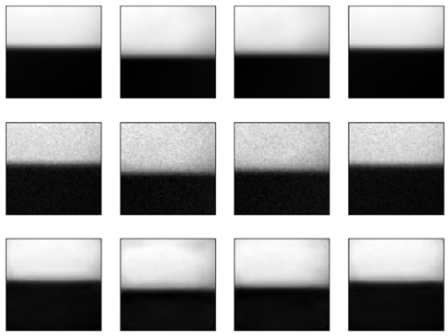

Fig. 2: Neural network denoiser. Top: Original noiseless images of the edges; Middle: Images after artificially adding photon noise (QWC = 1000); Bottom: Output of the trained U-Net (denoised images).

Both methods have been used in combination with a simple straight-forward moment-based edge localization algorithm but other, more sophisticated algorithms might be employed as well.

Supported by: German Research Foundation (DFG - Deutsche Forschungsgemeinschaft) Project: SFB1244

References:

(1) T. Haist, S. Dong, T. Arnold, M. Gronle, and W. Osten, “Multi-image position detection,” Opt. Express 22(12), 14450–14463 (2014).

(2) O. Ronneberger, P. Fischer, and T. Brox, “U-net: Convolutional networks for biomedical image segmentation,” in International Conference on Medical image computing and computer-assisted intervention, (Springer, 2015).

Characterization of slit homogenizers for the GeoCarb mission

T. Haist, M. Tscherpel, S. Hartlieb

Satellite-based hyperspectral imaging is typically performed in a push-broom configuration. One potentially important source of error is scene inhomogeneity of a spatial resolution cell. In other words: If within one resolution cell the spectroscopic and or polarimetric parameters of light spatially vary, the measurement uncertainty of the spectroscopic measurement will considerably increase.

Therefore, each photon that is detected is first homogenized by a so-called homogenization element. Different homogenization devices have been used and characterized in the past with respect to their optical performance.

In a cooperation with the University of Oklahoma, Lockheed and NASA we build a specialized characterization setup and used that setup for testing six slit homogenizers to be potentially used in the GeoCarb mission to monitor CO2 pollution from space.

Generally speaking, the near field output of the slit homogenizer with respect to diffraction and polarization effects is of interest if different input illumination scenes are used. The characterization is performed in the near-infrared and short-wave infrared spectral region. Several thousand high resolution images under different conditions (polarization, input scene, polarization) have been captured and evaluated.

Temporal coherence (as one will face it in a spectrometer) is achieved using different laser sources. Spatial incoherence with very good spatial homogeneity is achieved using a double diffuser approach when illuminating the “scene”, which in our experiments consisted of a changeable (position and geometry) slit. The Müller vector is measured pixelwise for certain given input polarization.

The major finding is that the homogenizer performance depends strongly on the polarization of the incoming light, with the sensitivity growing as a function of wavelength. The width of the ISRF is substantially smaller when the light is vertically polarized (orthogonal to the slit length) compared to horizontally polarized (parallel to the slit length), and the throughput is accordingly reduced. These effects are due to the effects of the gold coating and high incidence angles present in the GeoCarb homogenizer design, which was verified using a polarization-dependent model generalized from previous homogenizer modeling work.

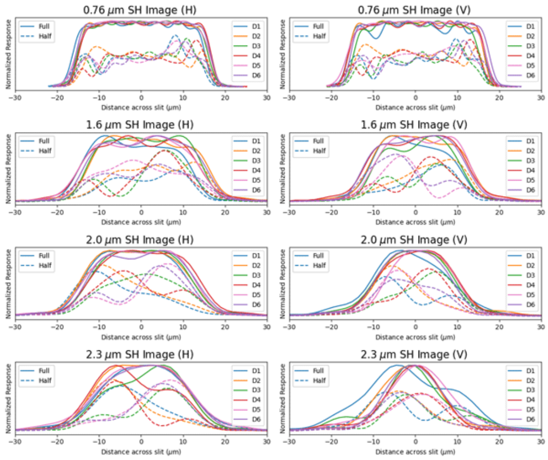

Fig. 1: Typical measurement results (intensity across slit) for different illuminations.

Supported by: NASA
In cooperation with: University of Oklahoma, Lockheed Martin, NASA

References:

(1) Crowell, S., Haist, T., Tscherpel, M., Caron, J., Burgh, E., & Moore III, B. (2023). Performance and polarization response of slit homogenizers for the GeoCarb mission. *Atmospheric Measurement Techniques*, *16*(1), 195-208.

Measurement of large-scale building deformations

F. Guerra, S. Hartlieb, T. Haist

Within the Sonderforschungsbereich 1244 new techniques for adaptive buildings are being be developed. For the control of such buildings (high rise buildings and bridges) ITO is developing new sensing methods to measure deformation. Two successful methods are based on using holograms in front of conventional photogrammetric camera systems.

For the multipoint technique, active emitters (LEDs) are mounted at the building. The computer-generated hologram in the imaging system (ideally located in the Fourier plane) replicated the image of each LED. On the image sensor we therefore have N copies of the imaged LEDs and straightforward center-of-gravity based evaluation of the LED's image position followed by averaging over the N copies leads to very precise measurements (precision in the range of thousands of a pixel).

Therefore, deformations of the building can be measured by the relative distance between the images of the LEDs.

For the demonstration high-rise building of the SFB 1244, which is located on the campus of the university, we are using two camera boxes, each of which is equipped with two cameras (for stereo processing).

A second method is using a long focal length (e.g. $f' = 500\,\mathrm{mm}$) imaging system in combination with a computer-generated hologram. The hologram leads to large field angles in certain (measurement) directions. In other words: One achieves a wide-angle long focal length imaging. The wide-angle is necessary to measure the large buildings and the long focal length leads to a large magnification and, therefore, to a good precision.

Both systems achieve fast (80 Hz) operation with low latency in a 24/7 operation scheme. The systems are robust and potentially cheap and can be easily retrofitted to existing buildings.

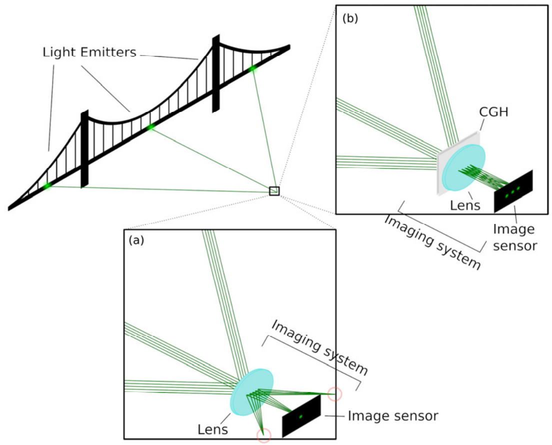

Fig. 1: Holographic wide-angle system.

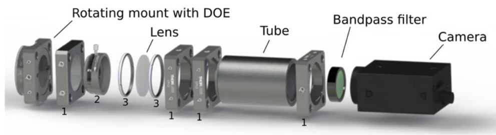

Fig 2.: Optical system for wide-angle measurements.

Supported by: DFG within SFB 1244
In cooperation with: ISYS University of Stuttgart

References:

(1) Guerra, Flavio, Philipp Wilhelm, and Tobias Haist. "Holographic Wide-Angle System for Deformation Measurement of Extended Structures." *Optics* 3.1 (2022): 79-87.

(2) Aslani, V., Guerra, F., Steinitz, A., Wilhelm, P., & Haist, T. (2022). Averaging approaches for highly accurate image-based edge localization. *Optics Continuum*, *1*(4), 834-845.

(3) Hartlieb, S., Schober, C., Haist, T., & Reichelt, S. (2022). Accurate single image depth detection using multiple rotating point spread functions. *Optics Express*, *30*(13), 23035-23049.

High Resolution Metrology and Simulation

ClearView3D – A robust sensor system for autonomous vehicles under harsh environmental conditions

C. M. Bett, M. Daiber-Huppert, K. Frenner, W. Osten

Reliable sensor performance under harsh environmental conditions is one of the main challenges for autonomously driven vehicles. Together with our partners from Fraunhofer Institut für Physikalische Messtechnik (IPM) and Institut für Autonome Intelligente Systeme Universität Freiburg (AIS) we have developed a sensor system that is able to cope with poor visibility conditions (1), see Fig. 1, and shows potential to detect objects reliably in real time (2,3,4). The system consists of a lidar sensor built by IPM (1) and a time-gated sensor from ITO (5). While the Lidar sensor provides a wide field-of-view (FOV) but a low resolution, our sensor can enrich the lidar data with high resolution images albeit at a lower FOV. Both sensors use photon path length differences to discriminate between ballistic object photons and noise photons scattered within the medium.

Within the scope of the project, we analyzed to what extent images of a time-gated camera are compressible and found that compression ratios of one percent or lower are feasible (4,5,6). By directly sensing in a compressed manner with a single-pixel-camera (7), we are thus able to meet the tight eye safety regulations as well as high frame rates necessary for save autonomous driving (5). In the future, we plan to implement a time-gated-single-pixel-camera for autonomous vehicles in the scope of the *innovation campus mobility of the future* and equip it with our direct object detection algorithms developed within the project "Deep Learning based Single Pixel Pose Estimation".

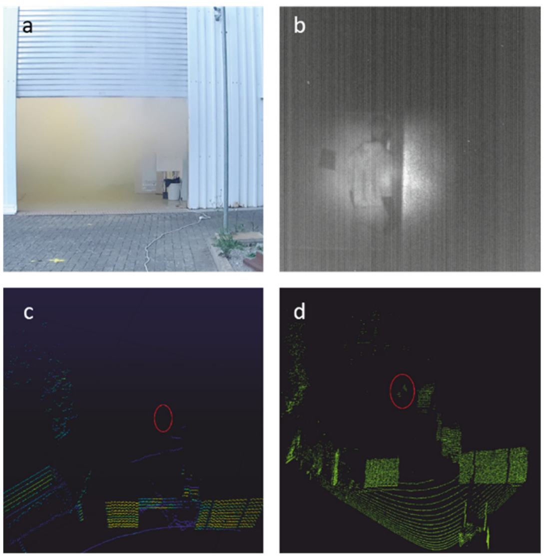

Fig. 1: Comparison of a conventional sensor system with velodyne lidar and camera and our sensor system for measurements within a fog-filled hall: Whereas the camera (a) and the velodyne lidar (c) fail to detect a person standing in thick fog, our time-gated camera (b) and the IPM lidar system (d) can detect it. Figure by V. Vierhub-Lorenz.

Financed by: Baden-Württemberg-Stiftung gGmbH
Project: Laser-basiertes 3D-Sensorsystem für das autonome Fahren unter schwierigen Wetter- und Sichtbedingungen ClearView-3D
In cooperation with: Fraunhofer Institut für Physikalische Messtechnik (IPM) and Institut für Autonome Intelligente Systeme Universität Freiburg (AIS)

References:

(1) V. Vierhub-Lorenz et al., "Development of a LiDAR system for low visibility conditions", Proc. SPIE Optical Measurement Systems for Industrial Inspection XIII 12618, 126181A, 2023.

(2) K. Sirohi et al., "Efficientlps: Efficient lidar panoptic segmentation," IEEE Transactions on Robotics, 38, 3, 2021.

(3) K. Sirohi et al., Uncertainty-aware Panoptic Segmentation. *arXiv preprint arXiv:2206.14554*, 2022.

(4) C.M. Bett, et al., „Towards image-free object detection for autonomous vehicles under harsh environmental conditions", Proc. SPIE Optical Measurement Systems for Industrial Inspection XIII 12618, 126181C, 2023.

(5) C.M. Bett, et al., "Evaluation of a time-gated-single-pixel-camera as a promising sensor for autonomous vehicles in harsh weather conditions," J. Eur. Opt. Society-Rapid Publ. 19(1), 27, 2023.

(6) Bett, C. M., et al., "Time-gated-single-pixel-camera: a promising sensor for robust object detection in adverse weather conditions for autonomously driven vehicles," ICMV2022 12701, 1270107, SPIE, 2023.

(7) M.F. Duarte et al., „Single-pixel imaging via compressive sampling", IEEE Signal Processing Magazine 25(2), 83-91, 2008.

Deep learning based single pixel pose estimation

A. Birk, K. Frenner, W. Osten

With the advent of technical devices that interact increasingly autonomously with their surroundings, the requirements for their optical feature detection increase sharply. Machine Vision (MV) – a technical system's capability to understand properties of its surroundings through optical means – is one of them.

While classic MV schemes rely heavily on processing images captured by conventional cameras, we investigate a different approach. Relying on the principles of Compressed Sensing, we capture and process the optical data in a compressed fashion. By cycling through pixel mask patterns applied to the illumination of a scene and capturing the backscattered light's intensity with a photodiode, we receive a set of intensities. A neural network processes it and directly returns exactly those features of the scene that are relevant to the MV task. The concept is based on the Single Pixel Camera by Duarte et al. (1) and illustrated in Fig. 1. A noteworthy detail is that in this scheme, we skip image reconstruction entirely, making it image free. The latter is in contrast to most established MV schemes and greatly reduces both sensing and processing workload, potentially enabling entirely new areas of application for MV. The use case we focus on is object detection and pose estimation, an MV problem that arises in robot path planning applications.

Work on this project has been underway for a few years already, with the basic principle showing very promising results. Now we expanded the principle with the capability to perform multi-object detection without dynamically increasing the amount of measurements, enhancing the overall usefulness of the approach significantly while keeping the physical detection step itself static in duration and execution (2).

In another work, we investigated how to influence mathematical properties of internal (hidden) data vectors in neural networks through appropriate training strategies, with promising results. We found that it is possible for neural networks to represent images in a compressed fashion such that the adding of two vectors yields a combination of the original images. Applied to the intensity representation in our approach, this enables further advances for iterative reconstruction and sensor fusion.

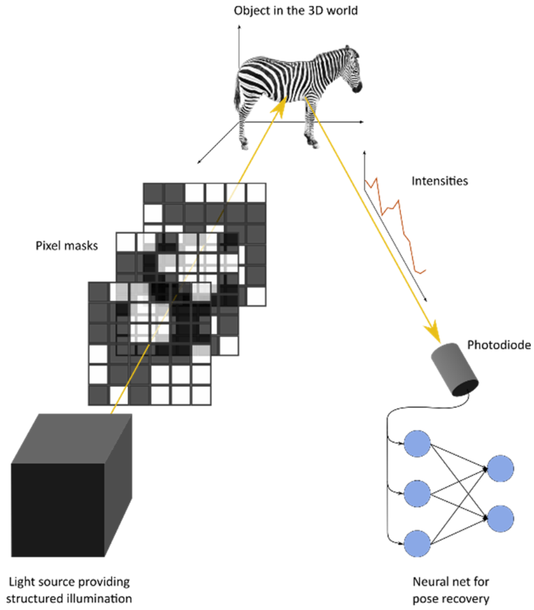

Fig. 1: The sensing principle: Light is modulated with intensity masks and projected onto the scene. Photodiode collects backscattered light. Neural network processes resulting intensities, recovering object information.

Supported by: Landesministerium für Wissenschaft, Forschung und Kunst Baden-Württemberg
Project: Single Pixel Camera with Deep ConvNet Signal Processing for Autonomous Robot Systems (GSaME F2-036)

References:

(1) M. F. Duarte et al., "Single-pixel imaging via compressive sampling", IEEE Signal Processing Magazine, vol. 25, no. 2, pp. 83-91, 2008.
(2) A. Birk, K. Frenner, and W. Osten, "Deep learning based compressed sensing in machine vision: an iterative approach to multi object detection", Fifteenth International Conference on Machine Vision (ICMV 2022), 12701, 2023.

Development of a digital twin for a confocal microscope

A. Birk, L. Fu, K. Frenner, S. Reichelt

Over the years, a multitude of optical devices for the precise measurement of structures on the Micrometer and Nanometer regime have been developed, such as white light interferometers or confocal microscopes. However, our understanding and examination capabilities of their systematic measurement errors and uncertainties is still very limited. Thus, to make full use of these precision devices in the future, it is desirable for users and manufacturers to have a reliable simulation that reflects optical capabilities and limitations of each device. This enables an a-priori calculation of the expected system response to a sample, allowing users to judge error margins and general usefulness of a tool for the current metrology task and increases traceability.

To fill this gap, we are developing a digital twin of a commercial confocal microscope from our project partner TWIP optical solutions GmbH. Our goal is to represent the entire imaging process of the microscope, including illumination, scattering on the sample, and propagation back to the sensor plane, as accurately as possible in a simulation tool chain. Prospectively, this will be evaluated against real-world measurements in cooperation with our project partners at Physikalisch-Technische Bundesanstalt (PTB).

We implemented the light scattering simulation on the sample using various methods. First, we implemented a Rigorous Coupled Wave Analysis (RCWA, Fig. 1a) solution based on our software package MicroSim for cases with 2D structures. We also implemented a method based on the Small Amplitude Perturbation Theory (SAPT) for simplified 3D cases. Finding that this is not precise enough in general 3D cases, we implemented a Boundary Element Method (BEM, Fig. 1b) using our software package SpeckleSim (1). By applying the latest developments and additions to our BEM implementation, such as the Multi-Level Fast Multipole Method (MLFMM), we are now able to compute scattering from comparatively large surface areas of 30 µm by 30 µm.

To simulate the propagation of light through the microscope's optical system, we use a Fourier propagation method where we apply the nominal system's aberrations in the Fourier domain, analogous to the method presented by Pahl et al. in (2).

Supported by: EMPIR European Metrology Programme for Innovation and Research Project: Traceable industrial 3D roughness and dimensional measurement using optical 3D microscopy and optical distance sensors – TracOptic (20IND07)
In cooperation with: Physikalisch-Technische Bundesanstalt (PTB), TWIP optical solutions GmbH

References:

(1) Fu, L., Daiber-Huppert, M., Frenner, K. & Osten, W., "Simulation of realistic speckle fields by using surface integral equation and multi-level fast multipole method", Optics and Lasers in Engineering 162, 107438, 2023.

(2) Pahl, T., Hagemeier, S., Bischoff, J., Manske, E. & Lehmann, P., "Rigorous 3D modeling of confocal microscopy on 2D surface topographies", Measurement Science and Technology 32, 094010, 2021.

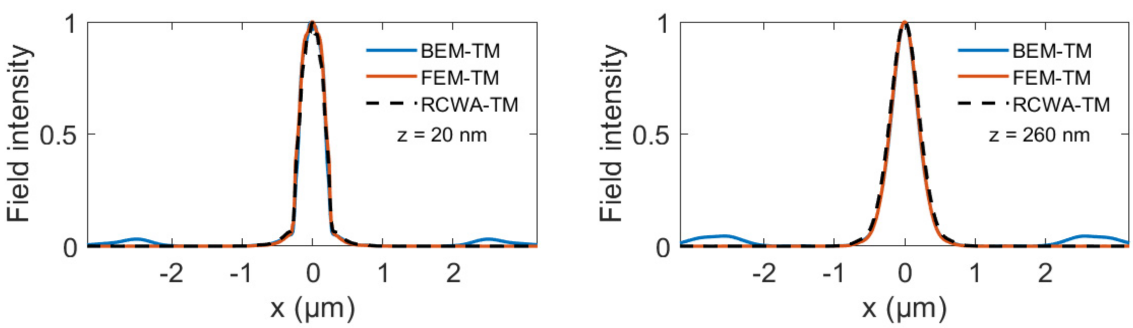

Fig. 1: Comparison between simulation methods: Single grating structure at different distances from the surface.

Multi-spectral attenuated total reflectance measurements

F. Fischer, K. Frenner, A. Herkommer

Infrared spectroscopy based on the principle of attenuated total reflectance (ATR) is a powerful method for analyzing material composition without extensive preparation. It is therefore potentially able to analyze and classify cancerous tissue even in an in-vivo environment. With the recently developed ultra-sparse multi-spectral ATR sensor principle (1), we intentionally acquire minimal spectral data with quantum cascade lasers (QCLs) as high-power illumination sources to streamline analysis and enhance sensitivity. By employing advanced signal processing and machine learning, meaningful spectral and spatial information can be extracted from a sparse dataset. This innovative technique holds the potential to revolutionize molecular analysis across diverse fields.

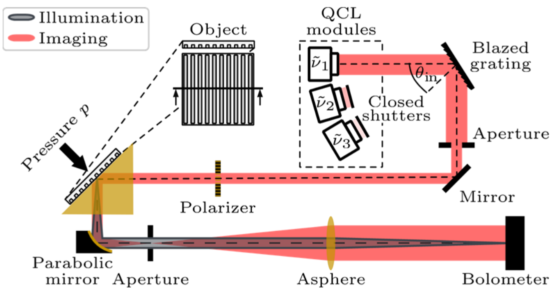

Fig. 1: Concept for a modular multi-spectral ATR sensor using a QCL-illumination. The imaging unit consists of a 4f-telecentric system and a thermoelectric micro-bolometer.

The concept for the laboratory setup used in this project is displayed in Fig. 1. During the measurement, the sample is sequentially illuminated by multiple narrow-bandwidth QCLs. In order to discover the spectral biomarkers with the highest amount of information, we have developed a novel feature selection algorithm embedded inside a classifier model that outperformed existing methods in terms of repeatability of results and discriminative power (2). Furthermore, we have shown that we can still achieve reasonable sensitivity and convincing specificity with ultra-sparse Raman spectra at a compression level of more than 99 % using only five spectral channels for the classification of differently treated bladder cancer organoids (3). Similar observations could also be made in the classification of bladder tissue (1).

Fig. 2 shows the signal of a silicone phantom, which is recorded with the micro-bolometer at the wavelength λ = 9.3 µm.

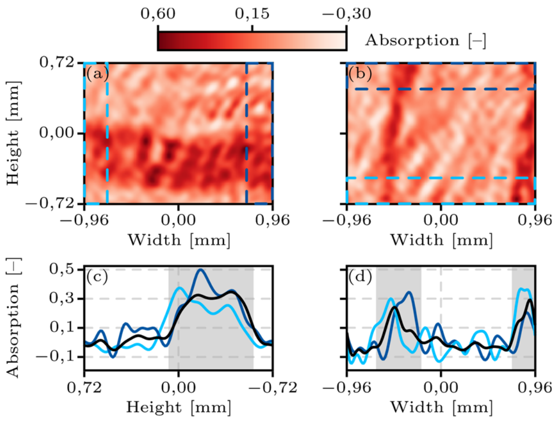

Fig. 2: Absorption measurements of a silicone (PDMS) grating with a period of g = 600 µm horizontally (a) and vertically (b) oriented. The line plots (c) and (d) are their respective mean signals averaged over 20 px (blue lines) and all pixels (black).

The maximum mean absorption coincides with comparative measurements (A_λ = 0.4), which indicates the capability to record spectrally correct images with the proposed ATR sensor in a dry measurement environment. However, this unfortunately does not hold for aqueous environments.

Supported by: DFG German Research Foundation
Project: Graduate School 2543/1 “Intraoperative Multi-Sensory Tissue-Differentiation in Oncology" (Project A2)

References:

(1) Fischer, F., Frenner, K., Herkommer, A., “Sparse Mid-Infrared Spectra Enable Real-time and In-vivo Applications in Tissue Discrimination”, EPJ Web of Conferences 266, 02004, 2022.

(2) Fischer, F. et al., “FeaSel-Net: A Recursive Feature Selection Callback in Neural Networks”, Machine Learning and Knowledge Extraction 4, 968-993, 2022.

(3) Becker, L. et al., “Data-Driven Identification of Biomarkers for In Situ Monitoring of Drug Treatment in Bladder Cancer Organoids”, International Journal of Molecular Sciences 23, 6956, 2022.

Reconstruction of refractive indices using Levenberg-Marquardt algorithm in Fourier scatterometry

L. Fu, K. Frenner, S. Reichelt

Fourier scatterometry is a powerful model-based inspection technique used in semiconductor industry for measuring the geometry of patterned features on wafers. Various methods can be employed to reconstruct the feature parameters, including library search (1), deep-learning (2), or iterative regression techniques (2). The first two methods require a large number of pre-prepared datasets, which is time consuming. In the case of the last method, such as Levenberg-Marquardt algorithm (LMA), parameters that best match the experimental data are iteratively determined through modeling. Our previous studies have demonstrated that the four parameters of a grating, including sidewall angles, top and bottom roundings as illustrated in Fig. 1(a), can be reconstructed with just several iterations by fitting the 0th order pupil image from a Fourier scatterometry setup (2). In this report, we study further the reconstruction of the refractive indices of the SiO_2 layer and the Si grating using the LMA, as these parameters are also dependent on the process and shape. The thickness of the SiO_2 remains at 3 nm.

The grating has a pitch and height of 100 nm and is illuminated by a focused TM-polarized laser beam with a numerical aperture (NA) of 0.7 or 0.95, operating at a wavelength of 405 nm. It is modelled using rigorous coupled wave analysis (RCWA) method and 30 Fourier modes are considered. The pupil image is sampled in the range of [-NA, NA] by equally distanced $N_p \times N_p$ points along the x- and y-directions. The image is subsequently converted into an array y with 709 effective points for N_p equal to 31, assuming an NA of 0.7, for example. A stop criterion of χ^2=10^{-5} is used as in Ref. (2).

We first concentrate on n_{SiO2}, the refractive index of SiO_2, as a single parameter to reconstruct using LMA. The true n_{SiO2} is varied randomly within a range of [1.4, 1.66], which is discretized into 14 steps with each 0.02. Thus n_{SiO2} = 1.4 + 0.02(P-1), where P is an integer varied from 1 to 14. For other parameter reconstructions, we use the same P array. The correlation coefficient R^2 is a convenient way to measure the goodness-of-fit, which is defined as

$$R^2 = 1 - \frac{\sum_{i=1}^{m}\left(y_{true} - y_{fit}\right)^2}{\sum_{i=1}^{m}\left(y_{true} - \bar{y}_{true}\right)^2}.$$

At first no noise is considered. To reconstruct n_{SiO2}, we test 20 fitting procedures using randomly selected true values as shown in Fig. 1(b). This process yields a highly accurate R^2 of 0.9958. Nevertheless, the variation step of 0.02 is relatively large. When a variation step of 0.01 is used, the fitting procedure fails due to the reduced data sensitivity. This outcome can be attributed to the smaller scattering volume of the SiO_2 layer in comparison to the bulk Si grating, due to its thinness and lower refractive index.

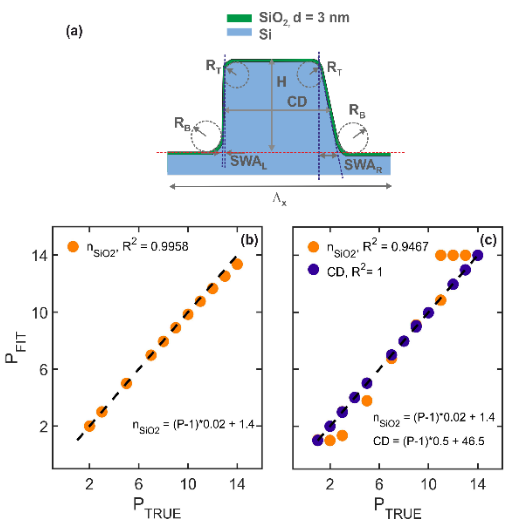

Fig. 1: (a) Schematic of a parameterized Si grating unit cell with a periodicity of Λ_x. Λ_x = H = 100 nm, R_T = R_B = SWA_R = SWA_L = 5 nm. (b) R^2 for the reconstructed refractive index of SiO_2. (c) R^2 for n_{SiO2} and CD when the two parameters are reconstructed simultaneously. For both (b) and (c), NA = 0.7 and N_p = 31.

The reconstruction of n_{SiO2} is further investigated using LMA when a second parameter such as critical dimension (CD) in a variation range of [46.5, 53] in nanometer is incorporated. As shown in Fig. 1(c), R^2 for n_{SiO2}

is reduced largely to 0.9467, although a highly accurate R^2 of 1.0 is obtained for CD. When more parameters such as SWA_R and SWA_L are incorporated into CD and n_{SiO2}, no acceptable R^2 can be obtained. We can thus conclude that the pupil image is insensitive to variation of n_{SiO2}.

We then proceed to investigate the reconstruction of n_{Si} together with CD. Specifically, we vary only its real part, while keep its imaginary part fixed at 0.33. This suffices to provide us a sense of the outcome. The variation ranges for the two parameters are $Re(n_{Si})$ = [5.3245, 5.52] and CD (nm) = [46.5, 53], respectively. Still with N_p = 31, we obtain R^2 of 0.776 for n_{Si} and of 0.9827 for CD, as illustrated in Fig. 2(a). Similar to the case of n_{SiO2}, the fitting quality for n_{Si} is much worse than for CD. To improve the fitting quality, we increase NA to 0.95 and the sampling point N_p is increased to 51. The results are shown in Fig. 2(b), by which R^2 is increased to 0.9814 for n_{Si} and to 0.9975 for CD. We have to emphasize that, increasing N_p and NA does not prove effective in reconstructing n_{SiO2} and CD due to the same issue with the SiO_2 layer.

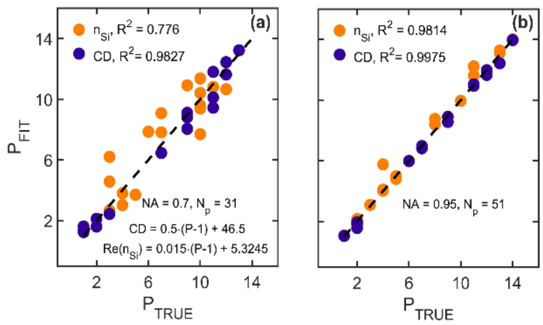

Fig. 2: (a) Correlation coefficient of R^2 for the reconstruction of $Re(n_{Si})$ and CD with NA = 0.7 and N_p = 31. (b) The same test for $Re(n_{Si})$ and CD but with NA = 0.95 and N_p = 51.

In summary, the Levenberg-Marquardt algorithm can effectively reconstruct the refractive index of Si, along with other parameters, by fitting the pupil images from Fourier scatterometry. Applying a larger NA results in an improvement in accuracy, as anticipated. However, reconstructing the refractive index of SiO_2 is less effective due to its smaller scattering volume and lower refractive index. It does not converge anymore when a random noise of 2% is added to the image. It would be interesting to explore how a deep learning network performs in reconstructing n_{SiO2}. Nevertheless, we demonstrate that LMA serves as a rapid and convenient approach for exploring parameter correlations and their sensitivity to variations. This aids in data preparation for deep learning or library search.

Supported by: DFG German Science Foundation
Project: Optische Metrologie und Computational Imaging mittels tiefer neuronaler Netze (FR 3383/2-1)

References:

(1) L. Gödecke, K. Frenner, W. Osten, “Model-based characterisation of complex periodic nanostructures by white-light Mueller-matrix Fourier scatterometry”, Light: Advanced Manufacturing 2, 237-250, 2021.

(2) L. Fu, X. Wang, K. Frenner, S. Reichelt, “Comparative analysis of grating reconstruction: deep learning versus Levenberg-Marquardt methods”, Proc. SPIE 1261907, 2023.

Real-time object detection through deep learning-based multi-sensor collaboration in forklifts

X. Wang, K. Frenner, S. Reichelt

With the rapid advances in machine learning and artificial intelligence, the realization of autonomous driving capabilities has received significant attention in recent years. When compared to conventional driving scenarios, where a car is driving on public roads, autonomous driving functionalities designed for industrial vehicles used in engineering and industrial settings encounter more challenges. These challenges arise from distinct factors, including more dangerous working conditions, three-dimensional movements of the machines, and the detection of specific objects.

In this project, an optoelectronic 3D sensor system supported by a neural convolutional network has been developed, to facilitate the cost-effective realization of autonomous driving functionalities specifically designed for forklifts in warehouse environments. In this sensor system, several sensors will work together, to collect important 3D data from the surroundings. Subsequently, the forklift will give appropriate responses according to the gathered 3D data, particularly when confronted with dangerous situations along its designated driving path.

ITO has worked on this project alongside two other industrial partners, namely tbm hightech control GmbH and Kölbl & Vogl GmbH. The main task of ITO is to train a neural network which can integrate data from diverse sensors and then provide the category and position information of objects detected in the surroundings.

Two different sensors are utilized in this project. One is an RGB camera, which provides conventional RGB images. The other one is a time-of-flight (ToF) camera which can provide 3D information, including coordinates and distance for each individual pixel.

A neural network, based on the 'You Only Look Once' (YOLO) network (1), has been trained to detect specialized objects that frequently appear in a warehouse, using conventional RGB images. Taking advantage of the pixel relationship between the RGB camera and ToF camera, the positions of the detected objects, presented as bounding boxes on conventional RGB images, will be projected onto a depth map obtained from the ToF camera. After some statistical analysis, the pixels belonging to an object are extracted. As illustrated in Fig 1, the left part of the figure shows a conventional RGB image utilized for object detection. The middle part shows the corresponding bounding boxes, transformed from RGB image onto a depth map. The right part shows the pixels belonging to a single object. Finally, the 3D position of the object in the surroundings will be calculated to facilitate the forklift in giving an appropriate response.

Fig. 1: schematic representation of pixel extraction through Neural Network.

To expedite the execution of this neural network, the network has been quantized and adapted to a cost-effective hardware.

Supported by: AiF
Project: NeuroSensor
In cooperation with: tbm hightech control GmbH, Kölbl & Vogl GmbH

References:

(1) Glenn Jocher et al., "ultralytics/yolov5: v7.0 - YOLOv5 SOTA Realtime Instance Segmentation", Zenodo (2022) [doi:10.5281/zenodo.7347926].

Interferometry and Diffractive Optics

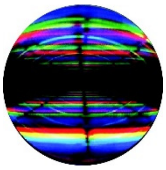

Calibration of unknown interferometer transmission spheres

R. Beißwanger, C. Pruß

Retrace errors are systematic errors that are especially important in non-null interferometric measurements. These errors are introduced by the optical components of the test setup. Their calibration is a non-trivial problem, since they depend on the specimen under test which defines the path that the object wavefront takes on its way to the camera of the interferometer.

In standard null tests, where the beam paths to and from the surface under test are typically the same, retrace errors are not a critical issue. Since the beam paths are identical, the systematic errors are easier to asses, e.g. when testing spherical surfaces with the help of a calibration sphere or using absolute tests like the 3 position Jensen test.

However, modern optical components such as aspheres and freeform surfaces require either null optics that also need to be calibrated or the flexibility of non-null tests. The tilted wave interferometry approach that has been invented at ITO in 2005 (1) and continuously developed since then is a non-null testing method that allows to measure aspheres and freeform surfaces with several hundred micrometers height deviation from their best fitting sphere. A major recent development has been the extension of the TWI principle to a Fizeau type setup (2,3). In this common path setup, the stability is greatly improved, see Fig 1. It relies on a black box calibration to eliminate retrace errors. This approach models the optical path lengths introduced by the optical system in a general, multidimensional polynomial approach. The coefficients of the polynomials are estimated using the nominal optical design of the setup and then adjusted in an iterative approach until the model reproduces the results of the calibration measurements.

We could show that this approach can be used even if the nominal optical design is not available, as is the case for most from-stock optical components. A generic approximation is sufficient as initial guess. The black box model calibration therefore is a generic tool for the calibration of retrace errors in interferometry.

In cooperation with: Mahr GmbH

References:

(1) J. Liesener et al., “Verfahren und Messvorrichtung zur Vermessung einer optisch glatten Oberfläche,” DPMA Patent DE 10 2006 057 606.3 (2006).

(2) R. Beisswanger et. al., „Tilted wave interferometer in common path configuration: challenges and realization” Proc. of SPIE Vol. 110561G.

(3) C. Schober et al., “Tilted Wave Fizeau Interferometer for flexible and robust asphere and freeform testing” [J]. Light: Advanced Manufacturing 3, 48(2022). doi: 10.37188/lam.2022.048.

(4) R. Beisswanger, C. Pruss, and S. Reichelt, "Retrace error calibration for interferometric measurements using an unknown optical system," Opt. Express 31, 27761-27775 (2023).

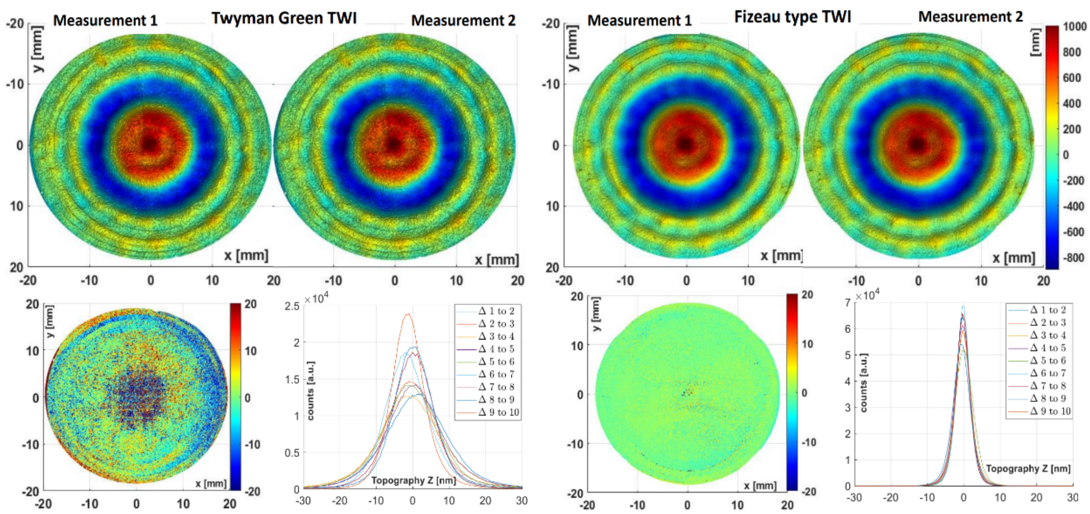

Fig. 1 Reproducibility of a Twyman-Green-TWI (left) vs. Fizeau-TWI (right). The experimental results indicate a noise decrease by a factor of about 3 for the Fizeau-TWI.

Absolute form interferometry for aspheres and freeform surfaces

A. Gronle, R. Beißwanger, C. Schober, C. Pruß, A. Herkommer

In interferometry, absolute length information is usually lost due to the 2π-ambiguity. In this project the aim is to recover this information using a multi wavelength approach. This opens the way to determine the absolute form of the surfaces under test (SUT).

For areal topography measurements of aspheres and freeforms the Tilted Wave Interferometer (TWI) is a flexible instrument. Its main feature is a 2D point source array, illuminating the SUT in four consecutive steps from different directions, compensating the aspheric deviations. The new setup in Fizeau configuration (1) uses standard Fizeau transmission spheres. This makes the setup more stable. For its realization, a new illumination scheme was developed to avoid masking of the reference wave. Interferograms are recorded at four different mask positions. A polynomial black box model of the interferometer serves as mathematical reference for their evaluation.

By using two different wavelengths in the setup, a phase map with a synthetic wavelength can be generated by subtracting the phase maps of the original wavelengths from each other. This synthetic wavelength is much longer than the original wavelengths, so the unambiguity range is extended. For example, if we use λ_1 = 619 nm and λ_2 = 638 nm, a synthetic wavelength of Λ = 21 µm is obtained. This principle is exemplary shown in Fig. 1 for the phase maps of a strong asphere at one mask position of the TWI.

By combining the multi-wavelength approach with the tilted wave interferometer, the position of the SUT relative to its nominal position can be unambiguously determined. Additionally, the mutual offsets of the interferometer patches can be measured rather than estimated, which is the current state of the art approach.

First results from simulations of a highly disturbed asphere show that the inverse problem that is solved to reconstruct the surface topography, converges much better when the patch offsets are known.

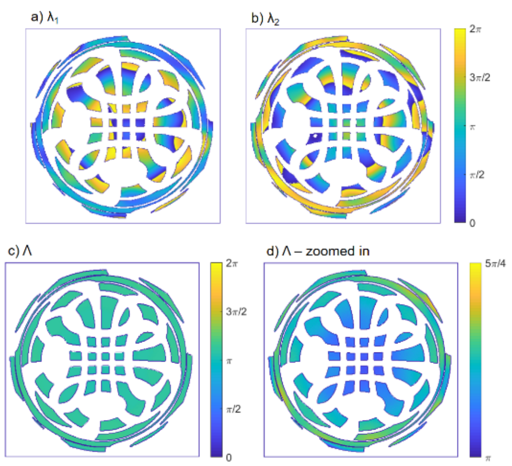

Fig. 1: Phase differences Φ_1 (a) and Φ_2 (b) between measured phase and reference phase at λ_1 and at λ_2, respectively. c), d): The combination of both phase differences ($\Phi_1-\Phi_2$) results in the phase difference between measured phase and reference phase at Λ within one period.

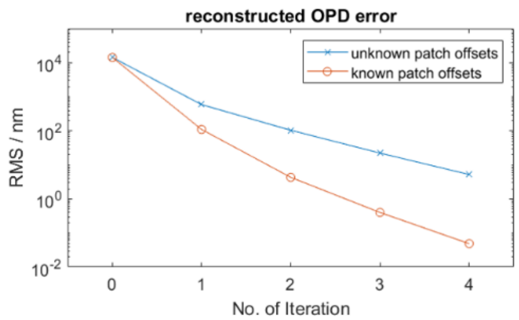

Fig. 2: RMS values of reconstructed OPD errors of a highly disturbed asphere. The convergence is much better if patch offsets are known.

Supported by: DFG German Science Foundation, Project: 496703792
In cooperation with: Physikalisch Technische Bundesanstalt

References:

(1) C. Schober, et al.: Tilted Wave Fizeau Interferometer for flexible and robust asphere and freeform testing, Light Advanced Manufacturing 3, 2022.

(2) I. Fortmeier, et al.: Evaluation of absolute form measurements using a tilted-wave interferometer. Optics Express 24 (2016).

Single-shot tilted wave interferometer

C. Schober, C. Pruß, S. Reichelt

Aspheric and freeform surfaces are important building blocks to reach the requirements of today’s optics products. A key aspect of current research and production of these optical surfaces is the measurement capability. Promising measurement techniques are full-field interferometric measurements. A standard solution for complex shaped surfaces is a compensator or null optics such as a computer-generated hologram. However, this approach is not flexible, since new surfaces require new compensators.

A technique for fast and flexible measurements of such surfaces is the tilted wave interferometer (TWI). It uses a special scheme of off-axis point sources to illuminate the system under test with light waves under different angles to compensate the local deviation from a spherical surface.

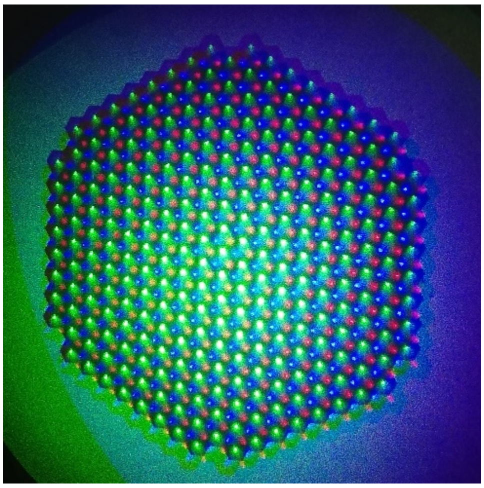

Fig. 1: RGB point sources in hexagonal geometry form the basis for single-shot TWI.

In the current realization of the system, the measurement time is about 30 seconds. In this time, 20 interferograms are captured and subsequently evaluated.

With our research project “Single-shot tilted wave interferometer”, we are bringing this measurement technique into a new measurement time regime.

Using a special sensor that captures the intensity, spectral information and the polarization state of the incident light, it is possible to reduce the entire measurement to a single captured camera image (1), thus reducing the measurement time of the system to the range of < 1 ms.

This will allow new possibilities for the measurement techniques such as high-volume production testing, measuring in unstable, changing environments or ophthalmic measurements.

The first demonstrator setup, uses three lasers, at 633 nm, 532 nm and 459 nm, respectively. It is designed to produce an evenly spaced hexagonal array of point sources, where no pair of neighboring point sources are emitting at the same wavelength. The resulting pattern can be seen in Fig. 1. The design uses multi-order diffractive optical elements and customized microprisms. The design avoids the use of spectral filters. This leads to a high light efficiency of the illumination unit.

Fig. 2: Higher order diffractive microlens array on a 45 mm substrate and aperture array on the backside.

The prototype was fabricated using two-photon grayscale lithography on a Nanoscribe Quantum X system, see Fig. 2. It produces 111 point sources.

Supported by: University of Stuttgart, Wissenstransferförderung

References:

(1) C. Pruss, C. Schober: “Single frame-tilted wave interferometer”, patent WO2022106694A1.

(2) C. Schober, L. Lausmann, K. Treptow, C. Pruss, S. Reichelt: „Neue Designmöglichkeiten durch Zweiphotonenlithographie für ein RGB-Interferometer-Beleuchtungsmodul“, Vortrag A3 auf der 124. Tagung der DGaO, 31.5.2023.

Event-based coherence scanning interferometry: eCSI

C. Schober, C. Pruß

Coherence scanning interferometry (CSI), also known as white light interferometry (WLI) or coherence radar is used for manifold applications in research and industry.

A short coherence light source illuminates an interferometric setup. The interference signals are captured with a camera sensor while the distance between the reference and the object beam path is scanned. The resulting image stack is then evaluated at every pixel to find the *z*-position where the contrast of the interferogram is maximum. This indicates that the optical path length of object and reference path are equal. Each pixel is evaluated individually, yielding a height map of the object as the result of the measurement.

If complex shaped surfaces with large height variations in the field of view are measured, the information density is low since interference contrast occurs only within the coherence length of the light source. The rest of the scan merely captures only constant background intensity. In addition, the scanning speed is limited by the frame capturing rate of the camera.

Our solution to this problem is the use of event-based sensors for capturing the interference signal.

Event-based sensors, also known as dynamic vision sensors, have led to a paradigm shift in visual information processing with digital systems. They are inspired by the principle of the human vision system: they only record changes in the scene. When the intensity at a pixel changes more than a given threshold, an event is issued. Therefore, they provide an asynchronous stream of information *when which* pixel has changed in which *direction*.

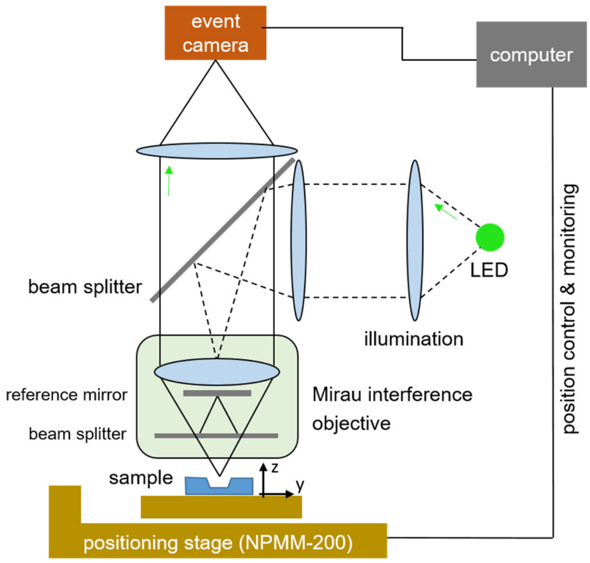

Fig. 1: Optical layout of the eCSI measurement system in combination with the NPMM-200. (1)

We built an interferometric microscope with an event sensor in combination with our nanopositioning and nanomeasuring machine NPMM-200. The optical layout of the system is shown in fig. 1. The event camera used is the SILKYEVCAM from Century Arks using the Prophesee Gen3 event-based image sensor.

Every pixel of the event sensor has a complex electronic realization containing a photodiode, logarithmic amplifiers and comparator. At every pixel the logarithm of the intensity is compared and when the change exceeds a certain threshold an event is generated and referenced with a timestamp with microsecond resolution. Apart from the location of the pixel, the event carries information on the polarity of the signal, i.e. whether the intensity has become brighter or darker. A simulation of event-based coherence scanning interferometry signals in one pixel is shown in fig. 2. Only when the interference fringes are visible in the signal the events are

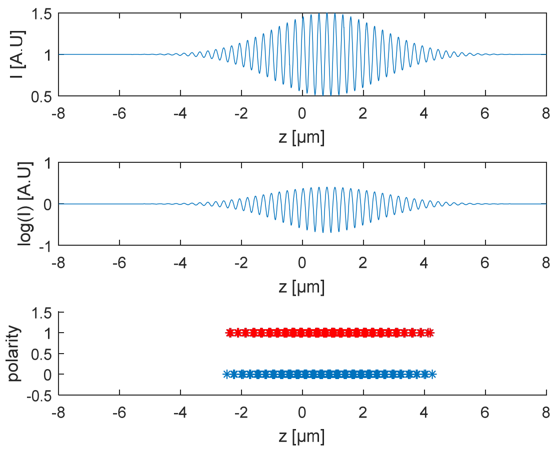

Fig. 2: Simulation of the event-based interference signal generation. It is visible that only in the region of the visible interference fringes event signals are generated. (1)

generated. Outside of the coherence length there is no additional signal generated.

The evaluation of the event stream requires a novel evaluation algorithm. In our new developed algorithm, the changes of the polarity of the registered events of the pixel are evaluated to identify the rising- and falling edges of the interference fringes. From the events next to a change of the polarity the maximum value of the interference fringe is estimated. For estimating the fringe order the center of gravity of all interference fringes is used.

We tested our system and the algorithm on different calibration artefacts on the calibration groove standard Halle LNT4080/30 as shown in fig. 3. The results of the measurement evaluation are shown in figure 4. We measured the 24 µm depth groove of the calibration standard. The evaluated value is 24.017 µm, which is in the center of the provided uncertainty range of 23.96 to 24.08 µm of the calibration standard. The upper and the lower region of the grove are measured with a FWHM of 20 nm.

To demonstrate the data reduction capability of the system, we analyzed the recorded data in comparison to a standard coherence scanning interferometer with a scan step of 50 nm and the same illumination settings. With the eCSI system, it is possible to reduce the recorded data by up to one order of magnitude.

The research was awarded with a UPOB Asphere Metrology Young Scientist Award 2022.

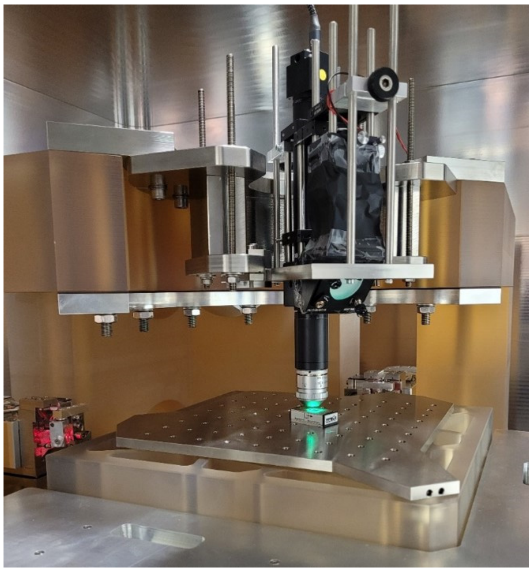

Fig. 3: eCSI system in the NPMM-200, measuring the groove calibration standard.

Supported by: DFG German Science Foundation
Project: 267094782

References:

(1) C Schober, et al., "Event based coherence scanning interferometry," Opt. Lett. 46, 4332-4335 (2021).
(2) C. Schober et al., "Ereignisbasierte Weißlichtinterferometrie (eCSI)" tm - Technisches Messen (2022).
(3) C. Schober, C. Pruss, A. Herkommer, " Integriertes Messkonzept zur Registrierung von Weißlichtinterferometriesignalen für Nanometrologie in großen Messvolumina", Proc. DGaO 122. Tagung, (2021)

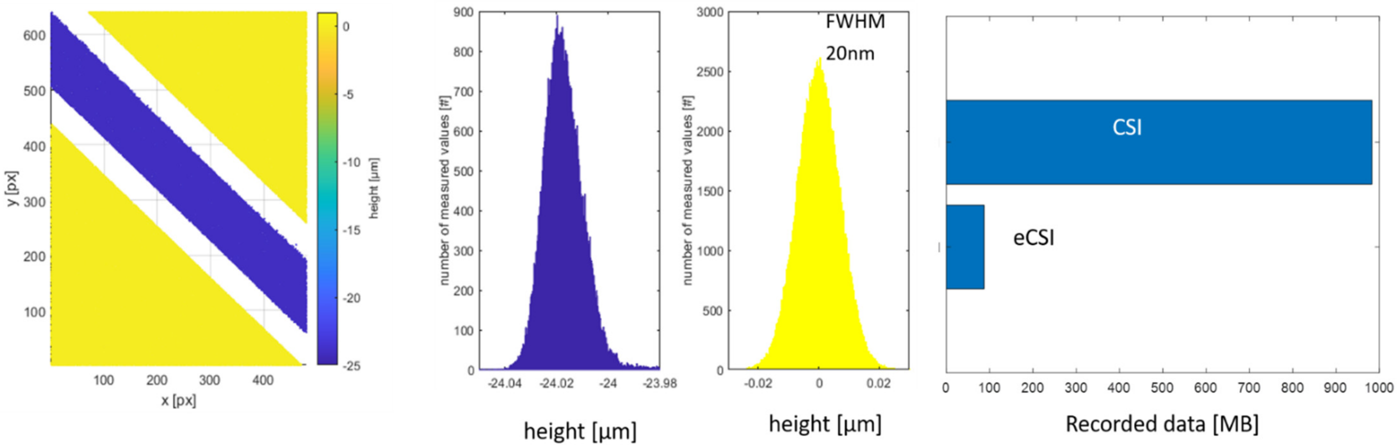

Fig. 4: Measurement result of a 24 µm groove of the Halle depth calibration standard KNT 4080/03. The measured depth is 24.017 µm, well within the provided uncertainty range of 23.96 to 24.08 µm. On the left the measured topography is shown. In the middle histograms for the upper and the lower region of the groove are shown. The FWHM is 20 nm. On the right the recorded data is compared to a measurement with a conventional CSI system. The reduction of the recorded data is about one order of magnitude.

Nanopositioning and nanomeasuring machine NPMM-200

C. Schober, C. Pruß

Nanometer positioning is an important topic in today's research areas. With our nanopositioning and nanomeasuring machine NPMM-200 built by the TU Ilmenau this nanometer precision is possible in a large positioning volume of 200 x 200 x 25 mm^3. Since its installation in 2018, the machine has undergone final testing and is in operation.

The positioning resolution is realized by six interferometers that measure the movement of a mirror-corner like sample carrier. The interferometers are fixed in a measurement frame made of ZERODUR glass ceramic. The measurement frame can accommodate different types of sensors. The easy exchange of the sensors enables a plentitude of possibilities for the use of the machine (1).

To stabilize the measurements against environmental influences of temperature, pressure and humidity, the machine is built in a vacuum chamber and the drives of the machine are temperature controlled with an active cooling system. The opened vacuum chamber is shown in fig. 1.

Fig. 1: The NPMM-200 at ITO. Machine in the opened vacuum chamber for thermal isolation. The measurement frame is made of ZERODUR.

One area of application for the machine is surface metrology. For measuring complex shaped surfaces with interferometric resolution, we built a custom-made white light interferometric measurement head for the use in the machine (2). It is designed for thermal stability using a system construction made of invar alloy (3). The light source has a central wavelength of 532 nm. The objective is a 20x0.4 Mirau interference objective. An image of the experimental realization of the sensor in the metrological frame of the machine is shown in fig. 2.

To measure large surfaces or areas, multiple subaperture measurements must be combined. In one subaperture measurement a *z*-scan is made with the axis of the machine. This results in an enormous scanning range of 25 mm, unlike conventional white light interferometer profilers that use piezo drives for scanning. The gathered data is analyzed using a lock-in phase evaluation method (4).

For the combination of different subaperture measurements, the lateral magnification and the orientation between the axis of the NPMM and the measurement head have to be calibrated. This is done by measuring a calibration target at different positions in one field of view. The rotation of the camera coordinate system to the axis of the NPMM is evaluated to 13.69±0.0049° and the lateral magnification factor of the camera is 401.28±0.04 nm / pixel.

With this measurement head, we measured a freeform surface and an aspheric surface with additional etched steps (5). The diameter of the surfaces was 50 mm. The samples are shown in fig. 3.

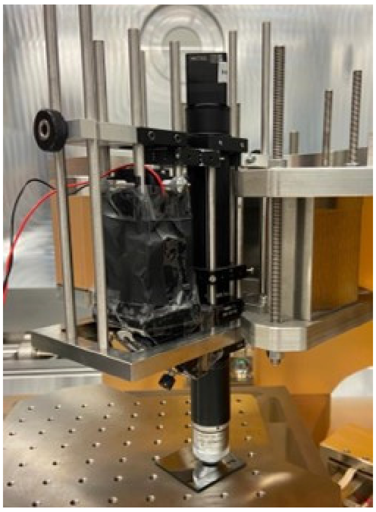

Fig. 2: Custom built white light interferometric measurement head in the NPMM-200.

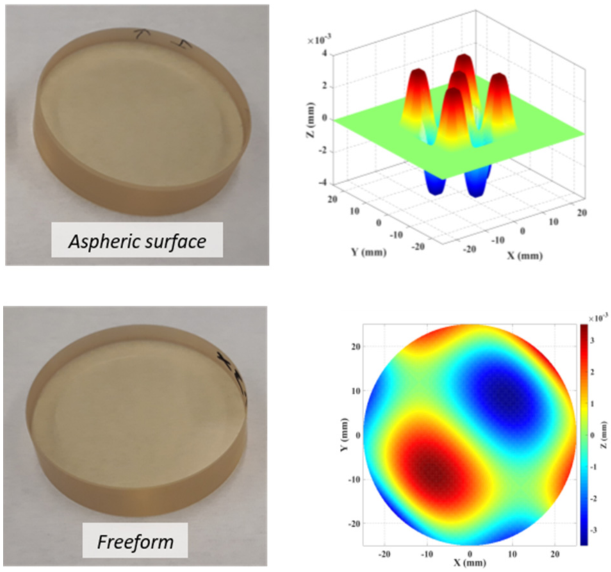

Fig. 3: The aspheric and the freeform surface measured with the NPMM-200 WLI. The surfaces are made of ZERODUR (5). The nominal design is shown on the right.

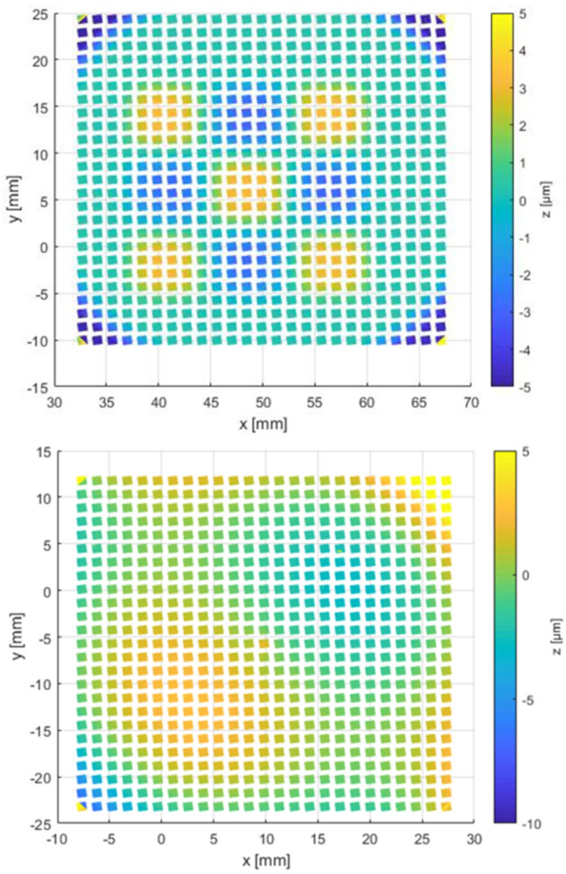

Fig. 4: Measurement results of the aspheric (top) and the freeform surface (bottom). 25 x 25 sub apertures. The measurements contain 2.6 billion data points. (3)

Each measurement consists of 25 x 25 subapertures that were performed on a rectangular grid on the surface. The stability of the metrological concept allows to measure the surface without the need for stitching and measurement with overlap of the subapertures.

The measurement results are shown in fig. 4. Each measurement consists of 2.621.440.000 measurement points. The steps in the aspheric surface are clearly visible. The measurements demonstrate the capability of large aperture measurements with high point density.

Supported by: DFG German Science Foundation
Project: 267094782

References:

(1) W. Osten, E. Manske, T. Haist, “How to drive optical measurement systems to outstanding performance”, Proc. SPIE 10557, (2018).

(2) C. Schober, C. Pruss, A. Herkommer, “Sensordesign für die NPMM-200 am Beispiel eines Weisslichtsensors“, Proc. DGaO 121. Tagung P3, (2020).

(3) C. Schober, C. Pruss, A. Herkommer, “Integriertes Messkonzept zur Registrierung von Weißlichtinterferometriesignalen für Nanometrologie in großen Messvolumina“, Proc. DGaO 122. Tagung, (2021).

(4) M. Fleischer, “Fast algorithm for data reduction in modern optical three-dimensional profile measurement systems with MMX technology,” Appl. Opt. 39,1290-1297 (2000).

(5) Y. Arezki, C. Schober, C. Pruss, et. al., “Traceable Reference Full Metrology Chain for Innovative Aspheric and Freeform Optical Surfaces Accurate at the Nanometer Level”, Sensors, (2021).

Fabrication of diffractive elements

K. Treptow, C. Pruß, T. Schoder, S. Reichelt

Diffractive optical elements (DOE) are valuable tools in optical design and for metrology applications. Typically, they are thin phase modulating structures with smallest dimensions in the (sub-) micrometer range, that operate by means of interference and diffraction. This is why their functionality differs from that of refractive optical elements.

At ITO we operate a clean room with the relevant fabrication equipment and metrology devices to produce a wide variety of diffractive elements. The DOE fabrication is mainly based on laser direct writing at 405 nm wavelength on specialized equipment, capable of processing also large precision substrates with a thickness of up to 20 mm and a diameter of 200 mm. The circular laser writing systems (CLWS) produce high-resolution binary and gray-scale structures in polar coordinates (1), comparable to a DVD writer. All process steps are controlled by adequate measurement systems including AFM, SEM, confocal and white light microscopy – an absolute necessity for the fabrication optimization.

Structures are directly written into photoresist to obtain binary or continuous structures. If required, the resulting microstructures can be transferred into the substrate using a dry etching process (reactive ion etching RIE using fluorine-based chemistry, typically into fused silica substrates, but also high-index dielectric layers). Alternatively, binary structures with high aspect ratio can be realized using a chromium layer as hard mask in the RIE process. The chromium layer is structured either with a thermochemical process or with a photoresist process, both followed by wet-chemical chrome etching.

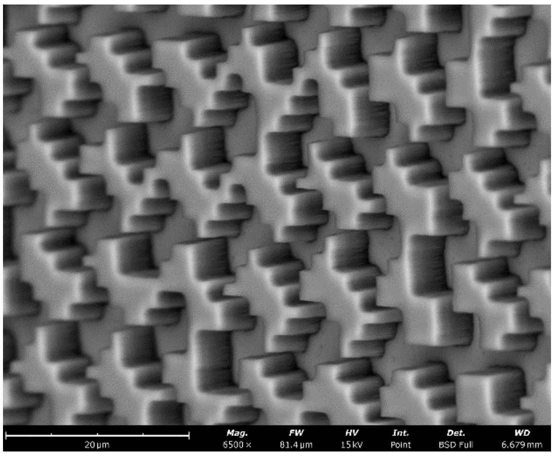

Fig. 1: SEM measurement of an achromatic CTIS element with a depth of 5 µm. The binary structure was etched against a microstructured chromium layer in fused silica.

There are numerous designs and applications for diffractive elements:

For CTIS (computed tomography imaging spectroscopy) we developed a new process chain for a multi-material prototype element. Binary structures in fused silica generated with an RIE process using a chromium hard mask were refilled with photoresist to create an achromatization effect. This design increases the diffraction efficiency for CTIS applications (Fig. 1).

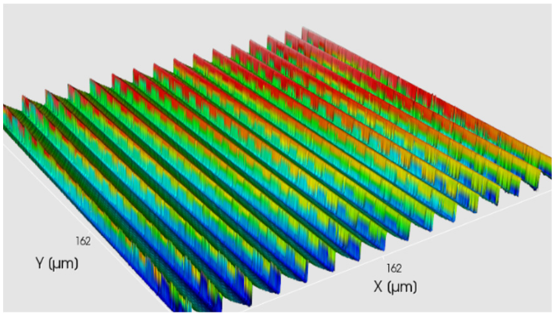

Fig. 2: Surface of a blazed mirror with a depth of 6 µm, measured with a confocal microscope.

Fig. 2 shows part of a blazed mirror structure that allows to obey the Scheimpflug principle in an optical metrology system. The blazed grating structures with a height of 6 µm and a period of 15 µm cover an area of 45x35 mm^2. They were fabricated on the CLWS using a gray scale photoresist process followed by a chromium sputter coating process to increase reflectivity.

Relatively large computer-generated holograms can be fabricated for large beam diameter setups. The element in Fig. 3 is a

90x90 mm^2 diffractive element used to generate multipoint patterns (3).

It is possible to implement multiple optical functionalities when designing a computer-generated hologram (2). Fig. 4 shows an element that combines two tasks: It replicates a single object point to a predefined pattern of several spots in the image plane and adds a vortex point spread function (PSF).

Not only diffractive optics can be manufactured with the CLWS and RIE. A benchmark structure with different layers was fabricated for comparison measurements. The element in Fig. 5 consists of different arrangements of glass substrate, photoresist, a chromium layer and gratings with varying depth and width in the micrometer range used to benchmark optical metrology devices such as white light interferometers.

Fig. 3: Large DOE with a footprint of 90x90mm^2. The element is illuminated across its entire surface to generate multipoint images.

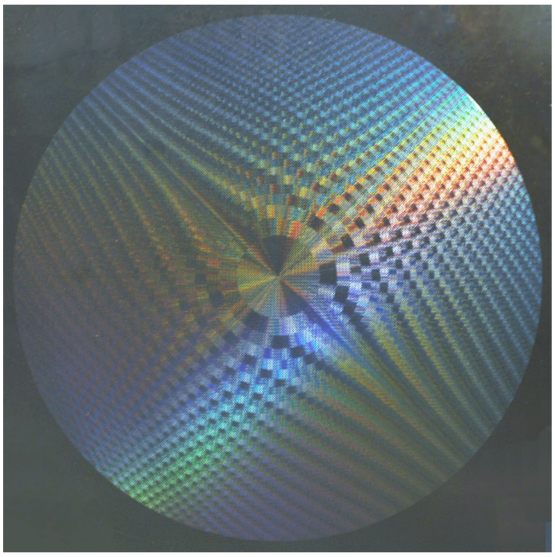

Fig. 4: DOE with combined tasks: replication of a single object point to a predefined pattern of several spots in the image plane and adding a vortex point spread function (PSF).

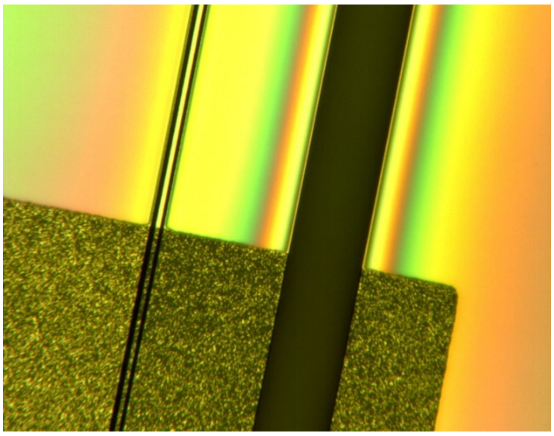

Fig. 5: Benchmark element with different arranged layer stacks, consists of glass substrate, photoresist and chromium layer.

References:

(1) Poleshchuk AG, Churin EG, Koronkevich VP, Korolkov VP, Kharissov AA, Cherkashin VV, Kiryanov VP, Kiryanov AV, Kokarev SA, Verhoglyad AG. Polar coordinate laser pattern generator for fabrication of diffractive optical elements with arbitrary structure. Appl Opt. 1999 Mar 10;38(8):1295-301. doi: 10.1364/ao.38.001295. PMID: 18305745.

(2) Simon Hartlieb, Christian Schober, Tobias Haist, and Stephan Reichelt, "Accurate single image depth detection using multiple rotating point spread functions," Opt. Express 30, 23035-23049 (2022).

(3) S. Hartlieb, M. Boguslawski, T. Haist, and S. Reichelt, „Holographical image based vibrometry with monochromatic and event based cameras“, in Optics and Photonics for Advanced Dimensional Metrology II, P. J. de Groot, R. K. Leach, and P. Picart, Hrsg., in Optics and Photonics for Advanced Dimensional Metrology II, vol. 12137. SPIE, 2022, S. 1213702.

Grating reflectors enabled laser applications and training

A. Savchenko, D. Bashir (IFSW), D. Didychenko (IFSW), C. Pruß

The international training network ITN GREAT is organized by a consortium of 16 renowned scientific institutions, academic partner organizations, as well as private sector partners from 4 countries: Germany, France Finland and the United Kingdom. Within this project 15 Early Stage Researchers (ESR) allocated in different institutions are working on the design, fabrication and implementation of Grating Waveguide Structures (GWS) in high power laser systems.

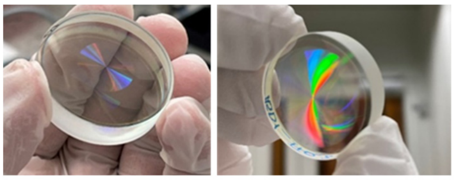

Fig. 1: Photo of the GWOC (left) and GWM (right).

GWS consist of a planar waveguide and a grating structure. A resonance effect can be observed in GWS under certain illumination conditions resulting in a high-finesse peak in reflection or transmission [1]. GWS with circular grating lines provide a solution for the generation of laser beams with axially-symmetric polarization directly out of the laser cavity [2].

We have developed a fabrication process tailored for circular GWS. It involves patterning of a substrate by our SBIL (Scanning Beam Interference Lithography) setup with a subsequent ICP (Inductively Coupled Plasma) etching step. Based on designs provided by IFSW (Institut für Strahlwerkzeuge) we successfully fabricated circular GWS of two different types.

The first is a grating waveguide output coupler (GWOC) that is designed as the output coupling mirror in a thin disk high power laser resonator. It has a shallow circular sub-micron diffraction grating etched directly into a fused silica substrate. This grating is then overcoated with a Nb_2O_5/SiO_2 multilayer coating sequence. A photo of one of the samples is shown in Fig.1. Results of reflectivity measurements and the corresponding design values made by IFSW are presented in Fig. 2.

The second type of GWS are grating waveguide mirrors (GWM) that are used as high-reflective end mirror in a thin disk laser cavity. They feature YAG substrates with Nb_2O_5/SiO_2 multilayer coating sequence and a sub-micron circular diffraction grating etched into the last high refractive index layer. A photo of one of the samples is shown in Fig. 1 on the right. Reflectivity measurements of the GWM can be seen in Fig. 3. For both GWOC and GWM measured reflectivity spectra are in good agreement with the simulation results. The samples were tested in the laser cavity and have shown promising results. Based on these results, a second generation of GWOCs and GWMs is planned with improved design and a further optimized fabrication process.

Supported by: European Union's Horizon 2020 research and innovation programme under the Marie Skłodowska-Curie grant agreement No 813159.
Project: ITN GREAT
In cooperation with: 15 academic and scientific partners from France, United Kingdom, Finland and Germany.

References:

(1) D. Rosenblatt, et al., "Resonant Grating Waveguide Structures", IEEE Journal of Quantum Electronics, vol. 33, no. 11, pp. 2038-2059 (1997).
(2) M. Abdou Ahmed, et al., "High-power thin-disk lasers emitting beams with axially-symmetric polarizations", *Nanophotonics* 11, no. 4, pp. 835-846 (2022).

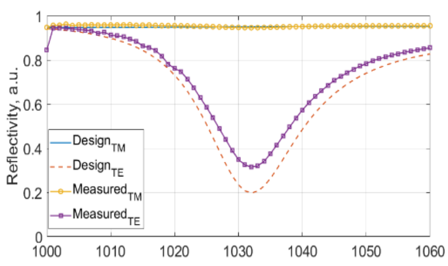

Fig. 2: Reflectivity of the fabricated GWOC.

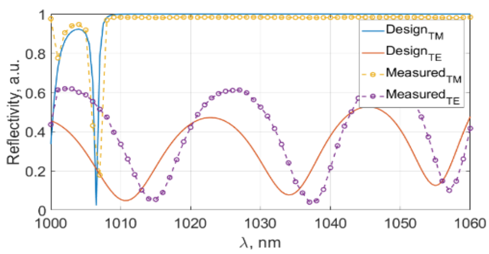

Fig. 3: Reflectivity of the fabricated GWM.

Three-dimensional scanning beam interference lithography

K. Treptow, C. Schober, C. Pruß, T. Haist, S. Reichelt

In the field of micro structuring glass surfaces, laser lithography is a proven means to fabricate almost arbitrary microstructures with high resolution. When large areas need to be structured, the writing time can take days. Also, typical lithography systems are limited to flat substrates. Within the new DFG project “3D-SBIL”, we are investigating methods that allow us to push the limits towards efficient parallel structuring of grating-like structures on 3D surfaces. The approach chosen in the project is scanning interference lithography (SBIL), a method that was first used for the efficient generation of large linear gratings on flat surfaces (1). The joint project goal is to extend this efficient method into 3D space while maintaining high positioning accuracy for the generated structures. Three partners join their expertise. The Institute of System Dynamics at the University of Stuttgart covers the control theory aspects and the Institute of Process Measurements and Sensor Technology at the TU Ilmenau investigates machine-concept and uncertainty aspects. The research at our institute covers the lithography aspects including referencing to already written structures and the integration of the results into a demonstrator system based on the nanopositioning and –measuring machine (NPMM-200) at ITO.

The demonstrator aims towards the following requirements:

The new system should structure gratings with variable periods between 300 nm and 1 µm on substrates with surface gradients up to 5°. In addition, the orientation of the grating lines can change during the patterning process. The maximum patterning speed should be 30 mm/s and the positioning accuracy of the grating lines targets below 10 nm.

For precise positioning, the nano positioning and metrology machine NPMM-200 (2) scans the substrate relative to the lithography head. In the quasi-static mode, it is possible to move the substrate with sub-nanometer precision with this machine. However, the high multi-axis dynamics combined with highest precision trajectories require new approaches for the control strategy.

With scanning beam interference lithography, it is possible to generate subwavelength periods and increase the patterning speed. Two laser beams overlap on the substrate surface and an interference pattern is created. The period depends on the angle of incidence between the two beams. Therefore, the movement of the interfering laser beams must be tracked and controlled during the process to minimize positioning errors.

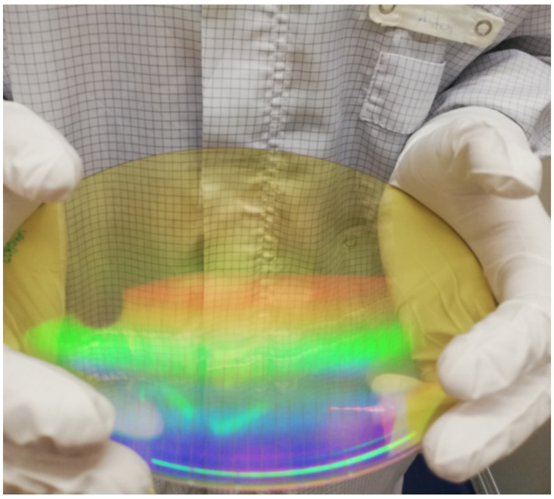

Fig. 1: Example of a linear grating pattern, manufactured by standard interference.

Project: DFG-Project 3D-SBIL 465642714

References:

(1) C. G. Chen and M. L. Schattenburg, „A brief history of gratings and the making of the MIT nanoruler,“ Space Nanotechnology Laboratory, MIT, Bd. 22, 2004.

(2) E. Manske, G. Jäger, T. Hausotte, A. Müller and F. Balzer: Nanopositioning and Nanomeasuring Machine NPMM-200 – sub-nanometre resolution and highest accuracy in extended macroscopic working areas; euspen’s 17th International Conference & Exhibition, Hannover, DE, May 2017.

Multipoint sensor system to enhance robot control

B. Bertschinger

In research, development and manufacturing of new innovative products versatile and highly flexible systems are required to reduce economical risks. Using high-precision optical measuring technologies and corresponding control systems, simple robot kinematics can become a universal tool for developers.

For this purpose, a real-time optical measuring method was implemented to accurately determine the dynamic and stationary positions of two robot arms. The measuring system has a high measuring accuracy of 5-10 µm, a fast measuring speed of 100 fps and a large measuring volume of up to (1000 x 1000 x 1000) mm³. It allows to create an accuracy map of the robot kinematics, which in turn will be used for software-driven configuration and path planning. Henceforth the trajectories of two cooperating robots are designed in such a way, that the resulting measurement and production volume represents an optimal solution for the required precision (1).

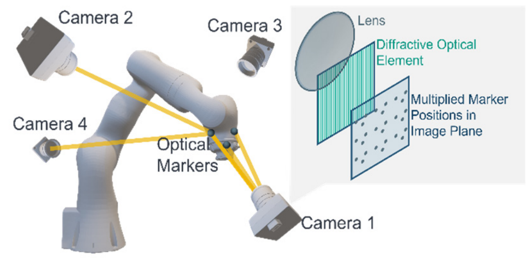

Fig. 1: Determination of the origin of two pixels in a stereoscopic measurement method using triangulation.

The measurement principle is based on holographic multi-point sensors. A diffractive optical element (DOE) in front of the sensor lens generates copies or diffraction orders from the imaged point.

These additional image points are arranged in a specific pattern, the so-called cluster. Their mutual distance depends on the properties of the diffractive optical element. The individual centers of gravity of these points are determined and averaged to obtain position information of the imaged point (2).

This requires a coarse detection of the cluster position. This can either be realized via the robot axis position or extrapolation from previous sensor states. Unfortunately, these approaches have shown to be error-prone. Instead a new approach was chosen on the basis of pyramid scaling (3). Here the cluster image is scaled such that the single points are merged into one, which can be detected via simple thresholding.

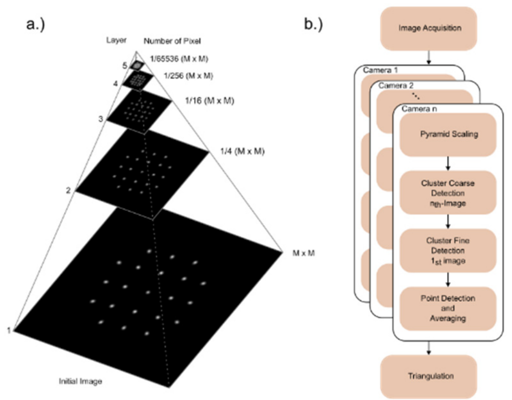

Fig. 2: a.) Scaling of a multipoint-cluster image via pyramid scaling b.) Image processing for multipoint detection with cluster coarse detection based on pyramid scaling.

These algorithms were implemented both on Graphic-Processing-Unit (GPU) and Central-Processing-Unit (CPU) and compared in terms of runtime. It was found that the use of both computational methods is highly situation-dependent. For regular use cases, a CPU-based implementation is usually sufficient.

Supported by: InnovationsCampus Mobilität der Zukunft (ICM)
Project: SDManu3 – Softwaredefinierte Präzision für hochflexible Roboterkinematiken

References:

(1) J. Baumgärtner, P. Gönnheimer, et al., “Optimal Robot Workpiece Placement for Maximized Repeatability”, Lecture Notes in Networks and Systems Vol. 546, 2022.

(2) S. Hartlieb, M. Tscherpel, F. Guerra, T. Haist, W. Osten. et al., “Remote Laboratories for Optical Metrology: From the Lab to the Cloud”, Optical Engineering, 52 (10) 101914, 2013.

(3) E.H. Adelson, et al., “Pyramid Methods in Image Processing”, RCA Engineer, Vol. 29, No. 6, p. 33.

Coherent Metrology

Holographic imaging through fog

A. Gröger, G. Pedrini

Digital holography benefits from interferometric amplification, which enhances sensitivity. Coherence-gated digital holography allows the suppression of noise sources such as multiple scattered photons and ambient light. In addition, digital holography provides access to optical phase information, which is an important metrological parameter for three-dimensional measurements.

The aim of this study is to investigate the potential of digital holography as a new sensor concept for the environmental perception of autonomous vehicles under difficult visibility conditions. Our experiments are conducted using a 27-meter-long fog tube and serve in particular to characterize the capacity to amplify ballistic photons and effectively discard multiple scattered photons based on their coherence property.

We use an off-axis holographic setup in image-plane configuration as illustrated in Fig.1. Light emitted from a pulsed Nd:YAG laser (SpitLight 600, Innolas) is divided into reference and object beam. The object beam is diverged by the lens L1 to produce a large illumination cone. The test object is positioned at the end of a tube filled with ultrasonically generated fog. The one-way distance through the fog is 27 meters. The reference beam is coupled into a single mode fiber and emitted at the pupil plane of the imaging lens L2. The optical path lengths in object and reference beams are matched. We use a gated InGaAs camera (WiDy Sens 640V-STP, NIT Vision) with a resolution of 640 by 512 pixels. Using an electronically controlled mechanical shutter in the reference beam path, we are able to switch between holographic and conventional imaging. By on-the-fly configuration of the camera, we can activate and deactivate the gated mode. In combination, the measurement setup can be switched between time-of-flight mode with 100 ns gate, gated holographic mode, holographic mode and conventional mode. Switching between modes is fully automated and takes less than a second. From the comparison of different imaging techniques, we are able to quantify the advantages of holographic imaging. Fig. 2 shows experimental results of the central letters on a car license plate obscured by fog in a distance of approximately 30 meters from the detector.

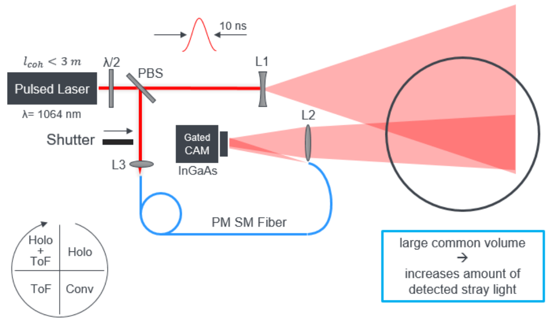

Fig.1: Experimental setup used to record image-plane holograms in off-axis configuration.

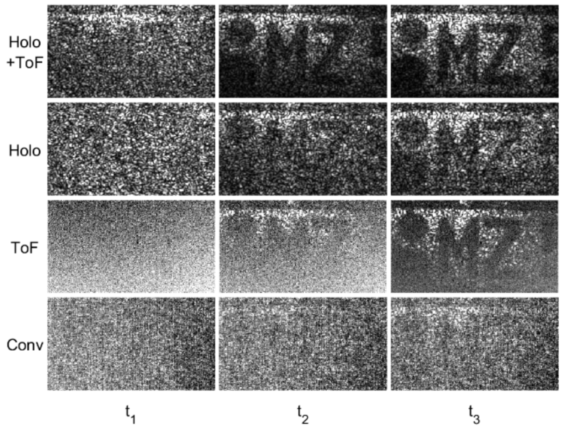

Fig. 2: Comparison of gated-holographic, holographic, gated and conventional imaging of a car license plate at decreasing fog densities (t1 to t3).

With the incorporation of a second wavelength, we are able to perform synthetic phase imaging to detect objects through extended bodies of fog.

Supported by: Baden-Württemberg Stiftung gGmbH.

References:

(1) A. Gröger, G. Pedrini, D. Claus, I. Alekseenko, F. Gloeckler, S. Reichelt, "Advantages of holographic imaging through fog," Appl. Opt. **62**, D68-D76 (2023).

(2) A. Gröger, G. Pedrini, F. Fischer, D. Claus, I. Aleksenko, S. Reichelt "Two-wavelength digital holography through fog" J. Eur. Opt. Society-Rapid Publ. 19 (1) 25 (2023) DOI: 10.1051/jeos/202.

Ultra-thin two-wavelength digital holographic endoscopy

A. Gröger, G. Pedrini

Holographic endoscopy represents a groundbreaking advancement in industrial and medical imaging. By employing coherent light and sophisticated recording systems, holographic imaging provides access to the optical amplitude and phase information. Utilizing the principles of digital holography, this technology offers high-resolution, three-dimensional visualizations of mechanical components or internal organs and tissues.

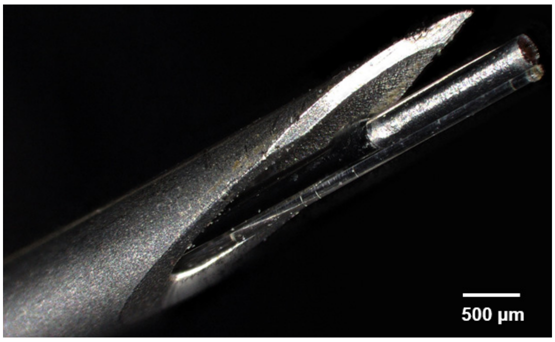

Fig. 1: Ultra-thin holographic endoscope (~400 µm diameter) inside a syringe needle and the section view of optical elements inside the endoscope head.

Coherent fiber bundles (CFBs) with their small diameter (less than 300 microns) and 10^3 to 10^4 individual cores pave the way towards ultra-thin holographic endoscopes. Fig. 1 shows an image of a prototype endoscope consisting of a multicore fiber and a single-mode fiber. We use two-photon-polymerization to print micro optics directly onto the multicore fiber and the illumination fiber.

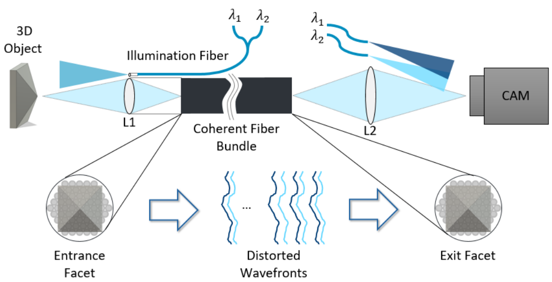

Fig. 2: Concept of experimental setup, the wavelength is provided using two tunable lasers at 780 nm ($\Delta\lambda \approx$ 300 pm)

In general, holographic imaging through multicore fibers suffers from random phase distortions introduced by the light transport through the individual fiber cores. For small wavelength differences however, spectral correlations in the wave front distortions can be exploited to perform synthetic phase imaging using two-wavelength digital holography. Fig. 2 illustrates the experimental setup. We use an off-axis holographic setup and two lasers at 780 nm with a wavelength difference of approximately 300pm to perform single-shot 3D shape measurement.

Both holograms are recorded simultaneously in one frame. The modulated object spectra for both wavelengths appear at different locations in the Fourier plane. Fig. 3 illustrates the signal processing steps to compute the surface geometry.

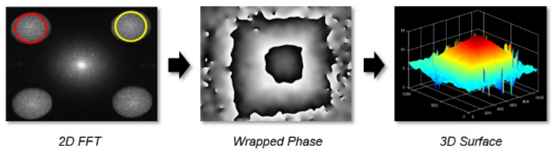

Fig. 3: Signal processing to compute the 3D surface of a test object

The reconstructed complex optical wave fields are computationally mixed, resulting in a synthetic wave probing the object. The wrapped phase signal of the synthetic wave contains the 3D shape information of the object. A promising deep learning approach for real-time phase unwrapping is currently under development.

References:

(1) A. Gröger, G. Pedrini, D. Claus, F. Fischer, S. Reichelt, S. Thiele, N. Fahrbach, "World's smallest single-shot two-wavelength holographic endoscope for 3D surface measurement," Proc. SPIE PC12356, Endoscopic Microscopy XVIII, PC123560P (17 March 2023); https://doi.org/10.1117/12.2662817

(2) A. Stickel, "Ultradünne holografische Endoskopie", Studienarbeit Master Medizintechnik.

(3) C. Ai, „Two Wavelength Digital Holography for the Investigation of Biological Tissue", Masterarbeit Medizintechnik.

(4) V. Vasileva, "Phase Unwrapping mittels Deep Learning für ultradünne zweiwellenlängen-holographische Endoskopie", Masterarbeit Medizintechnik.

(5) Sdougkou Marina, „Speckle decorrelation in holographic imaging through congruent fiber bundles", Studienarbeit Master Medizintechnik.

Lensless microscopy by multiplane recordings

E. Istrate, G. Pedrini, S. Reichelt

Lensless microscopy is attractive because lenses are often large, heavy and expensive. We report diffraction-limited, sub-micrometer resolution in a lensless imaging system. The experimental setup is shown in Fig. 1. We use measurements of the intensity of light scattered by the sample at multiple heights above the sample and a modified Gerchberg-Saxton algorithm to reconstruct the phase of the optical field. We introduce a pixel-splitting algorithm that increases resolution beyond the size of the sensor pixels, and implement high-dynamic-range measurements. The resolution depends on the numerical aperture of the first measurement height only, while the field of view (FOV) is limited by the last measurement height only. As a result, resolution and field of view can be controlled independently.

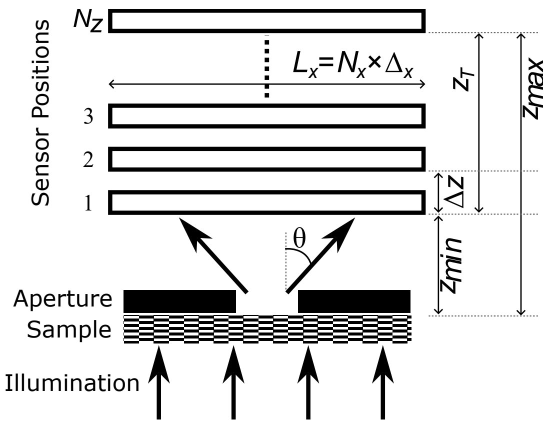

Fig. 1: Simplified experimental setup. Light is scattered by the sample and a portion passes through the aperture, after which it is measured by the movable sensor at N_z positions. z_{min}, z_{max}, z_T, Δz are respectively the minimum sample-sensor distance, the maximum distance, the total sensor travel distance and the distance between measurement planes. L_x, N_x, Δx are respectively the size of sensor, number of pixels and pixel size in x direction. (L_y, N_y, Δy, not shown, are defined similarly.) θ is the maximum angle of scattered rays that are captured

Fig. 2 shows the reconstruction of USAF 1951 target. Laser light of 633 nm is used in the experiment. A 220 µm diameter round aperture is placed above the target, to limit the FOV. We use $N_z = 26$ planes, separated by 100 µm. $N_x = N_y = 2048$ pixels. The closest and farthest planes are at z_{min} = 1.4 mm and z_{max} = 3.9 mm from the target. Group 9, Element 3 is resolved, with 0.78 µm features. We note that this is only slightly larger than the wavelength of 633 nm.

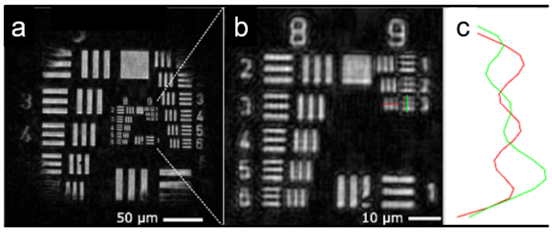

Fig. 2: Lensless reconstruction of USAF 1951 target. Entire aperture of 220 µm (a). Details (b). Amplitude profiles at the resolution limit (c), red lines show horizontal resolution, at the locations marked with red bars in (b), green lines show vertical resolution, at the green bars in (b).

The system also allows imaging with light of low spatial coherence. Using illumination from three LEDs, we produce full-color images of biological samples (see Fig. 3).

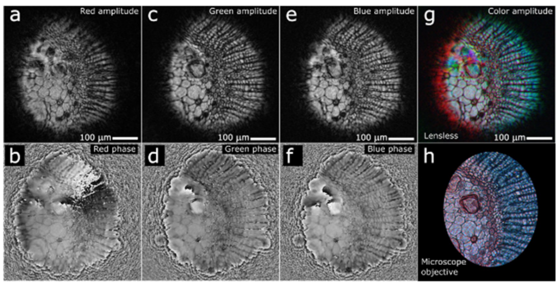

Fig. 3: Image of a biological sample (cross-section through a branch of wood). a,c,e: Amplitude reconstructions with red, green, blue light. b,d,f: Phase reconstructions with red, green, blue light. g: Full-color reconstruction combining information from a,c,e. h: Image of the same area of the sample using a microscope objective, for comparison.

References:

(1) E. Istrate, G. Pedrini, S. Reichelt, "Lensless microscopy by multiplane recordings: sub-micrometer, diffraction-limited, wide field-of-view imaging," Opt. Express 31, 36388-36401 (2023).

Physics enhanced neural network for phase retrieval from two diffraction patterns

R. Li, G. Pedrini, S. Reichelt

We propose a physics-enhanced two-to-one Y-neural network (two inputs and one output) for phase retrieval of complex wavefronts from two diffraction patterns. The learnable parameters of the Y-net are optimized by minimizing a hybrid loss function, which evaluates the root-mean-square error and normalized Pearson correlated coefficient on the two diffraction planes. An angular spectrum method network is designed for self-supervised training on the Y-net. Amplitudes and phases were retrieved using a Y-net with 100 learning iterations. Fast reconstructions could be realized without constraints or a priori knowledge of the samples. A schematic of the setup used for recording axially displaced diffraction patterns is shown in Fig. 1(a). The sample is illuminated by a plane wave and the diffraction patterns are recorded on two planes at distances of *z'* and *z'*+*z*. To reconstruct the complex-valued object, the phase on the two diffraction patterns is retrieved using a Y-net. The schematic for training the Y-net is shown in Fig.1 (b). In the first training loop, the learnable parameters are initialized. This initialization helps to prevent the signal from expanding to an extremely high value or going to zero. Then the learnable parameters are optimized by minimizing a hybrid loss function, which is built by following the optical diffraction model.

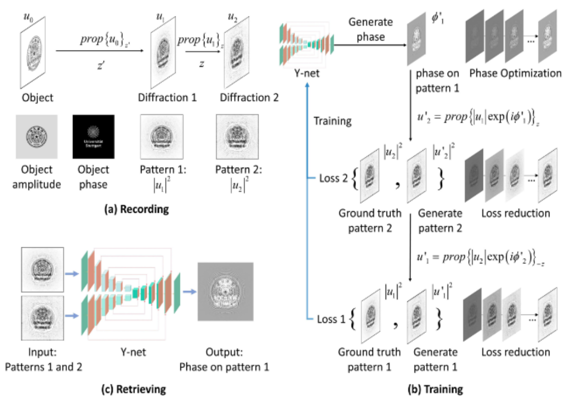

Fig. 1: (a) Recording two patterns diffracted by a complex object; (b) Training the Y-net based on diffraction between the two planes; (c) Retrieving the phase on the first pattern.

A skeletal muscle cell was used to demonstrate the capability of the Y-net. The sample in Fig. 2(a) was illuminated with a plane wave having wavelength of 632.8 nm. The first diffraction pattern was captured 39.4 mm away from the specimen, then the camera was shifted 1 mm for capturing the second pattern. The recorded patterns are shown in Figs. 2(b) and (c). The phase at the first plane was retrieved after training the Y-net with 100 iterations (see Fig. 2(d)). The reconstruction of the sample is obtained by propagating the retrieved wavefront. The reconstructed amplitude and phase of the skeletal muscle cell are shown in Figs. 2(e) and (f). The amplitude and phase show different structures of the skeletal muscle.

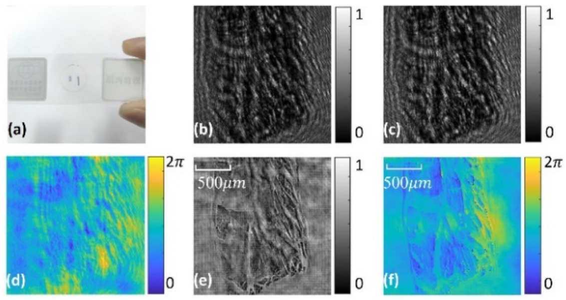

Fig. 2: Experimental result for a skeletal muscle cell. (a) Picture of the cell sample; (b) and (c) The recorded diffraction patterns on the two planes; (d) Retrieved phase on the plane of (b); (e) and (f) Amplitude and phase of the reconstruction using the Y-net with 100 iterations.

Supported by: Sino-German Centre (GZ 1391).

References:

(1) R. Li, G. Pedrini, Z. Huan, S. Reichelt, L. Cao, Physics-enhanced neural network for phase retrieval from two diffraction patterns. Opt. Express 2022; 30(18):32680-32692. doi: 10.1364/OE.469080.

Digital holographic microscope for the characterization of wave-fields transmitted and/or reflected from biological and technical samples

G. Pedrini

A microscope for the characterization of wave-fields transmitted and/or reflected from biological and technical samples was developed, built and tested. Fig. 1(a) shows the sketch of the system, which is the combination of two holographic in-line microscopes. The first one (red beam paths in Fig. 1(a)) measures the phase change of the wave transmitted by the sample. It uses as a light source a laser diode with a wavelength of 655 nm and a power of 2 mW. The second holographic microscope (see blue rays in Fig. 1(a)) measures the 3D relief of the sample. The light source in this case is a laser diode with wavelength of 405 nm (ultraviolet) and a power of 20 mW. We chose this laser because it has a short time coherence (approx. 100 µm), which means that the path lengths of the reference beam and the beam reflected by the sample must be equal. Only in this case, there will be interference for the holographic recording. We use holographic in-line setups where the phase is obtained by temporal phase shifting using piezo-electric devices.

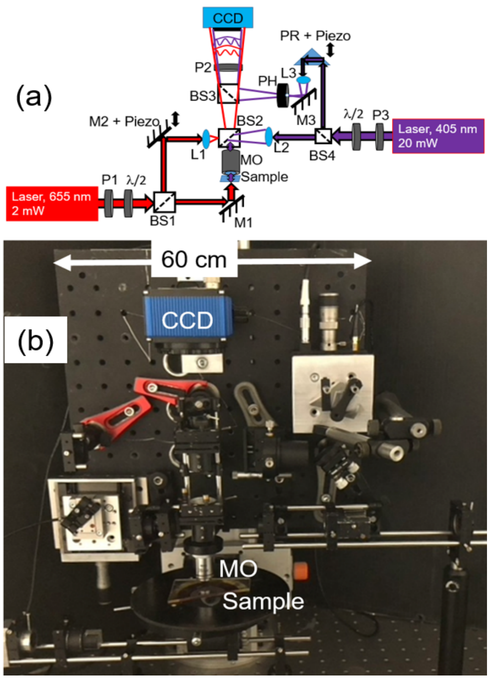

Fig. 1: Digital holographic microscope. Sketch (a) and built set-up (b).

Fig. 2 shows the result of measurement of a surface relief gratings (SRG) written on Chalcogenide As_2S_3–Se nano-multilayers. The surface relief $\Delta d(x,y)$ is calculated from the phase modulation $\Delta\phi(x,y)$ obtained by the holographic recording in reflection mode. $\Delta d(x,y) = \Delta\phi(x,y)\lambda_r/4\pi$, where λ_r = 405 nm, is the wavelength. The same sample area was investigated in transmission mode; this allowed determining that the sample has only very small refraction index modulation and that the diffraction of the grating is mostly produced by the 3D surface relief.

The setup was also used for the investigation of biological samples (see Ref. 2).

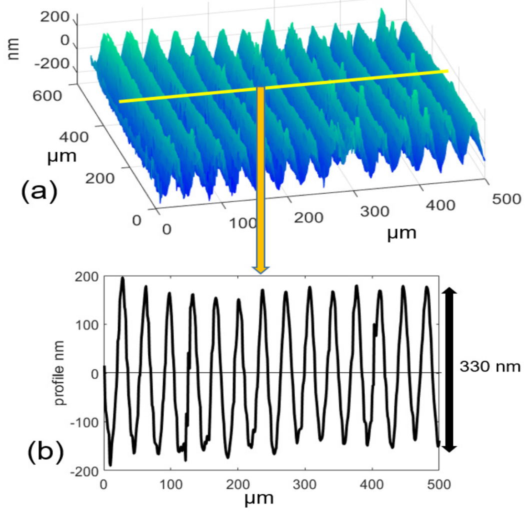

Fig. 2: Surface relief of the grating (a) and cross section (b).

Supported by: DLR-Era.Net (FKZ: 01DJ21002)

References:

(1) V. Cazac, A. Meshalkin, V. Abashkin, A. Achimova, V. Katkovnik, I. Shevkunov, D. Claus, and G. Pedrini. “Surface relief and refractive index gratings patterned in chalcogenide glasses and studied by off-axis digital holography”, Applied Optics, 57, 507-513 (2018).

(2) Quing Guo, “Digitales holographisches Mikroskop zur Untersuchung von reflektierenden und transmittierenden Proben”, Studienarbeit Master Medizintechnik, University of Stuttgart (2022).

Optical Design and Simulation

Project PRINTOPTICS: Looking back onto 6 years of successful development of high performance 3D-printed optical systems

A. Toulouse, S. Thiele, J. Drozella, A. Herkommer

The cooperative BMBF-funded project PRINTOPTICS was aimed to develop novel technologies, that lead to the realization of new types of printed complex micro-optical components and systems. From 2016 to 2022 the sub-project OptDesPrint allowed us together with the partners at 4'th Physics Institute of the University Stuttgart, Karl Storz, and Nanoscribe to extend the field of printed optics. Specific goal of the project was to realize the full value chain of optical design, simulation and manufacturing with suitable printing materials. Main benefit is a completely new generation of micro-optics, which combines free-form lenses in complex structures on a size of a few 10 to 1,000 µm.

During the project we were on the one hand able to improve simulations methods and on the other hand to develop novel optical design concepts for 3D-printed imaging and illumination systems.

For the wave-optical simulation of micro-printed systems, fast algorithms for light propagation were developed. These are based on an implementation of the so-called wave propagation method (WPM). After successful testing, the algorithms were integrated into ITO's own open-source suite ITOM. The suitability of the wave-optical models was tested in comparison against the experimental measured properties of real printed optics. One of the main goals here was to show that a wave-optically optimized system is superior to only ray-based modeling. This is particularly relevant as soon as diffraction effects are relevant or diffractive structures are used [1,2] as shown in Figure 1.

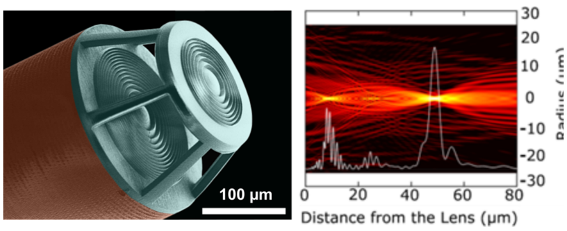

Fig. 1: 3D-printed diffractive focusing system for fiber-based trapping and wave-optical simulation of the focal region [2].

Regarding optical design concepts, a wide variety of imaging and illumination systems has been developed and optimized during the project under the constraints of 3D printing. For imaging applications wide-angle and tele systems, telecentric systems for endoscopic applications, hybrid refractive-diffractive, multi-aperture and off-axis systems have been designed, printed and tested. Figure 2 shows one example of an off-axis multi-channel imaging system, providing ultra-wide field of view [3].

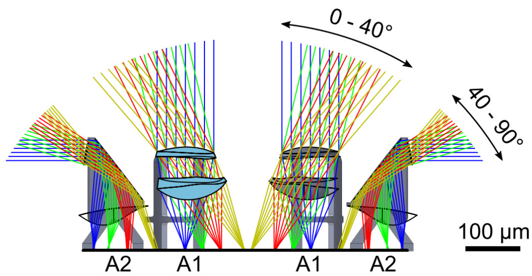

Fig. 2: Flat wide-angle multi-aperture system that can be integrated directly onto an image sensor [3].

Moreover, illumination optics, e.g. fiber-based optics, which enable extreme illumination angles, or optics which use total internal reflection or freeform surfaces to achieve complicated illumination distributions have been designed. Here, Figure 3 shows an example of a Ø 125 µm fiber-logo projector based on a hybrid refractive/diffractive freeform surface [4].

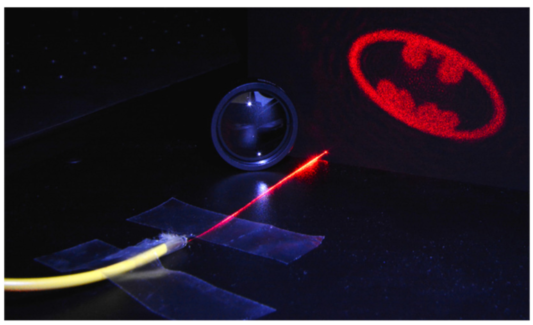

Fig. 3: Fiber illumination system with 3D-printed optics for logo projection.

For the manufacturing of such complex, small-scale, but high-performance optical systems, two aspects became very important: A method to generate absorbing apertures and stray-light shielding in the 3D-printed designs, and accurate tools to measure the complex surface profiles in order to correct their shape. For the creation of apertures, the ink-process which has already early been developed at ITO within the project [5] could be refined and was used in several demonstrators to increase contrast, or to provide apertures or entrance slits in imaging or metrology systems [6]. Figure 4 illustrates an ink-filled aperture to define the stop of an off-axis imaging system.

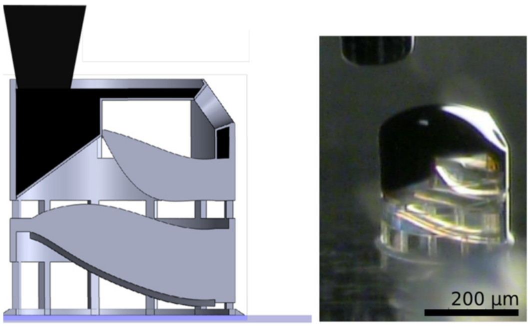

Fig. 4: Ink-filled cavities in the design of an off-axis imaging system in order to define the stop.

Regarding measurements of surfaces or 3D-geometries additional budget in the project allowed us to acquire a white light interferometer and a confocal microscope for 3D high resolution measurements of complex optical surfaces, together with a Desktop SEM and a digital microscope for inspection and analysis of 3D-printed structures. Only via the accurate measurements of optical surfaces and 3D-geometries a diffraction limited imaging quality can be achieved during iteration cycles of printing and measuring. However, for freeform surfaces additional effort is required to reference the surface measurements to the 3D-position of the surface in the system (Figure 5) [3].

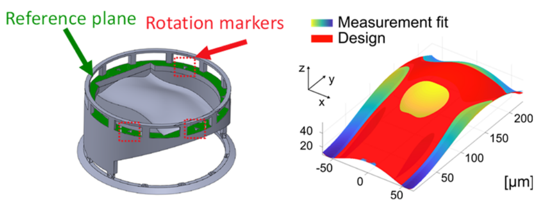

Fig. 5: Reference structures in the design of an off-axis imaging system for providing orientation of measurement data in the 3D-geometry [3].

In summary, the project PRINTOPICS over the years 2016 – 2022 allowed us to continuously improve and fine-tune our methods in 3D-printing of optics. The project has led to extensive and high-quality results: Both in terms of knowledge gain (measurable by the high number of publications and awards), in terms of exploitation opportunities (numerous patent applications), as well as in terms of the methodological competence and technological maturity achieved (measurable by the high quality and complexity of the prototypes and the professional simulation tools). The goal of the project to realize the full value chain of optical design, simulation and manufacturing was clearly reached.

One remarkable result of the project is the successful launch of the Start-Up Printoptix [7]. After several stages of start-up funding, fine-tuning the business-model and building up a customer base, the Printoptix GmbH was funded in December 2021. Since then, the company has shown a very impressive growth in revenue and employes, moreover they could win several funded projects.

In summary, the project PRINTOPICS is a success-story in terms of research, application and commercialization of a novel technology.

Supported by: BMBF
Project: OptDesPrint / PRINTOPTICS
In cooperation with: Karl Storz Se & Co. KG, Nanoscribe GmbH, 4'th Physics Institute

References:

(1) S. Thiele, C. Pruss, A.M. Herkommer, H. Giessen (2019), "3D printed stacked diffractive microlenses", Optics Express, 27(24), 35621-35630.
(2) A. Asadollahbaik, S. Thiele, K. Weber, A. Kumar, J. Drozella, et al. (2019), "Highly efficient dual-fiber optical trapping with 3D printed diffractive fresnel lenses", ACS photonics, 7(1), 88-97.
(3) A. Toulouse, J. Drozella, P. Motzfeld, N. Fahrbach, V. Aslani, S. Thiele, H. Giessen, A.M. Herkommer (2022), "Ultra-compact 3D-printed wide-angle cameras realized by multi-aperture freeform optical design", Optics Express, 30(2), 707-720.
(4) S. Schmidt, et al. (2020), "Tailored micro-optical freeform holograms for integrated complex beam shaping", Optica, 7(10), 1279-1286.
(5) A. Toulouse, S. Thiele, H. Giessen, A.M. Herkommer (2018), "Alignment-free integration of apertures and nontransparent hulls into 3D-printed micro-optics", Optics letters, 43(21), 5283-5286.
(6) A. Toulouse, J. Drozella, S. Thiele, H. Giessen, A. Herkommer (2021), "3D-printed miniature spectrometer for the visible range with a 100× 100 µm² footprint", Light: Advanced Manufacturing, 2(1), 20-30.
(7) www.Printoptix.com .

Miniaturized 3D printed fiber-optic probe for OCT and autofluorescence detection in medical applications

S. Thiele, A. Toulouse, F. Rothermel, A. Herkommer

Atherosclerosis is one of the leading cause of global mortality. Early diagnostics and research is therefore mandatory.

Intravascular optical coherence tomography (OCT) is a promising tool for visualising the structural features of the atherosclerotic plaque, for example, measuring the thickness of the fibrous cap. The research team around Prof. Robert McLaughlin and Dr. Jiawen Li at the University of Adelaide are leading researchers in that area. They have developed a fiber-based OCT-system which can be inserted into small blood vessels. A rotation of the fiber-probe results in a circular OCT-scan. As the OCT needs to look sideways, a small optical prism is used to redirect the focused beam. Additionally, the system is inside a glass catheter, which introduces optical aberrations. Therefore, a very small but complex optical focusing system is required for optimum performance.

This situation seemed to by a perfect synergy between a professional medical application and the 3D-printing activities at the Institute. Therefore, in 2019 a DAAD-based exchange program between the ITO and the University of Adelaide has been proposed and immediately got funded. During this project we could establish a very vivid and fruitful collaboration of both partners, which still lasts today.

As a first step, we designed and manufactured a 3D-printed focusing freeform prism for the OCT fiber probe, as shown in Figure 1.

The 3D printed lens is designed to correct the astigmatism that arises from the intravascular

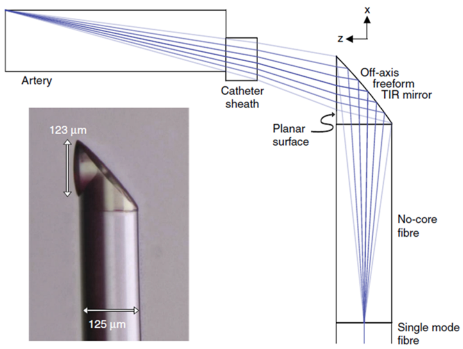

Fig. 1: 3D-printed OCT fiber optics for aberration correction, adapted form [1].

catheter used during imaging, thus providing improved OCT quality [1].

Encouraged by the sucessful application of the probe in mouse-vessels, the international team at ITO and Adelaide has in a next step developed a bimodal OCT and fluorescence intravascular imaging system that can simultaneously acquire both the structural (from OCT) and molecular information (from fluorescence) of atherosclerotic plaques [2]. We developed a miniaturised 3D-printed double-clad fibre intravascular probe with an outer diameter of 620 µm (including the catheter sheath). The optical design of the 3D-printed fiberhead is based on an inner OCT lens surface, surrounded by a complex TIR-Fresnel structure to collect the flourescence from a large solid angle, as shown in Figure 2.

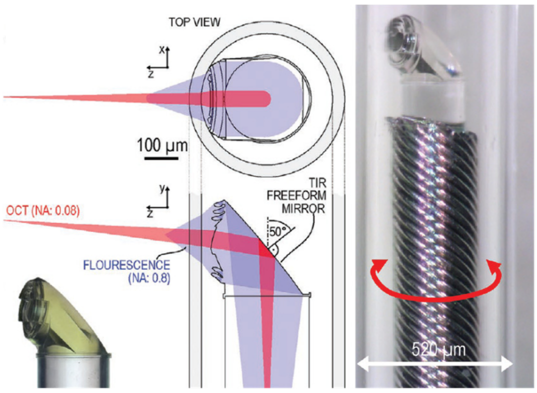

Fig. 2: Bi-modal OCT/ fluorescence fiber probe [2].

The partners in Adelaide are currently using the system to explore autofluorescence present in unstable human plaques. In the future we want to continue this successful cooperation.

Supported by: DAAD
Project: OptDesPrint / PRINTOPTICS
In cooperation with: University of Adelaide

References:

(1) Jiawen Li, et al. "Ultrathin monolithic 3D printed optical coherence tomography endoscopy for preclinical and clinical use." Light: Science & Applications 9.1 (2020): 124.
(2) Jiawen Li, et al. "3D‐Printed Micro Lens‐in‐Lens for In Vivo Multimodal Microendoscopy. Small 18.17 (2022): 2270087.

Magnetic Actuation of 3D-printed Micro-optical Elements

F. Rothermel, S. Thiele, C. Jung, H. Giessen, A. Herkommer

The actuation of optical components plays an important role in imaging systems as it allows for dynamic features, such as autofocusing or zoom. Implementing such features into additively manufactured micro-optical systems fabricated via two-photon polymerization however is a challenging task. Conventional micro-actuation methods (e.g. MEMS) require assembly of the system and thus would compromise the advantages of 3D-printing, while the use of stimuli-responsive resins is not suitable to fabricate optical elements of high quality.

We developed an actuation method that relies on magnetic forces and can easily be integrated into the fabrication process using only few post-processing steps. The 3D-printable, monolithic opto-mechanical design includes the actuatable micro-optical element, a mechanical restoring element (springs, flexures etc.) and a microfluidic reservoir. This reservoir is filled with a composite of ferromagnetic microparticles and epoxy resin, which can be permanently magnetized after curing. By applying an external magnetic field, the magnet and thus the optical element can be continuously positioned (Fig. 1). The magnetic field causes a displacement of the lens along the optical axis, which can be used for autofocusing as well as zooming, if the depth of field of the system is suitable.

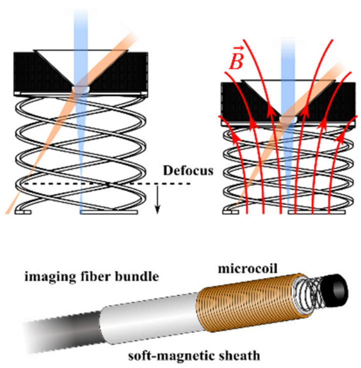

Fig. 1: Concept of the magnetic actuation method of a 3D-printed autofocus/zoom micro-system with a diameter of <500 µm.

The magnetic field can be generated by custom integrated microcoils, which allows for highly compact endoscopic actuated systems with total system diameters below 500 µm: The micro-optical system is fabricated directly on the end-facet of the imaging fiber bundle. The microcoil is then wound around a soft-magnetic sheath encasing the imaging fiber. Large displacements of >100 µm and straight translational motions of the lens can be achieved, which was experimentally demonstrated in an equivalent setup (Fig. 2). Here, a displacement of approximately 200 µm was achieved using a coil current of 170 mA, while the lens showed a minor tilt during actuation.

Besides translational motions, rotational actuation of small prisms in order to achieve a shiftable FOV has also been demonstrated [1].

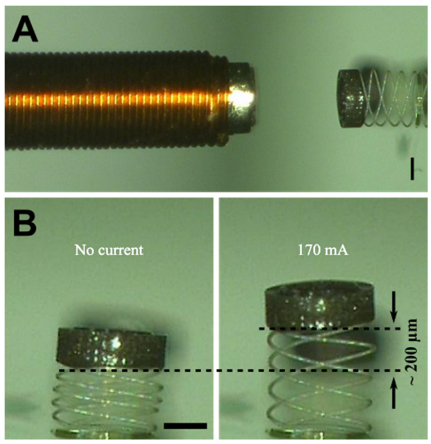

Fig. 2: Magnetic actuation experiment of the autofocus/zoom-system. The structure was printed onto a glass substrate and actuated using a microcoil wound around a soft-magnetic sheath. (A) Experimental setup. (B) Actuation of the structure with a coil current of 0 and 170 mA,

Supported by: DFG German Science Foundation
Project: Förderkennzeichen HE6363/5-1 (DFG-MiMAO)
In cooperation with: 4th Physics Institute, University of Stuttgart

References:

(1) F. Rothermel, S. Thiele, C. Jung, H. Gießen, A. M. Herkommer, „Towards magnetically actuated 3D-printed micro-optical elements“, Proc. SPIE 11816 (2021).

Advances in wave optical simulation of 3D printed micro optics

M. Wende, J. Drozella, A. M. Herkommer

The plugin WavePropagationMethods (WPM) for the software ITOM allows for fast and comfortable wave optical simulation of light propagation through micro optics. It enables user friendly creation of simulation models based on Zemax Optic Studio designs, measured surface data or custom refractive index distributions. The algorithm of the WPM is then used to calculate a step wise scalar electric field propagation through the simulation model (1). Compared to rigorous electromagnetic solvers like COMSOL, the WPM enables fast simulations of comparably large volumes in the range of up to 1 mm^3.

The WPM can simulate a wide range of micro optical systems which are manufactured using 2-photon lithography (2PL), yet the restriction on scalar electric fields and purely forwards directed propagation limits application e.g. for high numerical aperture lenses, high frequency gratings ($p < \lambda$) and systems with dominant reflective effects like resonators.

As a first step to address those limitations, we derived the “Fast Polarized Wave Propagation Method” (FPWPM) from the vector Helmholtz equation. The FPWPM allows for consideration of polarization in wave optical simulations, while the additional required simulation runtime minimal remains minimal (2).

The FPWPM shares the algorithmic structure of the scalar WPM, therefore all routines developed for the WPM plugin e.g. for generating simulation models can directly applied to this new simulation method. Straightforward integration of the FPWPM into the WPM plugin is therefore feasible.

In Fig. 1, a simulation example is depicted showcasing the use of the FPWPM algorithm for the simulation of a 3D-printed high-NA microlens, focusing a circularly polarized incident electric field carrying orbital angular momentum (OAM). Fig. 1 (a) shows a cross-section of the simulated electric field along the propagation axis. As can be observed by comparing Fig. 1 (b) and (c), the focal spot of the microlens strongly varies depending on the handedness of the circular polarization of the illumination light. Simulation results agree well with analytical references from literature, like the Richards-Wolf integral, proving that the FPWPM is well suited for accurate simulation of polarization effects in micro optical systems, while reducing the simulation runtime up to several 1000 x (2).

Current research is directed to expand simulation capabilities towards reflective optics by extending the FPWPM from a unidirectional to a bidirectional algorithm, allowing for simulation of e.g. micro resonators or catadioptric systems.

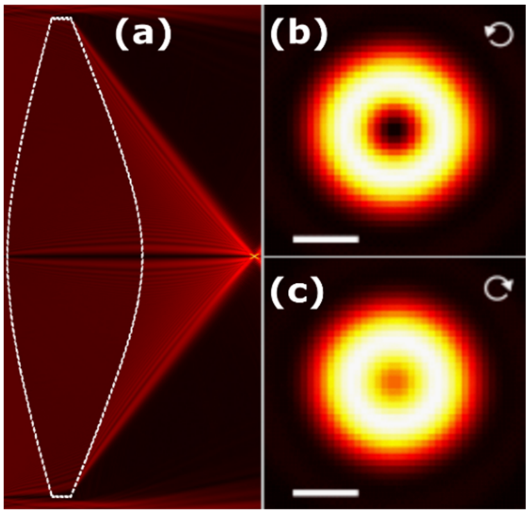

Fig. 1: **(a)** *Vector wave optical simulation of electric field propagation through a microlens.* **(b)** + **(c)** *Focal spots for LHC polarized and RHC polarized light, respectively. Bars: 0.5 µm.*

Supported by: Vector Stiftung (MINT Innovationen); Ministerium für Wissenschaft, Forschung und Kunst Baden-Württemberg (RiSC).

References:

(1) J. Drozella, A. Toulouse, S. Thiele, and A. M. Herkommer, “Fast and comfortable GPU-accelerated wave-optical simulation for imaging properties and design of highly aspheric 3D-printed freeform microlens systems,” in Novel Optical Systems, Methods, and Applications XXII, vol. 11105 (SPIE, 2019), pp.27-33.

(2) M. Wende, J. Drozella, A. Toulouse, and A. M. Herkommer, „Fast algorithm for the simulation of 3D-printed microoptics based on the vector wave propagation method,” Opt. Express 30, 4161-40173 (2022).

Additive manufacturing of volume scattering devices

J. Drozella, A. Herkommer

Additive Manufacturing using 2-photon-polymerization (2PP) revolutionized the possibilities of optical fabrication in recent years. It allows for complex 3-dimensional shapes including otherwise not producible undercuts and combinations of multiple surface types like refractive, diffractive, and meta structures.

The process involves photopolymerization of a usually liquid-phase photoresist followed by a development and rinsing step, which results in the targeted structures to be left standing.

3-dimensional modification of glass blocks has been shown (1) to be able to create targeted images in the far field, depending on the incoming illumination wavelength or angle. These structures are designed as individually placed volume pixels (voxels) in a 3D space. Their targeted positions can be calculated dependent on the position of *Ewald Spheres* within the spatial frequency representation of the physical volume (see Fig. 1) called the reciprocal lattice, which is obtained by a 3D Fourier transform.

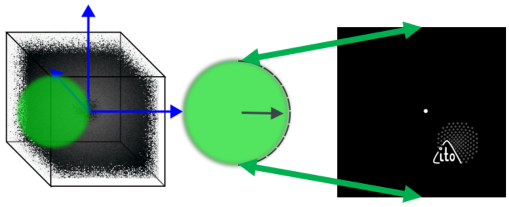

Fig. 1: Representation of an Ewald Sphere positioned in the reciprocal lattice of a 3D voxel distribution. Far field amplitudes of the scattered field can be adjusted on their surface.

Manufacturing within rigid glass substrates using modification of the local refractive index by the application of high energy laser pulses requires post-processing steps to cut down the substrate and mounting it in order to be applicable. Additive manufacturing overcomes these limitations, thus allowing for the fabrication of such structures on many types of substrates like glass slides, optical fibers, or directly onto sensors and sources. An obvious problem with this method is the work in liquid photoresist, which makes the precise positioning of individual voxels in a 3D space unlikely. We presented (2) an approach to enable the manufacture of fully targeted 3-dimensional voxel distributions within an additive process.

The additive manufacturing of 3-dimensional voxel distributions is made possible by a three-step process depicted in Fig. 2: Firstly, an enclosing volume is created within the liquid photoresist. This prohibits volume exchange between the interior volume and the surrounding photoresist caused by movement of the writing objective, for instance.

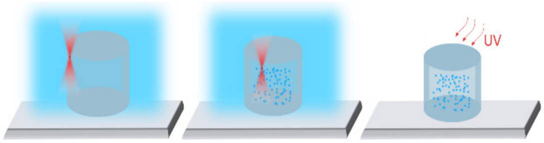

Fig. 2: Three-step process for the creation of arbitrary 3-dimensional voxel distributions in additive manufacturing. 1: creation of an enclosing volume. 2: writing of the voxel distribution. 3: development, rinsing, and flood illumination.

The voxel distributions can in a second step be written through the walls of the enclosing volume. Thirdly, a step of development and flood illumination results in the polymerization of the remaining enclosed liquid photoresist, ensuring long term stability.

Applied materials show refractive index variations between 2PP and 1PP illuminated photoresist. The manufactured voxel distributions project targeted far field images when illuminated with a plane wave (Fig. 3), showing that it is possible to create free floating voxel distributions in 3 dimensions using liquid phase photoresist.

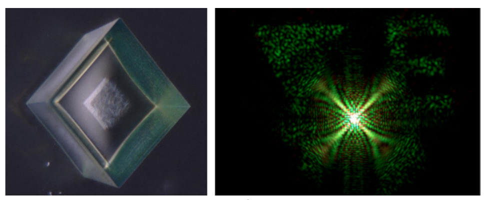

Fig. 3: An additively manufactured 3D voxel distribution (left), and targeted "triangle and E"-distribution (right).

Supported by MWK RISC Multiplexe Optiken

References:

(1) Gerke, T..; Piestun, R. (2010): Aperiodic volume optics. In Nature Photonics 4 (3), pp.188–193.

(2) Drozella, J.; et al. (2023): Towards additive manufacturing of multiplexed volume scattering devices using two-photon polymerization. In: Laser 3D Manufacturing X: SPIE (PC12412).

3D printed micro-optics for single photon sources

C. Jimenez, A. Toulouse, A. Herkommer

Reliable and high-quality single photon sources are crucial for scaling quantum information technology systems used in computing and encrypted communication channels. In order to take full advantage of what single photon sources (SPS) can provide, it is important to maximize the portion of photons being extracted and coupled into optical waveguides or single mode fibers (SMF). There exist different proposals for coupling photons from SPSs into SMFs, as illustrated in Fig. 1 and 2. Nevertheless, some of these methods rely on large optical systems (e.g. microscope lenses) in addition to complex positioning systems, which effectively limit the number of addressable emitters without increasing the overall space complexity. Such limitations can be circumvented with the help of 3D printed micro-optical components. In addition to facilitating compact integrated systems and direct coupling into optical fibers, these elements benefit from a process with an inherent high degree of spatial resolution that enables the use of a large variety of surface profiles.

In this regards, we have worked in a collaboration with the Institute of Solid State Physics from the technical University of Berlin in order to perform a numerical study for the case of integrating different 3D printed aspheric fiber lens structures with various single photon sources based on semiconductors Quantum Dots(QDs).

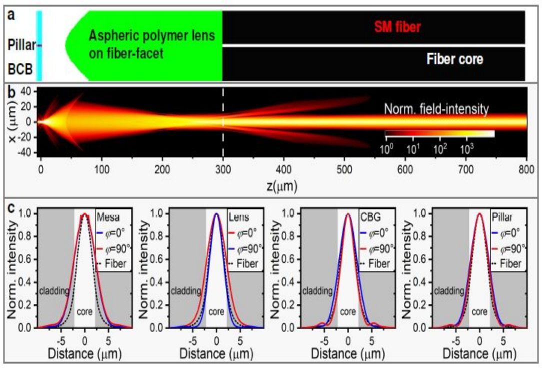

Fig. 1: FEM based simulation of semiconductor Quantum-Dot based single photon source integrated with aspheric 3D printed fiber-lens.

In the following, we have established a collaboration with the developers of the software package known as VirtualLab Fusion who are based at Jena, Germany. Such a software package allows us, to integrate different simulation methods within a single framework, enabling the extraction of information which cannot be obtained via the exclusive use of software packages based on ray-optics. In this way, we intend to gain additional insights into the different effects influencing the coupling performance of 3D printed optics in the context of single photon sources, facilitating at the end robust designs which can be tailored to different types of sources.

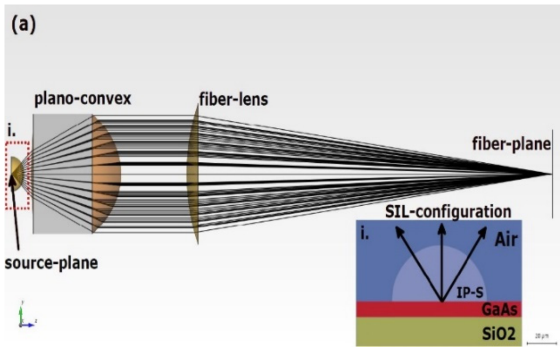

Fig. 2: Illustration of a system for coupling single photon sources to fibers.

Supported by:
DFG German Research Foundation
Project: GRK2642

References:

(1) L. Bremer, C. Jimenez, S. Thiele, K. Weber, T. Huber, S. Rodt, H. Gießen, A. M. Herkommer, S. Burger, S. Hofling, S. Reitzenstein “Numerical optimization of single-mode fiber-coupled single-photon sources based on semiconductor quantum dots“, Opt. Express 30, 15913 (202).

Microglass: Glass made from 3D-printed polymer structures

S. Thiele, A. Toulouse, A. Mrokon, L. Bülow, A. Herkommer

In recent years, the additive manufacturing of highly complex micro-optics by means of multiphoton polymerization has changed the production of tiny optical components in a revolutionary way. A major disadvantage is the process-related limitation of materials to polymers. These are far inferior to glass optics, especially in terms of temperature resistance, chemical resistance, mechanical stability, optical properties, and durability.

In the microglass project, we therefore investigated the extent to which the approach of optical 3D printing can be transferred to glass in order to open up new fields of research and opportunities for commercialization. The core idea was to use two photon lithography to print negative polymer molds, which were then molded into the positive via a glassomer [1] and converted into pure glass via a sintering process (Fig. 1).

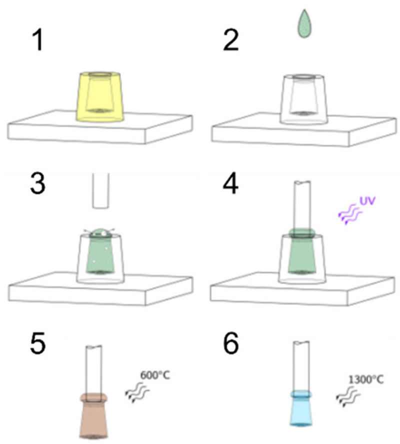

Fig. 1: A 6-step process to fabricate glass microoptics. 1. Fabrication of 3D-printed polymer mold, 2. Filling of the mold with "liquid glass", 3. Venting and joining of an optical fibre, 4. UV-curing of the glassomer, 5. Removal of the organic parts (600°C), 6. Sintering and shrinking (1300°C).

The 3D printed mold (step 1) can be almost arbitrarily complex due to the high flexibility of multiphoton lithography and is lost after the casting process (lost-form process). In addition to optically effective surfaces, it contains openings for the filling process, for venting and, if necessary, guide structures for mating parts. The actual filling with Glassomer is supported by capillary forces (step 2). After complete filling and joining of any counterparts (step 3), the Glassomer is cured by means of UV exposure (step 4). In the next step, all organic components are incinerated (step 5). This includes the mold as well as the polymer matrix of the glassomer, leaving only a brown body of bonded glass nanoparticles. This brown body is sintered in a final step 6, during which it undergoes significant shrinkage (~25%) and becomes monolithic glass.

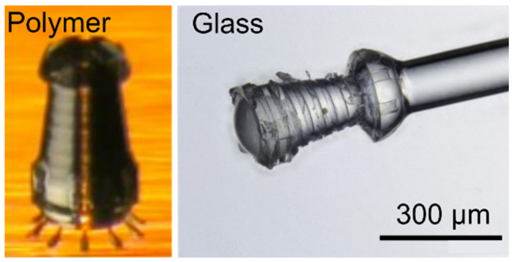

Fig. 2: Polymer mold and glass microlens fabricated from the mold on a fiber tip.

As a final milestone in the project, a lens sintered from glass on the tip of an optical fibre was successfully demonstrated (Fig. 2).

During the ongoing project, researchers at the University of Freiburg presented an adapted glassomer material that can be 3D printed and sintered directly on the microscale without the need to use a mold [2]. However, this process has increased processing time, introduced even more shrinkage due to the smaller fill factor in the polymer matrix, and shows an increased process sensitivity.

Supported by: Ministerium für Wissenschaft, Forschung und Kunst Baden-Württemberg (MWK)
Project: Microglass

References:

(1) F. Kotz et al. "Liquid glass: a facile soft replication method for structuring glass." Advanced Materials 28.23: 4646-4650, 2016.
(2) F. Kotz et al., „Two-Photon Polymerization of Nanocomposites for the Fabrication of Transparent Fused Silica Glass Microstructures", Adv. Mat. 33, 2006341, 2021.

3D-printed apertures, colored micro-optics & more

A. Toulouse, V. Aslani, S. Thiele, A. Herkommer

Most of our research on 3D-printed microoptics is based on a commercial two-photon 3D printer (Nanoscribe) and its proprietary materials and processes. However, there is a need for novel printing materials in microoptics, to enable aperture stops or integrated color filtering, for example. In dip-in lithography, Nanoscribe's mode of operation, the photoresists directly touch the microscope objectives used for printing and serve as immersion medium. This complicates work with novel photoresist formulations and inhibits use of aggressive materials that risk harming the objectives. We therefore developed a simple process to shield our objectives from the photoresist (Fig. 1) while verifiably conserving printing resolution [1].

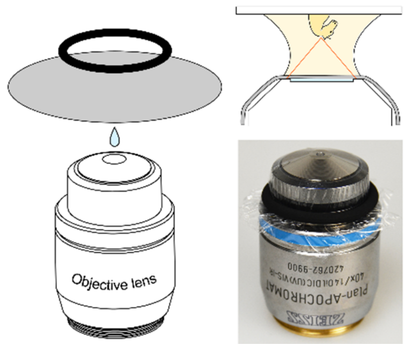

Fig. 1: A process to 3D-print experimental photoresists while protecting the writing objective using simple cling foil (1).

This modified printing process now enables us to develop new photoresists for contrast improvement of our microoptics, integrated hyperspectral applications or biological applications. In Fig. 2, we present successful fabrication of absorbing filters and apertures (top). A transmission of 5% can be reached with a filter thickness of 250 µm and we showed that apertures in this size range can lead to substantial contrast improvement in imaging applications. Furthermore, we were able to fabricate color filtering micro-objectives (middle), i.e. imaging optical systems with integrated color-filtering without the need for an additional explicit filter component. Finally, our process can be used to develop new aqueous protein bio-inks and fabricate metal structures (bottom).

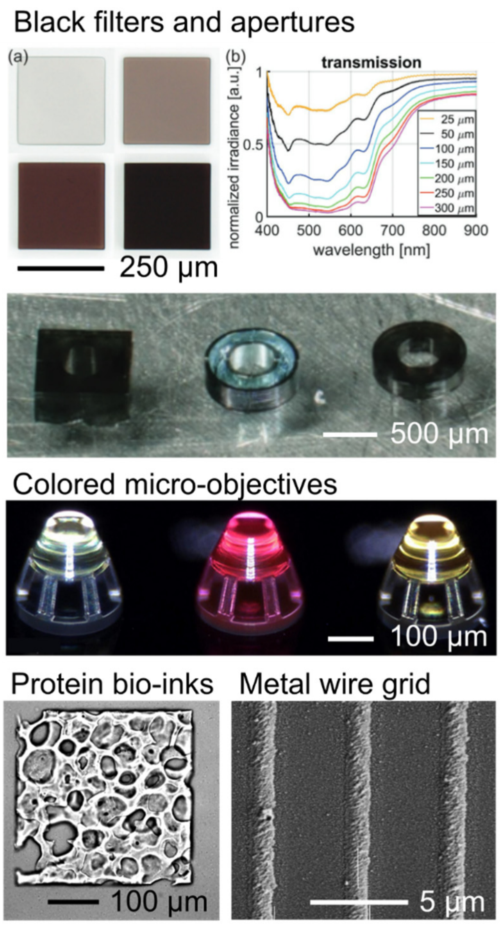

Fig. 2: Experimental photoresist applications [1,2,3].

Supported by: Deutsche Forschungsgemeinschaft (DFG)
Project: GRK 2543, A1

References:

(1) A. Toulouse, S. Thiele, K. Hirzel, M. Schmid, K. Weber, M. Zyrianova, H. Giessen, A. Herkommer, & M. Heymann „High resolution femtosecond direct laser writing with wrapped lens", Optical Materials Express, 12(9), 3801-3809, 2022.

(2) M. Schmid, A. Toulouse, S. Thiele, S. Mangold, A. Herkommer, & H. Giessen, "3D direct laser writing of highly absorptive photoresist for miniature optical apertures", Advanced Functional Materials, 2211159, 2022.

(3) V. Aslani, A. Toulouse, M. Schmid, H. Giessen, T. Haist, & A. Herkommer, „3D printing of colored micro-optics", Optical Materials Express, 13(5), 1372-1384, 2023.

Soft 3D fiber-optical actuation

J. Grunewald, A. Toulouse, F. Rothermel, M. Heymann, A. Herkommer

Accommodation is a milestone in the evolutionary development of the eye, as it allows focussing objects depending on their distance by a deformable lens. In technology, so-called liquid lenses, often realized by transparent and flexible PDMS-membranes deforming under pressure, can create adaptive optics/elements. With the possibilities of two-photon direct laser writing of 3D-microstructures using a recently developed PDMS resin, micro-optofluidic lenses can now be fabricated and incorporated in endoscopic micro-systems, ideal for minimally invasive biomedical applications.

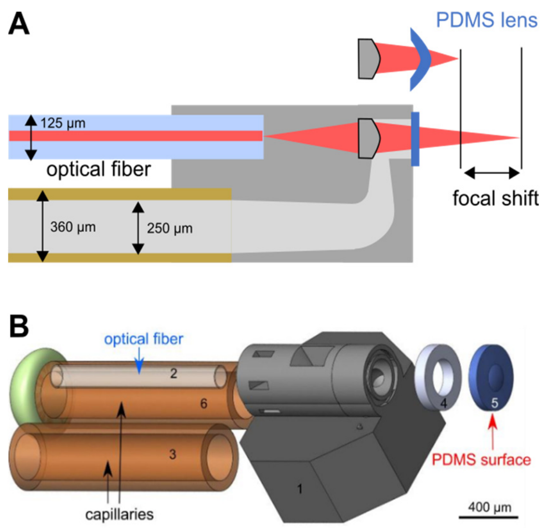

Fig. 1: Endoscopic micro-system with active focus-shifting containing an optofluidic PDMS-lens.(A) Concept of the assembly. (B) Exploded CAD view, denoting the order of the 6-step assembly procedure.

We developed an endoscopic system that allows for active transformation of its optical illumination distribution by deforming a 3D-printed PDMS-membrane through pressure application. The system consists of an IP-S optofluidic mount, containing an asphere for initial focussing, microfluidic channels and glass capillaries for development and pressure control, an optical fiber as well as the PDMS-membrane (Fig. 1). Although the final assembly requires 6 processing steps, including printing and gluing of several parts, it ultimately yielded reliable prototypes.

The on-fiber actuation of the membrane was successfully demonstrated. The static pressure was controlled in a range from 0.4 to 1.6 PSI, which resulted in an observable change in the curvature of the PDMS-membrane (Fig 2). However, the fabrication process of the membrane still needs improvement to achive optical surface quality.

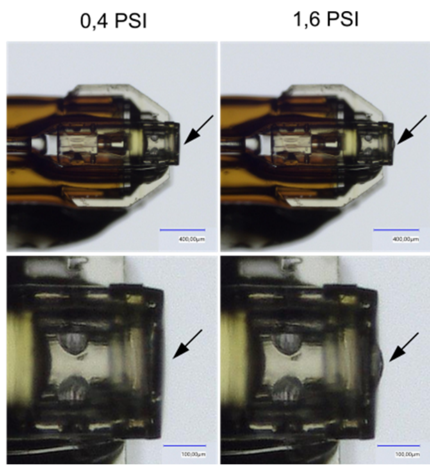

Fig. 2: When a static pressure change is applied, the curvature of the printed PDMS membrane changes.

Further research in this topic aims towards the improvement of surface quality of the PDMS-membrane as well as the implementation of custom-shaped membrane surfaces, such as aspheres or free-forms.

Supported by: Terra Incognita Program 2022, Biomedical Systems Seed Funding
Project: Soft 3D fiberoptical actuation
In cooperation with: Institute of Biomaterials and Biomolecular Systems (IBBS), University of Stuttgart

References:

(1) J. Grunewald „Weiche 3D-gedruckte faseroptische Aktuierung“, Bachelor Thesis (2022).

Spectral resolution enhancement for a tiny endoscope

A. Toulouse, J. Drozella, A. Herkommer

The smaller an endoscope, the greater its potential for minimally invasive surgical treatments. In conventional, flexible (fibre-based) endoscopes with small diameters (<200 µm), imaging is limited by the number of fibre cores. Due to this limitation, the image is pixelated (imaging fibre bundle) or, in the case of a single-mode fibre, consists of a single pixel.

In this project, an engineering approach is used to increase the number of pixels by spectral splitting. However, this requires very small color-splitting optical systems at the distal end of the endoscope. Such small spectral optics systems are practically impossible to fabricate directly on the fibre using conventional techniques. In this project, therefore, the idea is implemented using 3D-printed micro-optics. Preliminary work has shown that two-photon lithography is capable of producing spectroscopic and imaging systems on a micrometer size scale [1, 2].

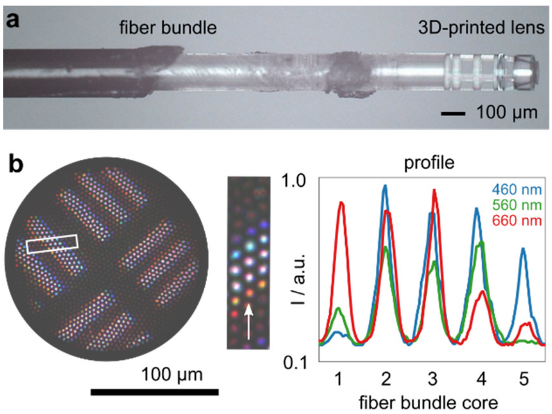

Fig. 1: (a) Dispersive imaging fibre bundle endoscope with 160 µm diameter. (b) Transmitted image and its spectral shift across the fibre cores.

We designed a dispersive objective lens and fabricated it directly on an imaging fibre bundle (Fig. 1). In a combined hyperspectral microscopic setup the color shift across the fibre cores can be measured. In a next step, the system is calibrated to shift the images corresponding to their wavelengths back to their original object positions. Each fibre core can thus be used to transmit multiple object points which leads to a single-direction resolution enhancement for our tiny endoscope.

The aim of this project is thus to combine the idea of spectral pixel multiplication with the innovative manufacturing process of 3D printing and open up new fields of application in medical engineering with extremely small and also flexible endoscopes. In the medium term, this could lead to improved diagnostics and treatment of strokes and heart attacks, for example.

Supported by: Vector Stiftung, Ministerium für Wissenschaft, Forschung und Kunst Baden-Württemberg (MWK)
Projects: TinyEndoscope3D, SpectraScope3D

References:

(1) T. Gissibl, S. Thiele, A. Herkommer, & H. Giessen, „Two-photon direct laser writing of ultracompact multi-lens objectives", Nature photonics, 10(8), 554-560, 2016.

(2) A. Toulouse, J. Drozella, S. Thiele, H. Giessen, & A. Herkommer, "3D-printed miniature spectrometer for the visible range with a 100×100 µm² footprint", Light: Advanced Manufacturing, 2(1), 20-30, 2021.

EndoPrint 3D - endoscopic Bio-3D-printing on the micro-scale

M. Wende, A. Toulouse, A. M. Herkommer

In order to allow for organ and tissue reconstruction on a cellular level, the goal of our new project "EndoPrint3D" is the development of a miniaturized endoscopic 3D-printer. With a diameter of just a few hundreds of microns, the small probe size allows access to tiny structures inside the human body, e.g. the inner ear, while keeping healthy tissue largely unaffected.

At the operation site, a bio-ink is used to print structures which act as a three dimensional framework for cellular growth, enhancing the self-regeneration of organ damage. To enable manufacturing of structures with subcellular feature size of just one micron, 2-photon lithography (2PL) is chosen as the method for 3D-printing.

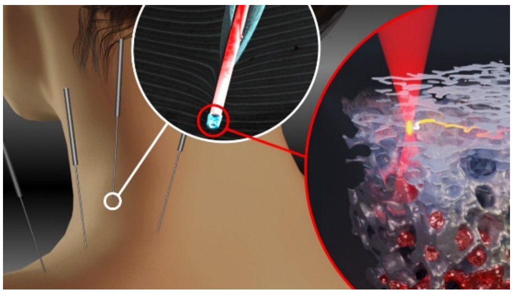

Fig. 1: Illustration how the final endoscopic 3D-printer could be applied to repair damaged tissue. Image credits: Kai Hirzel, Timo Gissibl, Florian Sterl.

In late 2022, the Carl Zeiss foundation decided to fund this interdisciplinary high-risk project in its "Wildcard" funding scheme. Since then, we chase our vision together with the biologists (IBBS, Prof. Heymann) and the physicists (4. PI, Prof. Giessen):

To enable endoscopic 2PL, a pulsed femtosecond (fs) laser has to be guided to the operation site through an optical fibre. At the fibre tip, a highly miniaturized objective lens tightly focuses the laser into a liquid bio-ink. In the focal region, the intensity exceeds a threshold to initiate multiphoton polymerization and the bio-ink solidifies. By moving the focus inside the bio-ink, structures with nearly arbitrary 3D shape can be created. The small size as well as high demands on the optical quality of the optical print head require a very accurate fabrication process. Therefore, we use a commercial 2PL-printer to manufacture the objective lens on top of the optical fibre.

Achieving a stable endoscopic 2PL printing process poses several challenges. Pulse compression for the fs laser has to be implemented in order to counteract dispersion inside the optical fibre (4. PI). If unattended, this would lead to temporal broadening of the fs laser's pulses, effectively diminishing the laser dose applied in the focal region of the objective lens. This is especially critical for the bio-ink, which is not as photosensitive as commercially available 2PL-photoresists and therefore requires high laser doses for the 2PL process.

Furthermore, the bio-ink itself is research objective with regard to toxicity and photo sensitivity as well as micromechanical properties (IBBS).

Finally, the 3D-printed objective lens has to be designed and highly corrected for aberrations in order to allow for consistent printing quality inside of the whole printing field (ITO). A mechanism has to be developed to encapsule and seal the objective lens in order to prevent the liquid bio-ink to enter the objective lens and compromise the optical performance. Additionally, we aim to implement an imaging system for real-time monitoring of the printing process.

Supported by: Carl-Zeiss-Stiftung
Project: EndoPrint3D
In cooperation with: 4th Physics Institute (4. PI) and Institute of Biomaterials and Biomolecular Systems (IBBS), University of Stuttgart

Photonic education kits and photonic modules for small/medium companies, start-ups and makers

C. Reichert, J. Trapp, K. Doth, T. Haist, A. Herkommer

Since 2016 the Institute participates in the BMBF initiative “Open Photonics”. This funding programm in the first phase was aimed at supporting schools, students and makers with low-cost and easy to use optics and photonics kits to understand and employ photonic principles for education and for realizing creative ideas. During this phase we developed a universal optical kit-box called BaKaRoS [1], together with partners from fischertechnik, Fraunhofer IAO and T-Systems. This kit contains 280 mechanical and optical parts and allows to assemble 14 different optical systems. The systems range from simple spectrometers, to telescopes, hand-held microscopes up to VR-googles. Not only the education kit was developed, but also open-software for optical design [2]. The project ended in 2020, however the optical kit is still used and was reconfigured for university students in 2022. To make the kit more usable we have split the large kit-box into smaller kits and have employed professional 3d-printed parts.

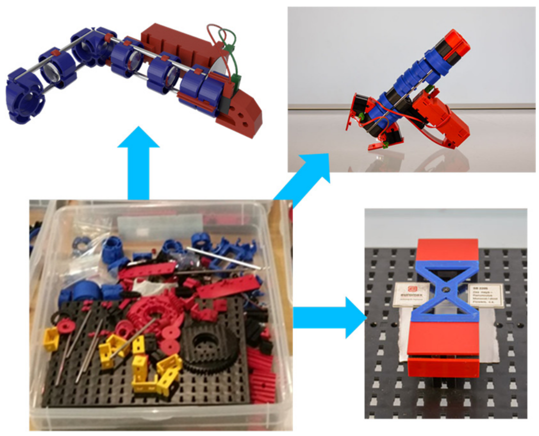

Fig. 1: Education kit “BaKaRoS” allowing the assembly of different types of optical systems.

In 2020 the BMBF launched a follow-up funding program called “Open Photonics Pro”, this time aimed to support small and medium companies with easy-to-use photonic modules to realize professional prototypes in a short time. Again the ITO successfully participated with the project MORPOA (modular system to realize photonic applications). In this project we could realize five different photonic modules together with the partners at Fraunhofer IAO and the company cirp, a professional 3D-printing SMB. Here we could realize modules for image projection, laser projection, illumination, image capture and hyperspectral sensing. All of the modules can be configured in terms of performance, size and outer shape. The outer shape can be realized by 3D-printing of an adaptive CAD-model. Moreover, open-source-software on the basis of ITOM was generated to use the modules for tracking, projection or detection purposes. The modules can also be combined, for example to realize a fringe projection system as shown in Figure 2.

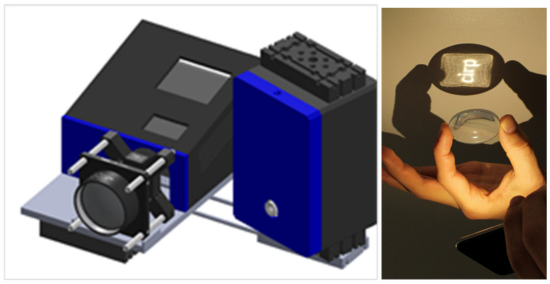

Fig. 2: Fringe projector (left) and 3D-printed freeform lens realized within the project MORPHOA.

Together with the partner cirp also 3D-printed transparent components could be realized [3]. Ranging from simple lenses, to light-guides, up to complex faceted lenticular surfaces a variety of ideas to employ 3d-printing for optical components was created.

Supported by: BMBF Projects: BaKaRoS and MORPHOA
In cooperation with: fischertechnik, Fraunhofer IAO, T-Systems, cirp GmbH

References:

(1) www.BaKaRoS.de
(2) C. Reichert, R. Knoll, P. Motzfeld, et. al. (2021).
(3) Evaluation and comparison of different materials for manufacturing of transparent optical components in additive manufacturing. Optical Engineering, 60(6), 067103-067103.
(4) C. Reichert, T. Gruhonjic, A. Herkommer (2020). „Development of an open source algorithm for optical system design, combining genetic and local optimization”, Opt. Eng., 59(5), 055111-055111.

Invited lectures on international conferences

A. Toulouse, J. Drozella, S. Thiele, H. Giessen, A. Herkommer

3D-gedrucktes Miniaturspektrometer für das sichtbare Spektrum mit einer Größe von 100x100x300 µm³

122. Jahrestagung der Deutschen Gesellschaft für angewandte Optik (DGaO), Bremen, September 2021

A. Toulouse, J. Drozella, S. Thiele, H. Giessen, A. Herkommer

Complex 3D printed microoptical systems: from a pinhole camera to a spectrometer

3D Printed Optics and Additive Photonic Manufacturing III, SPIE Photonics Europe, Strasbourg, Frankreich, April 2022

Awards

2021 – 2022

A. Toulouse

Young Scientist Award of the „Deutsche Gesellschaft für angewandte Optik (DGaO)“ for the best PhD thesis 2021

A. Toulouse, J. Drozella, S. Thiele, H. Giessen, A. Herkommer

Outstanding Paper Award 2021 of the Journal “Light: Advanced Manufacturing”. “3D-printed miniature spectrometer for the visible range with a 100 × 100 µm² footprint”

H. Giessen, A. Herkommer and Simon Thiele

Gips-Schüle-Forschungspreis 2021

C. Schober

CC UPOB Young Scientist Award 2022, second prize

R. Beißwanger, A. Harsch

EOS Prize 2022 for best paper in JEOS:RP for the article: “Round robin comparison study on the form measurement of optical freeform surfaces”

Membership of Editorial Boards

A. Herkommer

Member of the Editorial Board of the Journal “JPhys Photonics”

S. Reichelt

Section Editor of “Optics, Visual System, Human Factors” in Springer “Handbook of Visual Display Technology” (3rd Edition), Edited by: Karlheinz Blankenbach, Qun (Frank) Yan, Robert J. O'Brien

Reviewed Papers

2021

Y. Arezki, R. Su, V. Heikkinen, F. Leprete, P. Posta, V. Bitou, C. Schober, C. Mehdi-Souzani, B. Alzahrani, X. Zhang, Y. Kondo, C. Pruss, V. Ledl, N. Anwer, M. Bouazizi, R. Leach, H. Nouira

Traceable Reference Full Metrology Chain for Innovative Aspheric and Freeform Optical Surfaces Accurate at the Nanometer Level

Sensors Vol. 21, Nr. 4, 1103

F. Beirow, J. Wahl, R. Hohmuth, A. Richter, C. Pruß, C. Mateo, T. Graf, M. Abdou Ahmed

Increasing the efficiency of the intra-cavity generation of ultra-short radially polarized pulses in thin-disk resonators with grating waveguide structures

OSA Continuum Vol. 4, Nr. 2, pp. 262-278

A. Birk, Y. Wilhelm, S. Dreher, C. Flack, P. Reimann, C. Gröger

A Real-World Application of Process Mining for Data-Driven Analysis of Multi-Level Interlinked Manufacturing Processes

Procedia CIRP, Vol. 104, pp. 417-422

D. Claus, I. Alekseenko, M. Grabherr, G. Pedrini, R. Hibst

Snap-shot topography measurement via dual-VCSEL and dual wavelength digital holographic interferometry

Light : Advanced Manufacturing, Vol. 2, Nr. 4

F. Glöckler, F. Hausladen, I. Alekseenko, A. Gröger, G. Pedrini, und D. Claus

Two-photon-polymerization enabled and enhanced multi-channel fibre switch

Engineering Research Express, Vol. 3, Nr. 4, 045016

M. Gödecke, K. Frenner, W.Osten

Model-based characterisation of complex periodic nanostructures by white-light Mueller-matrix Fourier scatterometry

Light: Advanced Manufacturing, Vol. 2, Nr. 18

N. Harland, B. Amend, B., N. Lipke, S. Y. Brucker, F. Fend, A. Herkommer, H. Lensch, O. Sawodny, T. E. Schäffer, K. Schenke-Layland, C. Tarín Sauer, W. Aicher & A. Stenzl

Organoide zur Weiterentwicklung der intraoperativen Diagnostik

Der Urologe, Bd. 60, 1159–1166

S. Hartlieb, M.Tscherpel, F.Guerra, T. Haist, W. Osten, M. Ringkowski, O. Sawodny

Highly accurate imaging based position measurement using holographic point replication

Measurement, Vol. 172, 108852

S. Hartlieb, M. Ringkowski, T. Haist, O. Sawodny, und W. Osten

Multi-positional image-based vibration measurement by holographic image replication

Light: Advanced Manufacturing, Vol. 2, Nr. 32

B. Javidi, A. Carnicer, A. Anand, G. Barbastathis, W. Chen, P. Ferraro, J. W. Goodman, R. Horisaki, K. Khare, M. Kujawinska, R. A. Leitgeb, P. Marquet, T. Nomura, A. Ozcan, Y. Park, G. Pedrini, P. Picart, J. Rosen, G. Saavedra, N. T. Shaked, A. Stern, E. Tajahuerce, L. Tian, G. Wetzstein, and M. Yamaguchi

Roadmap on digital holography Invited

Optics Express, Vol. 29, Nr. 22, pp. 35078-35118

M.Joglekar, V. Trivedi, R. Bhatt, V. Chhaniwal, S. Dubey, D. Claus, G. Pedrini, R. Leitgeb, B. Javidi, A. Anand

Compact, low cost, large field-of-view self-referencing digital holographic interference microscope

Optik, Vol. 245, 167615

S. Ludwig, G. Pedrini, X. Peng, und W. Osten

Single-pixel scatter-plate microscopy

Optics Letters, Vol. 46, Nr. 10, pp. 2473-2476

S. Ludwig, P. Ruchka, G. Pedrini, X. Peng, und W. Osten

Scatter-plate microscopy with spatially coherent illumination and temporal scatter modulation

Opt. Express, Vol. 29, Nr. 3, pp. 4530-4546

Z. Meng, G. Pedrini, X. Lv, J. Ma, S. Nie, C. Yuan

DL-SI-DHM: a deep network generating the high-resolution phase and amplitude images from wide-field images

Optics Express Vol. 29, Nr. 13, p.19247-19261

H. Pang, T. Haist, T. Haecker

Absorption of tailored laser beams within 3D laser cutting kerfs

Journal of Laser Applications Vol. 33, Nr. 3, 032007

G. Pedrini, D. Claus

Phase retrieval using bidirectional interference

Applied Optics Vol. 60, Nr. 12, p. 3517-352

G. Pedrini, D. Claus

Phase retrieval using 3D Fourier transforms of volume diffraction pattern

Optics Letters Vol. 46, Nr. 7, p. 1716-1719

K. Prause, A. Herkommer, B. R. Pinzer, und M. Layh

Single-shot high speed aerial chromatic confocal metrology sensor

Optical Engineering, Vol. 60, Nr. 12, 124110

F. Reichenzer, M. Schneider, und A. Herkommer

Improvement in systematic error in background-oriented schlieren results by using dynamic backgrounds

Experiments in Fluids, Vol. 62, Nr. 196

C. Reichert, R. Knoll, P. Motzfeld, L. Diebold, M. Schmid, O. Schendel, T. Luck, A. Herkommer

Evaluation and comparison of different materials for manufacturing of transparent optical components in additive manufacturing

Optical Engineering Vol. 60, Nr. 6, 067103

M. Schmid, F. Sterl, S. Thiele, A. Herkommer, H. Giessen

3D printed hybrid refractive/diffractive achromat and apochromat for the visible wavelength range

Optics Letters Paper Vol.46, Nr. 10, p. 2485-2488

C. Schober, C. Pruß, A. Faulhaber, und A. Herkommer

Event based coherence scanning interferometry

Optics letters, Vol. 46, Nr. 17, pp. 4332-4335

A. Toulouse, J. Drozella, S. Thiele, H. Giessen, A. Herkommer

3D-printed miniature spectrometer for the visible range with a 100 × 100 µm2 footprint

Light: Advanced Manufacturing, Vol. 2, Nr. 2

Reviewed Papers

2022

M. A. Ahmed, F. Beirow, A. Loescher, T. Dietrich, D. Bashir, D. Didychenko, A. Savchenko, C. Pruss, M. Fetisova, F. Li, P. Karvinen, M. Kuittinen, T. Graf

High-power thin-disk lasers emitting beams with axially-symmetric polarizations

Nanophotonics, Vol. 11, Nr. 4, pp. 835-846

S. Amann, T. Haist, A. Gatto, M. Kamm, A. Herkommer

Design and realization of a miniaturized high resolution computed tomography imaging spectrometer

EPJ Web of Conferences Vol. 266, 02001

V. Aslani, F. Guerra, A. Steinitz, P. Wilhelm, T. Haist

Averaging approaches for highly accurate image-based edge localization

Optics Continuum, Vol. 1, Nr. 4, pp. 834-845

L. Becker, F. Fischer, J. L. Fleck, N. Harland, A. Herkommer, A. Stenzl, W. K. Aicher, K. Schenke-Layland, J. Marzi

Data-Driven Identification of Biomarkers for In Situ Monitoring of Drug Treatment in Bladder Cancer Organoids

International Journal of Molecular Sciences, Vol. 23, Nr. 13, 6956

R. Beisswanger, M. Weckerle, C. Pruss, S. Reichelt

Interferometric radius of curvature measurements: an environmental error treatment

Optics Express, Vol. 30, Nr. 14, pp. 25803-25816

L. Bremer, C. Jimenez, S. Thiele, K. Weber, T. Huber, S. Rodt, A. Herkommer, S. Burger, S. Höfling, H. Giessen, S. Reitzenstein

Numerical optimization of single-mode fiber-coupled single-photon sources based on semiconductor quantum dots

Optics Express, Vol. 30, Nr. 10, pp. 15913-15928

A. Faulhaber, C. Krächan, T. Haist

Depth from axial differential perspective

Optics Continuum, Vol. 1, Nr. 1, pp. 103-112

F. Fischer, A. Birk, P. Somers, K. Frenner, C. Tarín, A. Herkommer

FeaSel-Net: A Recursive Feature Selection Callback in Neural Networks

Machine Learning and Knowledge Extraction Vol. 4, Nr. 4, pp. 968-993

A. Gronle, C. Pruss, A. Herkommer

Misalignment of spheres, aspheres and freeforms in optical measurement systems

Optics Express, Vol. 30, Nr. 2, pp. 797-814

F. Guerra, P. Wilhelm, T. Haist

Holographic Wide-Angle System for Deformation Measurement of Extended Structures

Optics, Vol. 3, Nr. 1, pp. 79-87

R. Hahn, T. Haist, K. Michel, W. Osten

Diffraction-based hyperspectral snapshot imager

Optical Engineering, Vol. 61, Nr. 01, 015106

S. Hartlieb, C. Schober, T. Haist, S. Reichelt

Accurate single image depth detection using multiple rotating point spread functions

Optics Express, Vol. 30, Nr. 13, pp. 23035-23049

A. Kumar, A. Asadollahbaik, J. Kim, K. Lahlil, S. Thiele, A. M. Herkommer, S. N. Chormaic, J. Kim, T. Gacoin, H. Giessen, J. Fick

Emission spectroscopy of NaYF4: Eu nanorods optically trapped by Fresnel lens fibers

Photonics Research, Vol. 10, Nr. 2, pp. 332-339

J. Li, S. Thiele, R. W. Kirk, B. C. Quirk, A. Hoogendoorn, Y. C. Chen, K. Peter, S. J. Nicholls, J. W. Verjans, P. J. Psaltis, C. Bursill, A. M. Herkommer, H. Giessen, R. A. McLaughlin

3D-Printed Micro Lens-in-Lens for In Vivo Multimodal Microendoscopy

Small, Vol. 18, Nr. 17, 2107032

R. Li, G. Pedrini, Z. Huang, S. Reichelt, und L. Cao

Physics-enhanced neural network for phase retrieval from two diffraction patterns

Optics Express, Vol. 30, Nr. 18, pp. 32680-32692

M. Ringkowski, E. Arnold, S. Hartlieb, T. Haist, W. Osten, O. Sawodny

Precision tracking control of a dual-stage measuring machine

at - Automatisierungstechnik, Vol. 70, Nr. 7, pp. 646-661

W. Osten, G. Pedrini

55 Years of Holographic Non-Destructive Testing and Experimental Stress Analysis: Is there still Progress to be expected?

Light: Advanced Manufacturing, Vol. 3, Nr. 8

P. Ruchka, S. Hammer, M. Rockenhäuser, R. Albrecht, J. Drozella, S. Thiele, H. Giessen, T. Langen

Microscopic 3D printed optical tweezers for atomic quantum technology

Quantum Science and Technology, Vol. 7, Nr. 4, 045011

A. Schiebelbein, G. Pedrini

Lensless phase imaging microscopy using multiple intensity diffraction patterns obtained under coherent and partially coherent illumination

Applied Optics, Vol. 61, Nr. 5, pp. B271–B278

M. D. Schmid, A. Toulouse, S. Thiele, S. Mangold, A. M. Herkommer, H. Giessen

3D Direct Laser Writing of Highly Absorptive Photoresist for Miniature Optical Apertures

Advanced Functional Materials, p. 2211159

C. Schober, C. Pruss, A. Herkommer

Ereignisbasierte Weißlichtinterferometrie (eCSI)

tm - Technisches Messen, Vol. 89, Nr. 6, pp. 413-420

C. Schober, R. Beisswanger, A. Gronle, C. Pruss, W. Osten

Tilted Wave Fizeau Interferometer for flexible and robust asphere and freeform testing

Light: Advanced Manufacturing, Vol. 3, Nr. 48

J. Schwab, K. Weber, J. Drozella, C. Jimenez, A. Herkommer, L. Bremer, S. Reitzenstein, H. Giessen

Coupling light emission of single-photon sources into single-mode fibers: mode matching, coupling efficiencies, and thermo-optical effects

Optics Express, Vol. 30, Nr. 18, pp. 32292-32305

A. Toulouse, J. Drozella, P. Motzfeld, N. Fahrbach, V. Aslani, S. Thiele, H. Giessen, A. M. Herkommer

Ultra-compact 3D-printed wide-angle cameras realized by multi-aperture freeform optical design

Optics Express, Vol. 30, Nr. 2, pp. 707-720

A. Toulouse, S. Thiele, K. Hirzel, M. Schmid, K. Weber, M. Zyrianova, H. Giessen, A. M. Herkommer, M. Heymann

High resolution femtosecond direct laser writing with wrapped lens

Optical Materials Express, Vol. 12, Nr. 9, pp. 3801-3809

M. Wende, J. Drozella, A. Toulouse, A. M. Herkommer

Fast algorithm for the simulation of 3D-printed microoptics based on the vector wave propagation method

Optics Express, Vol. 30, Nr. 22, pp. 40161-40173

M. Zimmermann, S. Amann, M. Mel, T. Haist, A. Gatto

Deep learning-based hyperspectral image reconstruction from emulated and real computed tomography imaging spectrometer data

Optical Engineering, Vol. 61, Nr. 5, 053103

Reviewed Papers

2023 (until June 2023)

S. Amann, T. Haist, A. Gatto, M. Kamm, A. Herkommer

Design and realization of a miniaturized high resolution computed tomography imaging spectrometer

Journal of the European Optical Society-Rapid Publications, Vol. 19, Nr. 2, 34

V. Aslani, A. Toulouse, M. Schmid, H. Giessen, T. Haist, A. Herkommer

3D printing of colored micro-optics

Optical Materials Express Vol. 13, Nr. 5, pp. 1372-1384

C. M. Bett, M. Daiber-Huppert, K. Frenner, W. Osten

Evaluation of a time-gated-single-pixel-camera as a promising sensor for autonomous vehicles in harsh weather conditions

Journal of the European Optical Society-Rapid Publications, Vol. 19, Nr. 1, 27

S. Crowell, T. Haist, M. Tscherpel, J. Caron, E. Burgh, und B. Moore III

Performance and polarization response of slit homogenizers for the GeoCarb mission

Atmospheric Measurement Techniques, Vol. 16, Nr. 1, pp. 195-208

F. Fischer, K. Frenner, M. Granai, F. Fend, A. Herkommer

Data-driven development of sparse multi-spectral sensors for urological tissue differentiation

Journal of the European Optical Society-Rapid Publications, Vol. 19, Nr. 1, 33

L. Fu, M. Daiber-Huppert, K. Frenner, W. Osten

Simulation of realistic speckle fields by using surface integral equation and multi-level fast multipole method

Optics and Lasers in Engineering, Vol. 162, p. 107438

A. Gröger, G. Pedrini, D. Claus, I. Alekseenko, F. Gloeckler, S. Reichelt

Advantages of holographic imaging through fog

Applied Optics Vol. 62, Nr. 10, pp. D68-D76

A. Gröger, G. Pedrini, F. Fischer, D. Claus, I. Aleksenko, S. Reichelt

Two-wavelength digital holography through fog

Journal of the European Optical Society-Rapid Publications, Vol. 19, Nr. 1, 25

T. Haist, R. Hahn, S. Reichelt

Diffraction-based dual path multispectral imaging

tm - Technisches Messen, 2023

S. Hartlieb, C. Schober, T. Haist, S. Reichelt

Field evaluation of a novel holographic single-image depth reconstruction sensor

Journal of the European Optical Society-Rapid Publications, Vol. 19, Nr. 1, 20

H. Li, L. Fu, K. Frenner, W. Osten

Design studies of a far-field plasmonic superlens with an enlarged field of view

Optical Materials, Vol. 138, p. 113688

J. Liu, Ö. Atmaca, P. P. Pott

Needle-Based Electrical Impedance Imaging Technology for Needle Navigation

Bioengineering Vol. 10, Nr. 5, 590

S. Wagner, K. Treptow, S. Weser, M. Drexler, S. Sahakalkan, W. Eberhardt, T. Guenther, C. Pruss, A. Herkommer, A. Zimmermann

Injection Molding of Encapsulated Diffractive Optical Elements

Micromachines Vol. 14, Nr.6, 1223

S. Walz, V. Aslani, O. Sawodny, A. Stenzl

Robotic radical cystectomy – more precision needed?

Current Opinion in Urology Vol. 33, Nr. 2, p 157-162

Conference proceedings and journals

2021

S. Amann, A. Gatto, M. Kamm, G. Troll, T. Haist, A. Herkommer

Hyperspektrale Bildgebung mit Hilfe eines Computed Tomography Imaging Spectrometer unter Verwendung moderner Methoden

Proc. DGaO 122. Tagung B35

A. Asadollahbaik, S. Thiele, A. Kumar, K. Weber, J. Drozella, F. Sterl, M. Heymann, A. Herkommer, J. Fick, H. Giessen

Structured light to miniaturize optical micromanipulation

Proc. SPIE 11798, Optical Trapping and Optical Micromanipulation XVIII; 117981G (2021)

V. Aslani, T. Haist

Rauschreduktion durch den Einsatz von maschinellem Lernen in der Bildverarbeitung

Proc. DGaO 122. Tagung A36

L. Bremer, K. Weber, S. Fischbach, S. Thiele, M. Schmidt, A. Kaganskiy, S. Rodt, A. Herkommer, M. Sartison, S. L. Portalupi, P. Michler, H. Giessen, S. Reitzenstein

Quantum Dot Single-Photon Emission Coupled into Single-Mode Fibers with 3D Printed Micro-Objectives

OSA Technical Digest (Optical Society of America, 2021), paper ATu2S.5

L. Fu, M. Daiber-Huppert, K. Frenner, and W. Osten

Rigorous speckle simulator for large area rough penetrable surfaces using surface integral equations and multilevel fast multipole method

Proc. DGaO 122. Tagung A7

Y. Ganjkhani, A. Calabuig, G. Pedrini, A. Moradi

Oblique illumination in self-referencing digital holographic microscopy and its applications

Proc. SPIE 11786, Optical Methods for Inspection, Characterization, and Imaging of Biomaterials V, 117860K

R. Hahn, T. Haist, F. Hämmerling, D. Fleischle, O. Schwanke, O. Hauler, K. Rebner, M. Brecht, W. Osten

Detailed characterization of a hyperspectral snapshot imager for full-field chromatic confocal microscopy

Proc. SPIE 11352, 113520Y (published 2021)

T. Haist, A. Steinitz, F. Guerra

Increasing the accuracy of imaging-based dimensional measurements

Proc. SPIE 11352, 1135204 (published 2021)

S. Hartlieb, C. Erol, M. Tscherpel, T. Haist, F. Guerra, W. Osten, M. Ringkowski, O. Sawodny

Accurate 3D coordinate measurement using holographic multipoint technique

Proc. SPIE 11352, 1135203 (published 2021)

S. Hartlieb, M Ringkowski, T. Haist, W. Osten, O. Sawodny

Bildbasierte Vibrationsmessung mittels holografischer Mehrpunktgenerierung

Proc. DGaO 122. Tagung A4

S. Ludwig, G. Pedrini, X. Peng, W. Osten

Scatter-plate microscopy with coherent illumination and moving scattering media

Proc. DGaO 122. Tagung A6

S. Ludwig, G. Pedrini, X. Peng, W. Osten

Ensemble cross-correlation for image retrieval from the intensity signal recorded by a single pixel

Proc. SPIE 11782, Optical Measurement Systems for Industrial Inspection XII; 1178214 (2021)

E. Michalski, C. Schober, C. Pruß, A. Herkommer

Aufbau zur Charakterisierung der temperaturabhängigen Fokusverschiebung von Mikroskopobjektiven

Proc. DGaO 122. Tagung Poster: P14

C. Reichert, L. Diebold, R. Rausch, A. Herkommer

Entwicklung eines Algorithmus zur Ersetzung eines Optikdesigns durch Kataloglinsen mit kontinuierlicher Designanpassung

Proc. DGaO 122. Tagung B18

S. Ristok, S. Thiele, A. Toulouse, A. Herkommer, H. Giessen

Stitching-free 3D printing of millimeter-sized highly transparent spherical and aspherical optical components

Proc. SPIE 11677, Laser 3D Manufacturing VIII, 1167710

S. Ristok, S. Thiele, A. Toulouse, A. Herkommer, H. Giessen

Stitching-free 3D printing of millimeter-sized highly transparent spherical and aspherical optical components

OSA Technical Digest (Optical Society of America, 2021), paper ATh1R.1

F. Rothermel, S. Thiele, C. Jung, H. Giessen, A. Herkommer

Towards magnetically actuated 3D-printed micro-optical elements

Proc. SPIE 11816, Optomechanics and Optical Alignment; 118160I (2021)

S. Schmidt, S. Thiele, A. Toulouse, A. Herkommer, M. Hanft

Integrated structured illumination concepts by complex optical 3d-printing

Proc. DGaO 122. Tagung A26

M. Schmid, S. Thiele, A. Herkommer, H. Giessen

3D printed hybrid refractive/diffractive achromat and apochromat for the visible wavelength range

OSA Technical Digest (Optical Society of America, 2021), paper ATh1R.2

C. Schober, C. Pruss, A. Herkommer

Integriertes Messkonzept zur Registrierung von Weißlichtinterferometriesignalen für Nanometrologie in großen Messvolumina

Proc. DGaO 122. Tagung B19

A. Toulouse, J. Drozella, S. Thiele, H. Giessen, A. Herkommer

3D-gedrucktes Miniaturspektrometer für das sichtbare Spektrum mit einer Größe von 100 × 100 × 300 µm³

Proc. DGaO 122. Tagung H3

Conference proceedings and journals

2022

N. Borchers, M. Hillenbrand, T. Haist, A.M. Herkommer

Miniaturisierte optische 3D-Messtechnik für industrielle Bauteile mit beschränkter Zugänglichkeit

Proc. DGaO 123. Tagung A3

J. Drozella, A. Toulouse, P. Motzfeld, N. Fahrbach, V. Aslani, S. Thiele, A. Herkommer, H. Giessen

Micro-3D-printed multi-aperture freeform ultra-wide-angle systems: production, characterization, and correction

Proc. of SPIE 11989, Laser-based Micro- and Nanoprocessing XVI; 119890V (2022)

J. Drozella, M. Wende, A. Toulouse, R. Hahn, A. M. Herkommer

Wellenoptische Simulation 3D-gedruckter Mikrooptiken

Proc. DGaO 123. Tagung A22

F. Fischer, A. Birk, K. Frenner, A. Herkommer

FeaSel-Net: A Recursive Feature Selection Callback in Neural Networks

Machine Learning and Knowledge Extraction, Vol. 4, Nr.4, 968-993

F. Fischer, K. Frenner, A. M. Herkommer

Sparse Mid-Infrared Spectra Enable Real-time and In-vivo Applications in Tissue Discrimination

EPJ Web of Conferences 266, 02004

L. Fu, K. Frenner, S. Reichelt

Rigorous modelling of scattered light from large area 3D surfaces for a confocal microscope using surface integral equation method

Proc. DGaO 123. Tagung A24

A.Groeger, G. Pedrini, D. Claus, I. Alekseenko, F. Gloeckler, S. Reichelt

Coherence-gated digital holographic imaging through fog

Digital Holography and Three-Dimensional Imaging, M2A.2

R. Hahn, J. Görres, T. Haist, W. Osten, S. Reichelt

Novel snapshot hyperspectral imager based on diffractive elements

Proc. of SPIE 12139, Optical Sensing and Detection VII; 121390I (2022)

R. Hahn, T. Haist, S. Reichelt

Neuartiger Hyperspektralsensor basierend auf einem diffraktiven Element

Proc. DGaO 123. Tagung A26

S. Hartlieb, M. Boguslawski, T. Haist, S. Reichelt

Holographical image based vibrometry with monochromatic and event based cameras

Proc. of SPIE Vol. 12137, Optics and Photonics for Advanced Dimensional Metrology II; 1213702 (2022)

S. Hartlieb, C. Schober, T. Haist, S. Reichelt

Bildbasierte Abstandsrekonstruktion mittels holographisch vervielfältigter Doppel-Helix-PSF

Proc. DGaO 123. Tagung A2

S. Hartlieb, C. Schober, T. Haist, S. Reichelt

Holographic single-image depth reconstruction

EPJ Web of Conferences, Vol. 266. EDP Sciences, p.10005

G. Pedrini, A. Schiebelbein, E. Achimova, V. Abashkin

Lensless phase imaging microscopy by multiple intensity diffraction pattern

Proc. of SPIE Vol. 12136, Unconventional Optical Imaging III; 1213605 (2022)

K. Prause, B. Pinzer, A. Herkommer, M. Layh

Verification of a single-shot high speed aerial chromatic confocal metrology sensor

Proc. of SPIE Vol. 12008, Photonic Instrumentation Engineering IX; 120080G (2022)

A. Savchenko, C. Pruß, D. Bashir, D. Didychenko, M. Abdou-Ahmed

Fabrication of sub-wavelength circular diffraction gratings for high-power laser applications

Proc. DGaO 123. Tagung, Poster: B31THB

C. Schober, C. Pruss, A.M. Herkommer, S. Reichelt

Kurzkohärente Oberflächenmessung unter Verwendung von ereignisbasierten Sensoren

Proc. DGaO 123. Tagung A8

A. Toulouse, J. Drozella, P. Motzfeld, N. Fahrbach, V. Aslani, S. Thiele, H. Giessen, A.M. Herkommer

3D-gedruckte Freiformobjektive und Weitwinkelkameras mit einem extrem flachen Formfaktor

Proc. DGaO 123. Tagung B12

A. Toulouse, J. Drozella, S. Thiele, H. Giessen, A. Herkommer

Complex 3D printed microoptical systems: from a pinhole camera to a spectrometer

Proc. of SPIE Vol. PC12135, 3D Printed Optics and Additive Photonic Manufacturing III; PC1213504

K. Treptow, C. Schober, C. Pruss, S. Reichelt

Single-Shot Interferometrie fernab der Nulltest-Messung

Proc. DGaO 123. Tagung A29

M. Wende, J. Drozella, A.M. Herkommer

Schnelle vektorielle wellenoptische Simulation der Lichtausbreitung durch Mikrooptiken

Proc. DGaO 123. Tagung A23

Conference proceedings and journals

2023 (until June 2023)

S. Amann, T. Haist, A. Gatto, M. Kamm, S. Reichelt

Multi Aperture Computed Tomography Imaging Spectrometer

Proc. DGaO 124. Tagung B29

S. Amann, T. Haist, A. Gatto, M. Kamm, A. Herkommer

Intermediate image free computed tomography imaging spectrometer

Proc. of SPIE Vol. 12428, Photonic Instrumentation Engineering X; 124280G

S. Amann, M. Mel, P. Zanuttigh, T. Haist, M. Kamm, A. Gatto

Material Characterization using a Compact Computed Tomography Imaging Spectrometer with Super-resolution Capability

Optical Characterization of Materials. KIT Scientific Publishing, p. 139 – 148

V. Aslani, T. Haist, S. Thiele, A. Herkommer

Sensorsystem zur minimalinvasiven intraoperativen Gewebedifferenzierung in der Onkologie mittels endoskopischer Streifenprojektion

Proc. DGaO 124. Tagung A28

C. M. Bett, M. Daiber-Huppert, K. Frenner, W. Osten

Time-gated-single-pixel-camera: a promising sensor for robust object detection in adverse weather conditions for autonomously driven vehicles

Proc.of SPIE Vol. 12701, Fifteenth International Conference on Machine Vision (ICMV 2022); 1270107

A. Birk, K. Frenner, W. Osten

Deep learning based compressed sensing in machine vision: an iterative approach to multi object detection

Proc. of SPIE Vol. 12701, Fifteenth International Conference on Machine Vision (ICMV 2022); 1270109

J. Drozella, A. Toulouse, A. M. Herkommer

Zur additiven Herstellung von mikroskaligen multiplexen volumenstreuenden Elementen

Proc. DGaO 124. Tagung A4

A. Gröger, G. Pedrini, D. Claus, F. Fischer, S. Reichelt, S. Thiele, N. Fahrbach

World's smallest single-shot two-wavelength holographic endoscope for 3D surface measurement

Proc. of SPIE Vol. PC12356, Endoscopic Microscopy XVIII; PC123560P

S. Hartlieb, T. Haist, F. Guerra, S. Reichelt

Bildbasierte optische Messtechnik für zivile Bauwerke

Proc. DGaO 124. Tagung B16

A. Herkommer, C. Pruss, J. Trapp, T. Haist

Optik-Bausätze für die Nachwuchsförderung

Proc. DGaO 124. Tagung A33

S. Reichelt, G. Pedrini

Digital Holography vs. Display Holography - What are their differences and what do they have in common?

ICMVA '23: Proc. of the 2023 6th International Conference on Machine Vision and Applications, p.72–80

F. Rothermel, S. Thiele, R. Steinhoff, C. Jung, H. Gießen, A. M. Herkommer

Magnetisch aktuierbare 3D-gedruckte mikrooptische Elemente

Proc. DGaO 124. Tagung A1

C. Schober, L. Lausmann, K. Treptow, C. Pruss, S. Reichelt

Neue Designmöglichkeiten durch Zweiphotonenlithographie für ein RGB-Interferometer-Beleuchtungsmodul

Proc. DGaO 124. Tagung A3

K.Treptow, S. Wagner, C. Pruß, A. Zimmernann, A. Herkommer, S. Reichelt

Fertigung eines mikrostrukturierten Werkzeugeinsatzes zur kostengünstigen Herstellung von Hybridoptiken

Proc. DGaO 124. Tagung A9

M. Wende, A. Toulouse, M. Heymann, H. Giessen, A. M. Herkommer

Minimalinvasiver Bio 3D-Druck mittels endoskopischer Zwei-Photonen-Lithographie

Proc. DGaO 124. Tagung B31

Patents

Patent Applications

A. Asadollahbaik, S. Thiele, A. Herkommer, H. Giessen, J. Fick

Optische Pinzette basierend auf totaler interner Reflexion von Mikrooptiken, die an der Spitze einer optischen Singlemode-Faser angebracht ist

DE102021213647A1 Date of Publication: 09.06.2022
US020220181041A1 Date of Publication: 09.06.2022

F. Bienert, C. Pruß, M. Abdou-Ahmed

Gitterspiegel und Strahlungsbereitstellungssystem mit einem Gitterspiegel

EP000004092458A1 Date of Publication: 23.11.2022

A. Brueckner, E. Hegels, A. Herkommer, D. Manssen, S. Thiele

Compact catadioptric imaging apparatus

WO002022073592A1 Date of Publication: 14.04.2022

H. Giessen, A. Herkommer, J. Li, R. McLaughlin, S. Thiele

An optical element

WO002022016230A1 Date of Publication: 27.01.202

K. Körner, A. M. Herkommer

Verfahren und Fourier-Transformations-Spektrometer mit Zweistrahl-Interferometer zur Single-Shot-Imaging-Fourier-Spektroskopie

EP000003760992A1 Date of Publication: 06.01.2021
US020210310938A1 Date of Publication: 07.10.2021

K. Körner, A. M. Herkommer

Verfahren und Shear-Invariantes Michelsontyp-Interferometer zur Single-Shot-Imaging-FT-Spektroskopie

EP000003760990A1 Date of Publication: 06.01.2021
US020210310937A1 Date of Publication: 07.10.2021

C. Pruß, C. Schober

Einzelbild-Tilted Wave Interferometer

DE102020130814A1 Date of Publication: 25.05.2022
WO002022106694A1 Date of Publication: 27.05.2022

S. Thiele, C. Jung, H. Giessen, A. M. Herkommer

Aktuierbare optische Vorrichtung, Verfahren zur Herstellung der Vorrichtung, und Verwendung einer magnetischen Substanz

EP000003851892A1 Date of Publication: 21.07.2021
US020210221059A1 Date of Publication: 22.07.2021

Patents

Granted Patents

K. Arzenbacher, H. Giessen, T. Gissibl, A. Herkommer, S. Thiele

Method of fabricating a multi-aperture system for foveated imaging and corresponding multi-aperture system

US000011095813B2 Date of Publication: 17.08.2021

D. Claus, A. Herkommer, K. Körner, C. Pruss

Method and assembly for chromatic confocal spectral interferometry or spectral domain oct

US000011248900B2 Date of Publication: 15.02.2022

H. Giessen, W. Göbel, A. Herkommer, B. Häsler, K. Irion, S. Thiele

Endoscope and imaging device for an endoscope

US000011406249B2 Date of Publication: 09.08.2022

K. Körner, A. M. Herkommer

Verfahren und Fourier-Transformations-Spektrometer mit Zweistrahl-Interferometer zur Single-Shot-Imaging-Fourier-Spektroskopie

EP000003760992B1 Date of Publication: 20.04.2022
US000011530982B2 Date of Publication: 20.12.2022

K. Körner, W. Osten

Arrangement and method for robust single-shot interferometry

US000011231269B2 Date of Publication: 25.01.2022

K. Körner, W.Osten

Robustes One-Shot-Interferometer und OCT-Verfahren, insbesondere zur Materialmessung und auch Tumorzellen-Erkennung

EP000002843360B1 Date of Publication: 11.05.2022

Doctoral thesis, Master & Bachelor thesis and Student research thesis

Doctoral Thesis 2021- April 2023 (Month of the oral examination)

Buchta, Dominic

Simulationsgestützte Scherografie zur Defekterkennung an Kunstwerken

06/2021

Rausch, Denise

Design und Analyse von Beleuchtungs-optiken auf Basis des Phasenraumkonzepts

07/2021

Scholz, Sandy

Zur Verbesserung der Asphärenmesstechnik mittels Computer generierten Hologrammen

11/2021

Reichenzer, Frieder

Einfluss der Kesselraumgeometrie auf die Propagation eines Laserstrahls beim Laserschmelzschneiden

11/2021

Toulouse, Andrea

Komplexe 3D-gedruckte mikrooptische Systeme

12/2021

Reichert, Carsten

Ganzheitliche Optimierung und Auslegung von optischen Systemen

07/2022

Ludwig, Stephan

Beiträge zur Weiterentwicklung der Streuscheiben-Mikroskopie

11/2022

Hahn, Robin

Vollflächige konfokale Single-Shot Messtechnik unter Verwendung hyperspektraler Sensoren

11/2022

Zepp, Andreas

Modaler holografischer Wellenfrontsensor für Adaptive Optik

04/2023

Gödecke, Laura

Ein Beitrag zur modellgestützten Charakterisierung komplexer Halbleiter-Nanostrukturen mittels Weißlicht-Müller-Matrix-Fourier-Scatterometrie

04/2023

Master Thesis 2021-2022

Motzfeld, Pascal

Optimierung von 3D-gedruckten Mikro-Objektiven mit seitlicher Blickrichtung

1/2021

Zhao, Yuxuan

Characterization and numerical modelling of saturable absorber

2/2021

Steinitz, Adriana

Untersuchung einer Digitalholografie-Methodik zur Gewebedifferenzierung

3/2021

Wilhelm, Philipp

Multiimage-basierte Deformationsdetektion von Gebäuden

3/2021

Sun, Mingqian

Using GAN-based network for data augmentation and binary-classification in medicine

4/2021

Engel, Jonas

Regularisierung eines latenten Raums

4/2021

Kamin, David

Methoden zur Untersuchung von Stereo-Vision Algorithmen in der Robotik

8/2021

Wende, Marco

Effiziente Simulation der Propagation elektromagnetischer Vektorfelder durch Mikrooptiken

8/2021

Rehling, Dennis

Konzeption und Verifikation eines vollautomatischen, optischen Messplatzes zur Ermittlung relevanter Displayparameter im geometrischen Halbraum

8/2021

Nguyen, Duc Tien

Fertigungsgerechte Optimierung von diffraktiven optischen Elementen zur Herstellung mittels 2-Photonen-Polymerisation

9/2021

Fan, Hao

Nighttime pedestrian classification in infrared single-pixel imaging using deep learning approach

9/2021

Stassen, Lea

Optimierung diffraktiver Optik für die triangulierende Messtechnik

9/2021

Schiebelbein, Antonius

Phase Retrieval from Volume Intensity Recordings Obtained with Partially Coherent Illumination

10/2021

Chen, Lei

Autoencoder mit Regularisierungsunterstützung

10/2021

Koinzer, Ingo

Formabschätzung in der Tilted-Wave-Interferometrie durch merkmalbasierte Interferogrammauswertung

10/2021

Aisenbrey, Lena

Experimentalsystem zur optischen Mikromanipulation von Nano- und Mikroobjekten

11/2021

Kauke, Leonie

Steuerung von Injektionen in den subretinalen Spalt durch optische Verfahren

11/2021

Mrokon, Alexander

Auslegung und Realisierung eines neuartigen diffraktiven Hyperspektralsensors

2/2022

Lausmann, Lisa

Auslegung, Konstruktion und Erprobung einer neuen Beleuchtungseinheit für die Single-Shot-Tilted-Wave-Interferometrie

2/2022

Pfeiffer, Max

Entwicklung einer Zylinderabschnittsbeleuchtung für eine Panoramaoptik in der Koloskopie

2/2022

Weber, Steffen

Konzeption und Entwicklung eines Objektivmoduls zur Laserstrahlführung in 3D-Bearbeitungsmaschinen

4/2022

Pfau, Teresa

Detection of a human heartbeat with a highsensitivity diamond magnetometer

6/2022

Li, Jiaxin

Bildvorhersage und Kollisionsklassifizierung für autonomes Fahren mit Encoder-Decoder- und LSTM-Netzwerken

6/2022

Sauer, Tobias

Tiefenkartenvervollständigung von transparenten Objekten durch die Fusion von Punktwolken und Farbbildern

6/2022

Shakeri, Mahdiye

Rauschreduktionsalgorithmen für simulierte Lichtverteilungen

7/2022

Simmler, Stephan

Optimization of diffractive optical elements for CTIS

7/2022

Lang, Lukas

Weiterentwicklung und Charakterisierung eines Experimentalaufbaus für den parallelisierten optischen Einfang von Nano- und Mikroobjekten

8/2022

Bolter, Dominik

Implementierung einer Plattform zur Vervielfältigung von holografisch optischen Elementen

9/2022

Hellstern, Fiona

NV-Zentrum-basierte Quantensensorik für die Erkennung von Tumorzellen

9/2022

Stark, Jonas

Optische Konzeptionierung eines Echtzeit-OP-Systems zur quantitativen PpIX-Bestimmung in niedriggradig malignen Gliomen

10/2022

Ai, Congcong

Two Wavelength Digital Holography for the Investigation of Biological Tissue

10/2022

Ademaj, Jete

Adaptive Cu Optik zur Intensitätsformung beim Laserschneiden

11/2022

Dreshaj, Nora

Auslegung des optischen Strahlenganges für die intraoperative Swept-Source-OCT Bildgebung

11/2022

Boguslawski, Maciej

Eventbasierte Vibrationsmessung mittels computergenerierter Hologramme

11/2022

Beeh, Marie

Analyse, Optimierung und Entwicklung eines Fertigungsprozesses für schluckbare diagnostische Kapseln unter Berücksichtigung der optischen Parameter

12/2022

Ede, Svenja

Optimierung des Konturtrennprozesses von Glas mittels Strahlformung von ultrakurzen Laserpulsen

12/2022

Bachelor Thesis 2021-2022

Michalski, Emanuel

Prüfstand für die temperaturbedingte Änderung des Brennpunktes

1/2021

Richter, Constantin

Unterdrückung von akustischen Störeinflüssen auf die Nanomess- und Nanopositioniermaschine NPMM-200

2/2021

Grimm, Adrian

Scanning beam interference lithography mit der NPMM-200: Systemcharakterisierung und Modellierung des Belichtungsprozesses

3/2021

Weichert, Insa-Marie

Digital Holography for the Investigation of Polarizing Samples

10/2021

Kurz, Lukas

Interferometrische Detektion von biologischen Pathogenen

12/2021

Sipple, Lukas Wendelin

Aufbau und Modellierung einer programmierbaren Lichtquelle

2/2022

Reguigui, Hajer

Calibration and characterization of a new type of hyperspectral sensor in the biomedical field

6/2022

Grunewald, Jule

Weiche 3D-gedruckte faseroptische Aktuierung

7/2022

Laudenbach, Xenia

Lithographische Realisierung und Charakterisierung einer Beleuchtungseinheit für das Single-Shot Tilted-Wave Interfereometer

10/2022

Schwanke, Jakob

Optimierung einer mittels Zwei-Photonen-Lithographie 3D-gedruckten Alvarez-Linse

12/2022

Student Research Thesis 2021-2022

Ly, Toni

Entwicklung eines Deep-Learning-basierten Algorithmus zur Auswertung von störreflexbehafteten Interferogrammen

1/2021

Bauer, Niklas

Charakterisierung einer Polarisationsfarbkamera für die Interferometrie

1/2021

Ilgen, Pascal

Realisierung und Charakterisierung eines Weißlichtinterferometers für den Einsatz in der NPMM-200

2/2021

Atmaca, Ömer

Entwicklung eines Algorithmus zur stereoskopischen Entfernungsbestimmung für Single-Pixel-Kameras mittels Deep-Learning-basierter Signalverarbeitung

5/2021

Qi, Zheng

Generation of spectral datasets for disease detection using deep learning

6/2021

Ai, Congcong

Digital holography for visualizing droplets produced during coughing

7/2021

Krächan, Clara

Algorithmik zur Entfernungsmessung mittels differentieller Perspektive

9/2021

Röckel, Felix

Robuste 3D-Vermessung durch lateral bewegtes Single-Lens-Stereo

9/2021

Ademaj, Jete

Erstellung und Erprobung eines Simulationsmodells für die Nanopositionier- und Nanomessmaschine NPMM200

12/2021

Diebold, Linda

Implementierung und Vergleich verschiedener Ersetzungsreihenfolgen eines Optikdesigns durch Kataloglinsen mit kontinuierlicher Designanpassung

12/2021

Schittenhelm, Helena

Aufbau und Untersuchung eines FD-OCT für die Auswertung 3D-gedruckter Fasersensoren

1/2022

Xu, Siyuan

Vergleich verschiedener Weißlicht-Interferometrie-Algorithmen für die NPMM

4/2022

Lodholz, Felix

Algorithmen zur Distanzmessung mittels differentieller Perspektive

5/2022

Görres, Johannes

Kalibrierung eines chromatisch konfokalen Mikroskops mit hyperspektraler snapshot Technologie

6/2022

Shi, Yuanmeng

Hochgenaue Positionsbestimmung durch breitbandige holografische Multipoints

09/2022

Jäger, Patrick

3D Szenenerfassung mittels Ereigniskamera

09/2022

Guo, Qing

Digitales holographisches Mikroskop zur Untersuchung von reflektierenden und transmittierenden Proben

11/2022

Stickel, Aileen

Ultradünnes Holographisches Single-Shot Endoskop

11/2022

Gedemer, Aaron

Objektklassifikation mittels Dichtekarten

11/2022

Optik-Kolloquium 2023

34. Optik-Kolloquium
mit Antrittsvorlesung Prof. Dr. Stephan Reichelt

Optik und Photonik in der Produktionstechnik

am 23. März 2023, Teilnehmer: ca. 150

Begrüßung und Einführung	Prof. Dr. Stephan Reichelt ITO, Universität Stuttgart
Antrittsvorlesung Prof. Dr. Stephan Reichelt Engineering Optics – Entwicklung optischer Systeme in der Praxis	Prof. Dr. Stephan Reichelt ITO, Universität Stuttgart
Fortschritte in der Optischen Dünnschichttechnik	Dr. Andreas Wienke Laser Zentrum Hannover e.V., Hannover
3D printed holograms onside of the multicore fiber facet for lensless 3D imaging with keyhole access	Prof. Dr. Jürgen Czarske Professur Mess- und Sensorsystemtechnik (MST) TU Dresden
Komplexe mikrooptische Komponenten und Systeme durch 3D-Druck	Dr. Simon Thiele Printoptix GmbH, Stuttgart
Optische Prüftechnik bei Carl Zeiss SMT - Der Weg zu EUVL-Genauigkeiten	Stefan Schulte Carl Zeiss SMT GmbH, Oberkochen
Digital Holography – from the lab into the production line	Dr. Daniel Carl Fraunhofer-Institut für Physikalische Messtechnik (IPM), Freiburg
Zentriermessung in der Montage asphärischer Linsensysteme	Dr. Aiko Ruprecht TRIOPTICS GmbH, Wedel
Optische Metrologie für den Maschinenbau: Aufgaben, Herausforderungen, Treiber	Dr. Andreas Lange Mahr GmbH, Göttingen
Structured light for ultrafast laser micro- and nanoprocessing	Dr. Daniel Flamm TRUMPF SE + Co. KG, Ditzingen
Optische Systeme in der Lasermaterialbearbeitung – Lösungen und Herausforderungen	Prof. Dr. Andreas Michalowski Institut für Strahlwerkzeuge (IFSW), Universität Stuttgart

Organized International Conferences: 2021 - 2022

A. Toulouse (program committee):

SPIE LASER, Photonics West
Laser 3D Manufacturing
San Francisco, USA, March 8-11, 2021

A. Herkommer (program committee):

International Optical Design Conference IODC
Optical Design and Fabrication
Online, USA, June 27 – July 1, 2021

A. Herkommer (program committee):

EOS Optical Technologies
TOM 2: Computational, Adaptive and Freeform Optics
TOM 3: Optical System Design, Tolerancing and Manufacturing
Rome, Italy, September 6-10, 2021

A. Toulouse (program committee):

SPIE LASER, Photonics West
Laser 3D Manufacturing
San Francisco, USA, January 22-27, 2022

A. Herkommer (program committee):

EOS Optical Technologies
TOM 2: Computational, Adaptive and Freeform Optics
TOM 3: Optical System Design, Tolerancing and Manufacturing
Porto, Portugal, September 12-16, 2022

Impressum:

Publisher: Institut für Technische Optik
Universität Stuttgart
Pfaffenwaldring 9
D-70569 Stuttgart
www.ito.uni-stuttgart.de

Editor: Dipl.-Ing. (FH) Erich Steinbeißer

ISBN: 978-3-948570-20-0

ISBN 978-3-948570-20-0